LSDS-1574
Version 5.0

Department of the Interior
U.S. Geological Survey

Landsat 8 (L8)
Data Users Handbook

Version 5.0

November 2019

USGS
science for a changing world

Landsat 8 (L8)
Data Users Handbook

November 2019

Document Owner:

VAUGHN IHLEN Digitally signed by VAUGHN IHLEN
Date: 2019.11.26 15:30:49 -06'00'

Vaughn Ihlen Date
LSRD Project Manager
U.S. Geological Survey

Approved By:

KAREN ZANTER Digitally signed by KAREN ZANTER
Date: 2019.11.26 15:17:11 -06'00'

Karen Zanter Date
LSDS CCB Chair
U.S. Geological Survey

EROS
Sioux Falls, South Dakota

Executive Summary

The Landsat 8 (L8) Data Users Handbook is prepared by the U.S. Geological Survey (USGS) Landsat Project Science Office at the Earth Resources Observation and Science (EROS) Center in Sioux Falls, SD, and the National Aeronautics and Space Administration (NASA) Landsat Project Science Office at NASA's Goddard Space Flight Center (GSFC) in Greenbelt, Maryland.

The purpose of this handbook is to provide a basic understanding and associated reference material for the L8 Observatory and its science data products. In doing so, this document does not include a detailed description of every technical detail for the L8 mission but instead focuses on the information that the users need to gain an understanding of the science data products.

This handbook includes various sections that provide an overview of reference material followed by a more detailed description of applicable data user and product information. This document includes the following sections:

- Section 1 describes the background for the L8 mission as well as previous Landsat missions
- Section 2 provides a comprehensive overview of the current L8 Observatory, including the spacecraft, the Operational Land Imager (OLI) and Thermal Infrared Sensor (TIRS) instruments, and the L8 concept of operations
- Section 3 includes an overview of radiometric and geometric instrument calibration as well as a description of the Observatory component reference systems and the Calibration Parameter File (CPF)
- Section 4 includes a comprehensive description of Level 1 products and product generation
- Section 5 addresses the conversion of Digital Numbers (DNs) to physical units
- Section 6 includes an overview of data search and access using the various online tools
- Appendix A contains the list of known issues associated with L8 data
- Appendix B describes the 10 observatory component reference systems used by L8 geometric algorithms
- Appendix C contains an example of the Level 1 product metadata
- Appendix D contains reference materials applicable to L8 missions, systems, and data products
- Appendix E provides a listing of the acronyms used in this document

This document is controlled by the Land Satellites Data System (LSDS) Configuration Control Board (CCB). Please submit changes to this document, as well as supportive material justifying the proposed changes, via a Change Request (CR) to the Process and Change Management Tool.

Document History

Document Number	Document Version	Publication Date	Change Number
LSDS-1574	Version 1.0	June 2015	CR 12286
LSDS-1574	Version 2.0	March 2016	CR 12749
LSDS-1574	Version 3.0	October 2018	CR 14516
LSDS-1574	Version 4.0	April 2019	CR 14815
LSDS-1574	Version 5.0	November 2019	CR 15147

Contents

List of Figures

List of Tables

Section 1 Introduction

1.1 Foreword

The Landsat Project has provided calibrated high-quality moderate spatial resolution data of the Earth's surface to a broad and varied user community since 1972. Landsat images provide information that meets the broad and diverse needs of agribusiness, global change researchers, academia, state and local governments, commercial users, national security agencies, the international community, decision-makers, and the public.

The mission of the Landsat Project is to provide repetitive acquisition of moderate-resolution multispectral data of the Earth's surface on a global basis. Landsat represents the only source for global, calibrated, moderate spatial resolution measurements of the Earth's surface that are preserved in a national archive and freely available to the public. Data from the Landsat spacecraft constitute the longest record of the Earth's continental surfaces as seen from space. It is a record unmatched in quality, detail, coverage, and value.

Launched in 2013, the Landsat 8 satellite has contributed to an uninterrupted multispectral record of the Earth's land surfaces since 1972. Landsat 8 orbits in an eight-day offset with Landsat 7, which was launched in 1999. Landsat 8's space-borne data acquisition combines with the USGS archival and distribution systems, which includes the data processing techniques required to render Landsat 8 data into a scientifically usable format. With Landsat 8, special emphasis has been placed on periodically refreshing the global data archive, maintaining an accurate instrument calibration, providing data in accordance with national policy directives, and ensuring there is a data processing system that creates publically accessible products of superior quality.

The Landsat satellites carry a variety of components, including remote sensing systems, data relay systems, attitude-control and orbit-adjustment subsystems, a power supply, and receivers and transmitters for ground station communications.

The Landsat 8 (L8) Observatory offers the following features:

- **Data Continuity**: L8 is the latest in a continuous series of land remote sensing satellites that began in 1972.
- **Global Survey Mission**: L8 data systematically build and periodically refresh a global archive of Sun-lit, substantially cloud-free images of the Earth's landmass.
- **Free Standard Data Products**: L8 data products are available through the USGS EROS at no charge.

- **Radiometric and Geometric Calibration**: Data from the two sensors, the Operational Land Imager (OLI) and the Thermal Infrared Sensor (TIRS), are calibrated to better than 5 percent uncertainty in terms of Top of Atmosphere (TOA) reflectance or absolute spectral radiance and have an absolute geodetic accuracy better than 65 meters (m) circular error at 90 percent confidence (CE 90).
- **Immediate Delivery**: Products available for download immediately; higher-level products available for download within 72 hours.

The continuation of the Landsat Project is an integral component of the U.S. Global Change Research Program (USGCRP) and addresses a number of science priorities, such as land cover change and land use dynamics. L8 is part of a global research program known as NASA's Science Mission Directorate (SMD), a long-term program that studies changes in Earth's global environment. In the Landsat Project tradition, L8 continues to provide critical information to those who characterize, monitor, manage, explore, and observe the land surfaces of the Earth over time.

The USGS has a long history as a national leader in land cover and land use mapping and monitoring. Landsat data, including L8 and archive holdings, are essential for USGS efforts to document the rates and causes of land cover and land use change, and to address the linkages between land cover and use dynamics on water quality, water quantity, biodiversity, energy development, and many other environmental topics. In addition, the USGS is working toward the provision of long-term environmental records that describe ecosystem disturbances and conditions.

1.2 Background

The Land Remote Sensing Policy Act of 1992 (U.S. Code Title 15, Chapter 82) directed the Federal agencies involved in the Landsat Program to study options for a successor mission to Landsat 7 (L7), which ultimately launched in 1999 with a five-year design life, that could maintain data continuity with the Landsat System. The Act further expressed a preference for the development of this successor System by the private sector if such a development met the goals of data continuity.

The L8 Project suffered several setbacks in its attempt to meet these data continuity goals. Beginning in 2002, three distinct acquisition and implementation strategies were pursued: (1) the purchase of imagery from a commercially owned and operated satellite system partner (commonly referred to as a government "data buy"), (2) flying a Landsat instrument on National Oceanic and Atmospheric Administration's (NOAA's) National Polar-orbiting Operational Environmental Satellite System (NPOESS) series of satellites, and finally (3) the selection of a "free-flying" Landsat satellite. As a result, the Project incurred considerable delays to L8 implementation. The matter was not resolved until 2007, when it was determined that NASA would procure the next mission space segment and the USGS would develop the Ground System and operate the mission after launch.

The basic L8 requirements remained consistent through this extended strategic formulation phase of mission development. The 1992 Land Remote Sensing Policy Act

(U.S. Code Title 15, Chapter 82) established data continuity as a fundamental goal and defined continuity as providing data “sufficiently consistent (in terms of acquisition geometry, coverage characteristics, and spectral characteristics) with previous Landsat data to allow comparisons for global and regional change detection and characterization”. This direction has provided the guiding principal for specifying L8 requirements from the beginning, with the most recently launched Landsat satellite at that time, L7, serving as a technical minimum standard for system performance and data quality.

1.2.1 Previous Missions

Landsat satellites have provided multispectral images of the Earth continuously since the early 1970s. Thanks to these efforts, a unique data record of the Earth's land surface now exists. This one-of-a-kind retrospective portrait of the Earth’s surface has been used across several disciplines to achieve an improved understanding of the Earth's land surfaces and the impact of humans on the environment. Landsat data have been used in a variety of government, public, private, and national security applications. Examples include land and water management, global change research, oil and mineral exploration, agricultural yield forecasting, pollution monitoring, land surface change detection, and cartographic mapping.

L8 is the latest satellite in this series. The first (Landsat 1, originally known as ERTS-1) was launched in 1972 with two Earth-viewing imagers – a Return Beam Vidicon (RBV) and an 80-meter 4-band Multispectral Scanner (MSS). Landsat 2 and Landsat 3, launched in 1975 and 1978 respectively, were configured similarly. In 1984, Landsat 4 was launched with the MSS and a new instrument called the Thematic Mapper (TM). Instrument upgrades included improved ground resolution (30 m) and 3 new channels/bands. In addition to using an updated instrument, Landsat 4 made use of the Multimission Modular Spacecraft (MMS), which replaced the Nimbus-based spacecraft design employed for Landsat 1 – Landsat 3. Landsat 5, a duplicate of Landsat 4, was launched in 1984 and returned scientifically viable data for 28 years – 23 years beyond its 5-year design life. Landsat 6, equipped with an additional 15-meter panchromatic (Pan) band, failed to achieve orbit in 1993.

L7 was launched in 1999 and performed nominally until the Enhanced Thematic Mapper Plus (ETM+) sensor’s Scan Line Corrector (SLC) failed in May 2003. Since that time, L7 has continued to acquire useful image data in the “SLC-off” mode. All L7 SLC-off data are of the same high radiometric and geometric quality as data collected prior to the SLC failure.

Figure 1-1 shows the continuity of multispectral data coverage provided by Landsat missions, beginning with Landsat 1 in 1972.

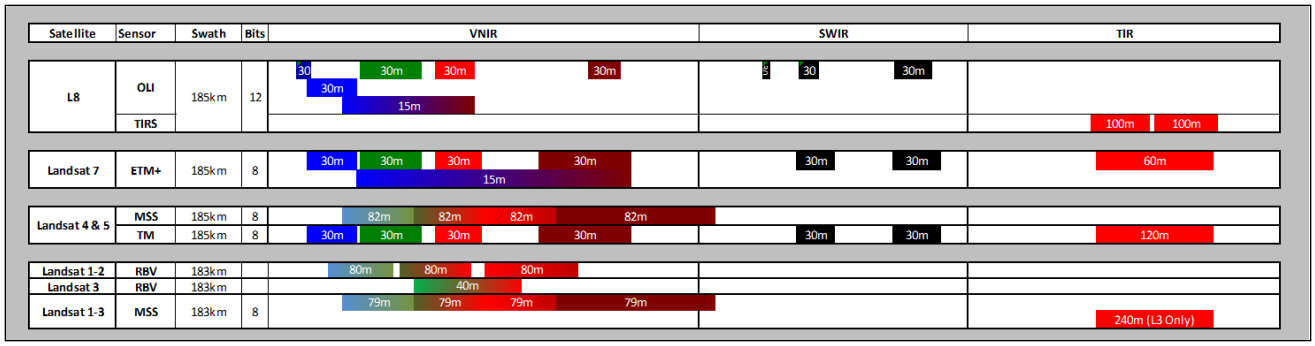

Figure 1-1. Continuity of Multispectral Data Coverage Provided by Landsat Missions

1.2.2 Operations and Management

The L8 management structure is composed of an ongoing partnership between NASA and USGS for sustainable land imaging. NASA contracted with Ball Aerospace & Technologies Corp. (BATC) to develop the OLI and with Orbital Sciences Corporation to build the spacecraft; NASA GSFC built the TIRS. NASA was also responsible for the satellite launch and completion of a 90-day on-orbit checkout before handing operations to the USGS. The USGS was responsible for the development of the Ground System and is responsible for operation and maintenance of the Observatory and the Ground System for the life of the mission. In this role, the USGS captures, processes, and distributes L8 data and maintains the L8 data archive.

The Landsat Project at USGS EROS manages the overall L8 mission operations. In this capacity, USGS EROS directs on-orbit flight operations, implements mission policies, directs acquisition strategy, and interacts with International Ground Stations (IGSs). USGS EROS captures L8 data and performs pre-processing, archiving, product generation, and distribution functions. USGS EROS also provides a public interface into the archive for data search and ordering.

1.3 Landsat 8 Mission

The L8 mission objective is to provide timely, high-quality visible and infrared images of all landmass and near-coastal areas on the Earth, continually refreshing an existing Landsat database. Data input into the system are sufficiently consistent with currently archived data in terms of acquisition geometry, calibration, coverage, and spectral characteristics to allow for comparison of global and regional change detection and characterization.

1.3.1 Overall Mission Objectives

L8 has a design life of 5 years and carries 10 years of fuel consumables. The overall objectives of the L8 mission are as follows:

- Provide data continuity with Landsat 4, 5, and 7.
- Offer 16-day repetitive Earth coverage, and an 8-day offset with L7.

- Build and periodically refresh a global archive of Sun-lit, substantially cloud-free land images.

1.3.2 System Capabilities

The L8 System is robust, high performing, and of extremely high data quality. System capabilities include the following:

- Provides for a systematic collection of global, high-resolution, multispectral data.
- Provides for a high volume of data collection. Unlike previous missions, L8 far surpasses the average collection of 400 scenes per day. L8 routinely acquires about 700 scenes per day; these are all stored in the USGS archive.
- Uses cloud cover predictions to avoid acquiring less useful data.
- Ensures all data imaged are collected by a U.S. Ground Station.

The L8 Observatory offers many improvements over its predecessor, L7. See Table 1-1 for a high-level comparison of L7 and L8 Observatory capabilities. The following subsections contain further details.

	Landsat 7	Landsat 8
Scenes / Day	~450	~700
SSR Size	378 Gbits, block-based	3.14 Terabit, file-based
Sensor Type	ETM+, Whisk-Broom	OLI / TIRS, Pushbroom
Compression	No	~2:1 Variable Rice Compression
Image D/L	X-Band GXA × 3	X-Band Earth Coverage
Data Rate	150Mbits/sec × 3 Channels / Frequencies	384 Mbits/sec, CCSDS Virtual Channels
Encoding	Not fully CCSDS compliant	CCSDS, LDPC FEC
Ranging	S-Band 2-Way Doppler	GPS
Orbit	705 km Sun-sync 98.2° inclination (WRS-2)	705 km Sun-sync 98.2° inclination (WRS-2)
Crossing Time	~10:00 AM ± 15 minutes	~10:00 AM ± 15 minutes

Table 1-1. Comparison of Landsat 7 and Landsat 8 Observatory Capabilities

1.3.3 Global Survey Mission

An important operational strategy of the L8 mission is to establish and maintain a global survey data archive. L8 follows the same Worldwide Reference System (WRS) used for Landsat 4, 5, and 7, bringing the entire world within view of its sensors once every 16 days.

In addition, L8 operations endeavor to systematically capture Sun-lit, substantially cloud-free images of the Earth's entire land surface. Initially developed for L7, the Long-Term Acquisition Plan (LTAP) for L8 defines the acquisition pattern for the mission to create and update the global archive to ensure global continuity.

1.3.4 Rapid Data Availability

L8 data are downlinked and processed into standard products within 24 hours of acquisition. Level 0 Reformatted (L0R), Level 1 Systematic Terrain Corrected (L1Gt),

Level 1 Precision Terrain Corrected (L1TP), and LandsatLook products are available through the User Portal (UP). All users must register through EarthExplorer (EE) at https://ers.cr.usgs.gov/register/.

All products are accessible via the Internet for download via Hypertext Transfer Protocol Secure (HTTPS); there are no product media options.

As with all Landsat data, products are available at no cost to the user. The user can view available data through the following interfaces:

1. EarthExplorer: https://earthexplorer.usgs.gov
2. Global Visualization Viewer: https://glovis.usgs.gov
3. LandsatLook Viewer: https://landsatlook.usgs.gov

1.3.5 International Ground Stations (IGSs)

Landsat has worked cooperatively with IGSs for decades. For the first time in the history of the Landsat mission, all data downlinked to IGSs are written to the Solid State Recorder (SSR) and downlinked to USGS EROS for inclusion in the USGS Landsat archive. No unique data are held at the IGSs. For updated information and a map displaying the IGSs, please see the following: https://landsat.usgs.gov/igs-network.

1.4 Document Purpose

This Landsat 8 (L8) Data Users Handbook is prepared by the USGS Landsat Project Science Office at the EROS Center in Sioux Falls, SD, and the NASA Landsat Project Science Office at NASA's GSFC in Greenbelt, Maryland. The purpose of this handbook is to provide a basic understanding and associated reference material for the L8 Observatory and its science data products.

1.5 Document Organization

This document contains the following sections:

- Section 1 describes the background for the L8 mission as well as previous Landsat missions
- Section 2 provides a comprehensive overview of the current L8 Observatory, including the spacecraft, the OLI instrument, the TIRS instrument, and the L8 concept of operations
- Section 3 includes an overview of radiometric and geometric instrument calibration as well as a description of the Observatory component reference systems and the CPF
- Section 4 includes a comprehensive description of Level 1 products and product generation
- Section 5 addresses the conversion of DNs to physical units
- Section 6 includes an overview of data search and access using the various online tools
- Appendix A contains the list of known issues associated with L8 data

- Appendix B describes the 10 observatory component reference systems used by L8 geometric algorithms
- Appendix C contains an example of the Level 1 product metadata
- Appendix D contains reference materials applicable to L8 missions, systems, and data products
- Appendix E provides a listing of the acronyms used in this document

Section 2 Observatory Overview

The L8 Observatory is designed for a 705 kilometer (km), Sun-synchronous orbit, with a 16-day repeat cycle, completely orbiting the Earth every 98.9 minutes. S-Band is used for commanding and housekeeping telemetry operations, while X-Band is used for instrument data downlink. A 3.14 terabit SSR brings back an unprecedented number of images to the USGS EROS archive.

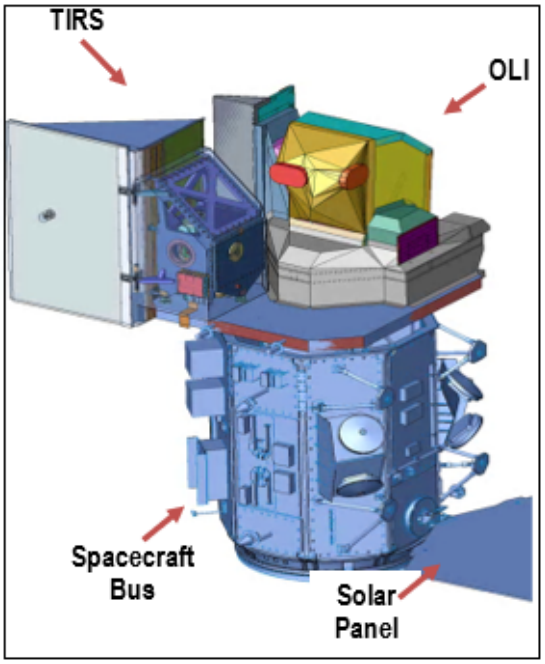

Figure 2-1. Illustration of Landsat 8 Observatory

L8 carries a two-sensor payload: the OLI, built by BATC, and the TIRS, built by NASA GSFC. Both the OLI and TIRS sensors simultaneously image every scene but are capable of independent use if a problem in either sensor arises. In normal operation, the sensors view the Earth at-nadir on the Sun-synchronous Worldwide Reference System 2 (WRS-2) orbital path/row coordinate system, but special collections may be scheduled off-nadir. Both sensors offer technical advancements over earlier Landsat instruments. The spacecraft, with its two integrated sensors, is referred to as the L8 Observatory.

2.1 Concept of Operations

The fundamental L8 operations concept is to collect, archive, process, and distribute science data in a manner consistent with the operation of the L7 satellite system. To that end, the L8 Observatory operates in a near-circular, near-polar, Sun-synchronous orbit with a 705 km altitude at the Equator. The Observatory has a 16-day ground track repeat cycle with an equatorial crossing at 10:11 a.m. (+/−15 min) Mean Local Time (MLT) during the descending node. In this orbit, the L8 Observatory follows a sequence of fixed ground tracks (also known as paths) defined by the WRS-2. The L8 launch and initial orbit adjustments placed the Observatory in an orbit to ensure an 8-day offset between L7 and L8 coverage of each WRS-2 path.

The Mission Operation Center (MOC) sends commands to the satellite once every 24 hours via S-Band communications from the Ground System to schedule daily data collections. Landsat 8 Long-Term Acquisition Plan (LTAP-8) sets priorities for collecting data along the WRS-2 ground paths. LTAP-8 is modeled on the systematic data acquisition plan developed for L7 (Arvidson et al., 2006). OLI and TIRS collect data jointly to provide coincident images of the same surface areas. The MOC nominally schedules the collection of 400 OLI and TIRS scenes per day, where each scene covers a 190-by-180 km surface area. The objective of scheduling and data collection is to provide near cloud-free coverage of the global landmass for each season of the year.

Since the 2014 growing season, however, the L8 mission has been routinely acquiring approximately 700 scenes per day.

The L8 Observatory initially stores OLI and TIRS data on board in an SSR. The MOC commands the Observatory to transmit the stored data to the ground via an X-Band data stream from an all-Earth omni antenna. The L8 Ground Network (GN) receives the data at several stations, and these stations forward the data to the EROS Center. The GN also includes IGS (referred to as International Cooperators (ICs)) operated under the sponsorship of foreign governments. Data management and distribution by the ICs is in accordance with bilateral agreements between each IC and the U.S. Government. No unique data are held at the IGSs.

The data received from the GN are stored and archived at the EROS Center, where L8 data products are also generated. The OLI and TIRS data for each WRS-2 scene are merged to create a single product containing the data from both sensors. The data from both sensors are radiometrically corrected and co-registered to a cartographic projection, with corrections for terrain displacement resulting in a standard orthorectified digital image called the Level 1 Terrain Corrected (L1T) product. The interface to the L8 data archive is called the UP, and it allows anyone to search the archive, view browse images, and request data products that are distributed electronically through the Internet at no charge (see Section 6).

2.2 Operational Land Imager (OLI)

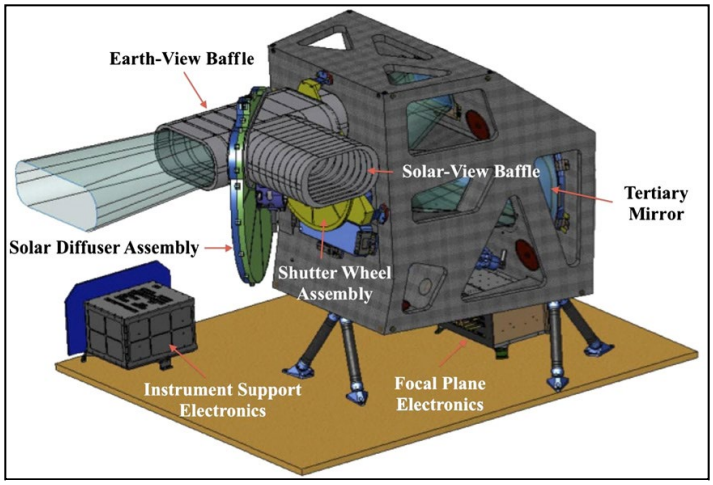

Figure 2-2. OLI Instrument

The OLI sensor, which has a five-year design life, is similar in design to the Advanced Land Imager (ALI) that was included on Earth Observing 1 (EO-1) and represents a significant technological advancement over L7's ETM+ sensor. Instruments on earlier Landsat satellites employed oscillating mirrors to sweep the detectors' Field of View (FOV) across the swath width ("whisk-broom"), but OLI instead uses long linear detector arrays with thousands of detectors per spectral band. Detectors aligned across the instrument's focal planes collect imagery in a "push-broom" manner, resulting in a more sensitive instrument with fewer moving parts. OLI has a 4-mirror telescope, and data generated by OLI are quantized to 12 bits, compared to the 8-bit data produced by the TM and ETM+ sensor.

The OLI sensor collects image data for 9 shortwave spectral bands over a 190 km swath with a 30 meter (m) spatial resolution for all bands except the 15 m Pan band. The widths of several OLI bands are refined to avoid atmospheric absorption features within ETM+ bands. The biggest change occurs in OLI Band 5 (0.845–0.885 micrometer (µm)) to exclude a water vapor absorption feature at 0.825 µm in the middle of the ETM+ near-infrared band (Band 4; 0.775–0.900 µm). The OLI Pan band, Band 8, is also narrower relative to the ETM+ Pan band to create greater contrast between vegetated areas and land without vegetation cover. OLI also has two new bands in addition to the legacy Landsat bands (1-5, 7, and Pan). The Coastal / Aerosol band (Band 1; 0.435-0.451 µm), principally for ocean color observations, is similar to ALI's band 1, and the new Cirrus band (Band 9; 1.36-1.38 µm) aids in the detection of thin clouds comprised of ice crystals (cirrus clouds appear bright, while most land surfaces appear dark through an otherwise cloud-free atmosphere containing water vapor).

Landsat-7 ETM+ Bands (µm)			Landsat-8 OLI and *TIRS* Bands (µm)		
			30 m Coastal/Aerosol	0.435 - 0.451	Band 1
Band 1	30 m Blue	0.441 - 0.514	30 m Blue	0.452 - 0.512	Band 2
Band 2	30 m Green	0.519 - 0.601	30 m Green	0.533 - 0.590	Band 3
Band 3	30 m Red	0.631 - 0.692	30 m Red	0.636 - 0.673	Band 4
Band 4	30 m NIR	0.772 - 0.898	30 m NIR	0.851 - 0.879	Band 5
Band 5	30 m SWIR-1	1.547 - 1.749	30 m SWIR-1	1.566 - 1.651	Band 6
Band 6	60 m TIR	10.31 - 12.36	*100 m TIR-1*	*10.60 – 11.19*	Band 10
			100 m TIR-2	*11.50 – 12.51*	Band 11
Band 7	30 m SWIR-2	2.064 - 2.345	30 m SWIR-2	2.107 - 2.294	Band 7
Band 8	15 m Pan	0.515 - 0.896	15 m Pan	0.503 - 0.676	Band 8
			30 m Cirrus	1.363 - 1.384	Band 9

Table 2-1. OLI and TIRS Spectral Bands Compared to ETM+ Spectral Bands

OLI has stringent radiometric performance requirements and is required to produce data calibrated to an uncertainty of less than five percent in terms of absolute, at-aperture spectral radiance and to an uncertainty of less than three percent in terms of TOA spectral reflectance for each of the spectral bands in Table 2-1. These values are comparable to the uncertainties achieved by ETM+ calibration.

The OLI Signal-to-Noise Ratio (SNR) specifications, however, were set higher than ETM+ performance based on results from the ALI. Table 2-2 and Figure 2-3 show the OLI specifications and performance compared to ETM+ performance for SNR at specified levels of Typical Spectral Radiance (Ltypical) for each spectral band.

Ltypical SNR				
ETM + Band	OLI Band	ETM+ Performance	OLI Requirement	OLI Performance
N/A	1	N/A	130	238
1	2	40	130	364
2	3	41	100	302
3	4	28	90	227
4	5	35	90	204
5	6	36	100	265
7	7	29	100	334
78	8	16	80	149
N/A	9	N/A	50	165

Table 2-2. OLI Specified and Performance Signal-to-Noise (SNR) Ratios Compared to ETM+ Performance

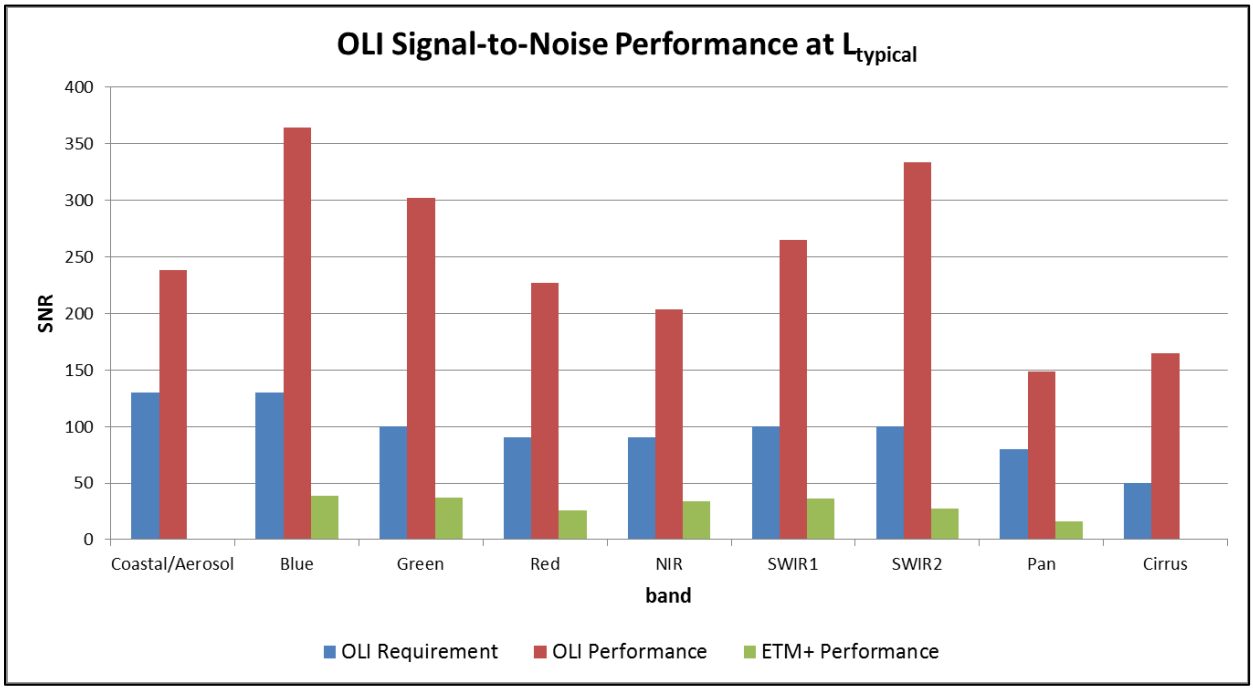

Figure 2-3. OLI Signal-to-Noise (SNR) Performance at Ltypical

The OLI is a push-broom sensor that employs a four-mirror anastigmatic telescope that focuses incident radiation onto the focal plane while providing a 15-degree FOV covering the 190 km across-track ground swath from the nominal L8 Observatory altitude. Periodic sampling of the across-track detectors as the Observatory flies forward along a ground track forms the multispectral digital images. The detectors are divided into 14 identical Sensor Chip Assemblies (SCAs) arranged in an alternating pattern along the centerline of the focal plane (Figure 2-4).

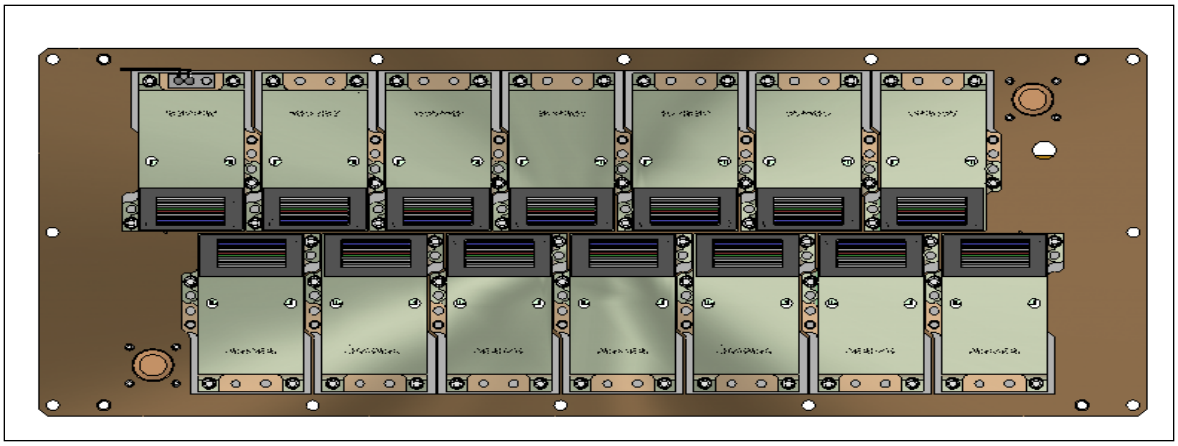

Figure 2-4. OLI Focal Plane

Each SCA consists of rows of detectors, a Read-Out Integrated Circuit (ROIC), and a nine-band filter assembly. Data are acquired from 6916 across-track detectors for each spectral band (494 detectors per SCA), except for the 15 m Pan band, which contains 13,832 detectors. The spectral differentiation is achieved by interference filters arranged in a “butcher-block” pattern over the detector arrays in each module. Even- and odd-numbered detector columns are staggered and aligned with the satellite's flight track. Even-numbered SCAs are the same as odd-numbered SCAs, only the order of the detector arrays is reversed top to bottom. The detectors on the odd and even SCAs are oriented such that they look slightly off-nadir in the forward and aft viewing directions. This arrangement allows for a contiguous swath of imagery as the push-broom sensor flies over the Earth, with no moving parts. One redundant detector per pixel is in each Visible and Near Infrared (VNIR) band, and two redundant detectors per pixel are in each Short Wavelength Infrared (SWIR) band. The spectral response from each unique detector corresponds to an individual column of pixels within the Level 0 product.

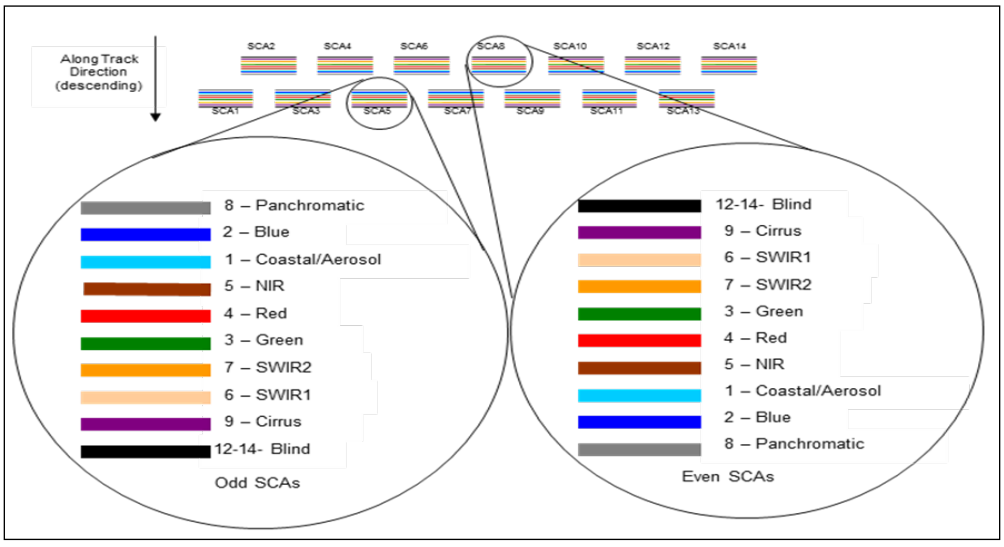

Figure 2-5. Odd/Even SCA Band Arrangement

Silicon PIN (SiPIN) detectors collect the data for the visible and near-infrared spectral bands (Bands 1 to 4 and 8). Mercury–Cadmium–Telluride (MgCdTe) detectors are used for the shortwave infrared bands (Bands 6, 7, and 9). An additional 'blind' band is shielded from incoming light and used to track small electronic drifts. There are 494 illuminated detectors per SCA, per band (988 for the Pan band); therefore, 70,672 operating detectors must be characterized and calibrated during nominal operations.

2.3 Thermal Infrared Sensor (TIRS)

Like OLI, TIRS is a push-broom sensor employing a focal plane with long arrays of photosensitive detectors. TIRS uses Quantum Well Infrared Photodetectors (QWIPs) to measure longwave Thermal Infrared (TIR) energy emitted by the Earth's surface, the intensity of which is a function of surface temperature. The TIRS QWIPs are sensitive to two thermal infrared wavelength bands, enabling separation of the temperature of the Earth's surface from that of the atmosphere. QWIPs' design operates on the complex principles of quantum mechanics. Gallium arsenide semiconductor chips trap electrons in an energy state 'well' until the electrons are elevated to a higher state by thermal infrared light of a certain wavelength. The elevated electrons create an electrical signal that can be read out, recorded, translated to physical units, and used to create a digital image.

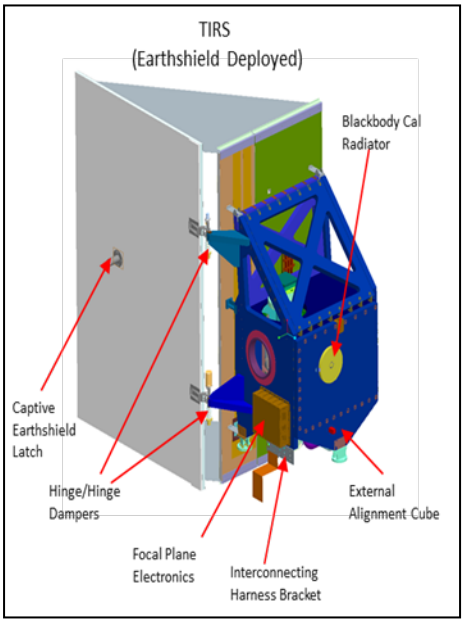

Figure 2-6. TIRS Instrument with Earthshield Deployed

The TIRS sensor, which has a three-year design life, collects image data for two thermal bands with a 100 m spatial resolution over a 190 km swath. The two thermal infrared bands encompass the wavelength range of the broader TM and ETM+ thermal bands (10.0–12.5 µm) and represent an advancement over the single-band thermal data. Data generated by TIRS are quantized to 12 bits. Although TIRS has a lower spatial resolution than the 60 m ETM+ Band 6, the dual thermal bands should theoretically enable retrieval of surface temperature, but stray light issues with Band 11 preclude the use of this approach.

Like OLI, the TIRS requirements also specify: cross-track spectral uniformity; radiometric performance, including absolute calibration uncertainty, polarization sensitivity, and stability; ground sample distance and edge response; and image geometry and geolocation, including spectral band co-registration. The TIRS noise limits (Table 2-3) are specified in terms of noise-equivalent change in temperature (NEΔT) rather than the signal-to-noise ratios used for OLI specifications. The radiometric calibration uncertainty is specified to be less than 2 percent in terms of absolute, at-aperture spectral radiance for targets between 260 Kelvin (K) and 330 K (less than 4 percent for targets between 240 K and 260 K and for targets between 330 K and 360 K), which is much lower than ETM+ measurements between 272 K and 285 K.

Currently, the performance of TIRS Band 11 is slightly out of specification because of stray light entering the optical path.

TIRS Noise-Equivalent Change in Temperature (NEΔT)				
Band	**NEDT@240**	**NEDT@280**	**NEDT@320**	**NEDT@360**
TIRS 10	0.069	0.053	0.046	0.043
TIRS 11	0.079	0.059	0.049	0.045
ETM+		0.22		

Table 2-3. TIRS Noise-Equivalent Change in Temperature (NEΔT)

The TIRS focal plane contains three identical SCAs, each with rows of QWIPs (Figure 2-7). The QWIP detectors sit between a ROIC and a two-band filter assembly. An additional masked or 'dark' band is used for calibration purposes. TIRS has 640 illuminated detectors per SCA, with approximately 27-pixel overlap to ensure there are no spatial gaps. Each TIRS SCA consists of a 640-column by 512-row grid of QWIP detectors. Almost all of the detectors are obscured except for two slits that contain the spectral filters for the 12.0 µm and 10.8 µm bands. These filters provide unvignetted illumination for approximately 30 rows of detectors under each filtered region.

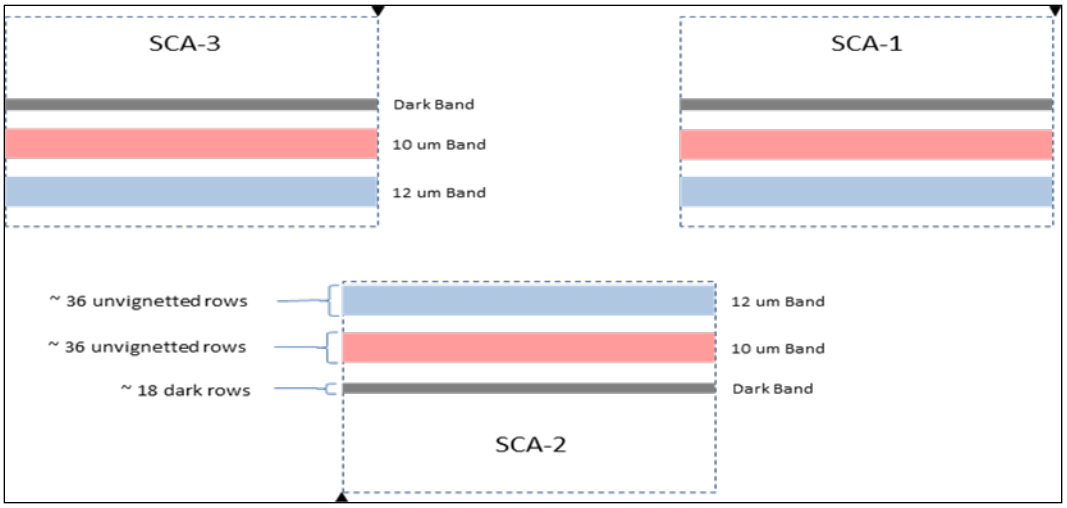

Figure 2-7. TIRS Focal Plane

Thermal energy enters the TIRS instrument through a scene select mirror and a series of four lenses before illuminating the QWIP detectors on the Focal Plane Array (FPA). Two rows of detector data from each filtered region are collected, with pixels from the second row used only as substitutes for any inoperable detectors in the primary row. The CPF specifies these rows.

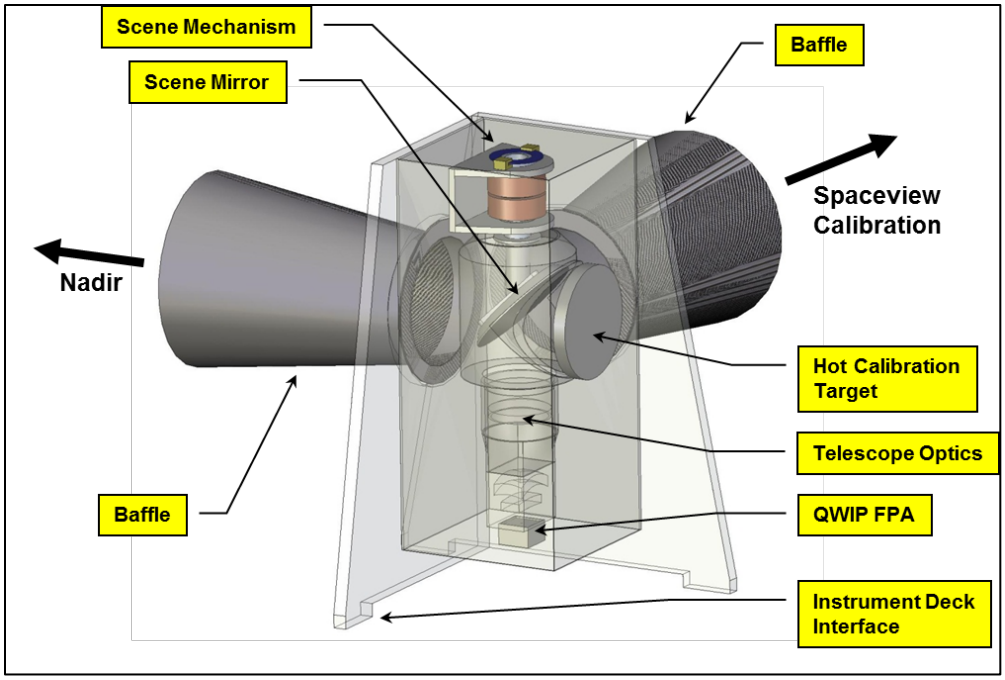

Figure 2-8. TIRS Optical Sensor Unit

2.4 Spacecraft Overview

Orbital Sciences Corporation built the L8 spacecraft at its spacecraft manufacturing facility in Gilbert, Arizona. The contract to build the spacecraft was originally awarded to General Dynamics Advanced Information Systems (GDAIS) in April 2008 but was subsequently acquired by Orbital Sciences Corporation in 2010. Orbital assumed responsibility for the design and fabrication of the L8 spacecraft bus, integration of the two sensors onto the bus, satellite level testing, on-orbit satellite checkout, and continuing on-orbit engineering support under GSFC contract management (Irons & Dwyer, 2010). The specified design life is 5 years, with an additional requirement to carry sufficient fuel to maintain the L8 orbit for 10 years. However, the hope is that the operational lives of the sensors and spacecraft will exceed the design lives and fuel will not limit extended operations.

The spacecraft supplies power, orbit and attitude control, communications, and data storage for OLI and TIRS. The spacecraft consists of the mechanical subsystem (primary structure and deployable mechanisms), command and data handling subsystem, attitude control subsystem, electrical power subsystem, Radio Frequency (RF) communications subsystem, hydrazine propulsion subsystem, and thermal control subsystem. All the components, except for the propulsion module, are mounted on the exterior of the primary structure. A 9×0.4 m deployable Sun-tracking solar array generates power that charges the spacecraft's 125 amp-hour nickel–hydrogen (Ni–H2) battery. A 3.14-terabit solid-state data recorder provides data storage aboard the spacecraft, and an Earth-coverage X-Band antenna transmits OLI and TIRS data either in real time or played back from the data recorder. The OLI and TIRS are mounted on an optical bench at the forward end of the spacecraft. Fully assembled, the spacecraft,

without the instruments, is approximately 3 m high and 2.4×2.4 m across, with a mass of 2071 kg fully loaded with fuel.

2.4.1 Spacecraft Data Flow Operations

The L8 Observatory receives a daily load of software commands transmitted from the ground. These command loads tell the Observatory when to capture, store, and transmit image data from the OLI and TIRS. The daily command load covers the subsequent 72 hours of operations, with the commands for the overlapping 48 hours overwritten each day. This precaution is taken to ensure that sensor and spacecraft operations continue in the event of a one- or two-day failure to successfully transmit or receive commands. The Observatory's Payload Interface Electronics (PIE) ensures that image intervals are captured in accordance with the daily command loads. The OLI and TIRS are powered on continuously during nominal operations to maintain the thermal balance of the two instruments. The two sensors' detectors continuously produce signals that are digitized and sent to the PIE at an average rate of 265 megabits per second (Mbps) for the OLI and 26.2 Mbps for TIRS.

Ancillary data, such as sensor and select spacecraft housekeeping telemetry, calibration data, and other data necessary for image processing, are also sent to the PIE. The PIE receives the OLI, TIRS, and ancillary data, merges these data into a Mission Data stream, identifies the Mission Data intervals scheduled for collection, and performs a lossless compression of the OLI data (TIRS data are not compressed) using the Rice algorithm (Rice et al., 1993). The PIE then sends the compressed OLI data and the uncompressed TIRS data to the 3.14 terabit SSR. The PIE also identifies the image intervals scheduled for real-time transmission and sends those data directly to the Observatory's X-Band transmitter. The IC receiving stations only receive real-time transmissions, and the PIE also sends a copy of these data to the onboard SSR for playback and transmission to the L8 Ground Network Element (GNE) receiving stations (USGS captures all of the data transmitted to ICs). OLI and TIRS collect data coincidently; therefore, the Mission Data streaming from the PIE contain both OLI and TIRS data as well as ancillary data.

The Observatory broadcasts Mission Data files from its X-Band, Earth-coverage antenna. The transmitter sends data to the antenna on multiple virtual channels, providing for a total data rate of 384 Mbps. The Observatory transmits real-time data, SSR playback data, or both real-time data and SSR data, depending on the time of day and the Ground Stations within view of the satellite. Transmissions from the Earth coverage antenna allow a Ground Station to receive Mission Data as long as the Observatory is within view of the station antenna. OLI and TIRS collect the L8 science data. The spacecraft bus stores the OLI and TIRS data on an onboard SSR and then transmits the data to ground receiving stations.

The Ground System provides the capabilities necessary for planning and scheduling the operations of the L8 Observatory and the capabilities necessary to manage the science data following transmission from the spacecraft. The real-time command and control subsystem for Observatory operations is known as the Mission Operations Element

(MOE). A primary and back-up MOC house the MOE, with the primary MOC residing at NASA GSFC. The Data Processing and Archiving System (DPAS) at the EROS Center ingests, processes, and archives all L8 science and Mission Data returned from the Observatory. The DPAS also provides a public interface to allow users to search for and receive data products over the Internet (see Section 6).

Section 3 Instrument Calibration

3.1 Radiometric Characterization and Calibration Overview

The L8 calibration activities began early in the instrument development phases, continued through On-orbit Initialization and Verification (OIV), and went on through mission operations. This section describes the instrument calibration activities for the OLI and TIRS from development and preflight testing, through OIV, and into nominal mission operations, as this is how the verification of instrument performance requirements proceeded. Table 3-1 provides a summary of the various calibration measurements.

	Purpose	How This is Used to Develop Calibration Parameters
OLI Preflight Activity		
Radiance of integrating sphere measured at multiple illumination levels	Establish linearity of detectors and focal plane electronics	Known radiance levels of the integrating sphere allow for linearity coefficients to be determined
Integration time sweeps of integrating sphere	Establish linearity of detectors and focal plane electronics	Known effective radiance levels allow for linearity coefficients to be determined and compared to multiple illumination levels of the integrating sphere; these measurements can be repeated on-orbit
Heliostat illumination of the solar diffusers	Derive a measure of the transmission of the heliostat and the reflectance of the solar diffuser panels	Verify effectiveness of the solar diffuser panels on-orbit
Measurement of the spectral reflectance of the solar diffuser panels	Determine in-band spectral reflectance of the solar diffuser panels	With the known spectral reflectance of the solar diffuser panels, coefficients are determined to convert the OLI response, in DNs, to spectral reflectance
Measurement of the Bi-directional Reflectance Distribution Function (BRDF) of the solar diffuser panels	Determine the reflectance of the solar diffuser panels in on-orbit orientation	Also to determine the coefficients to convert the OLI response to spectral reflectance
Transfer radiometer measurements of the integrating sphere and solar diffuser panels at the same illumination levels as measured by the OLI	Ensure traceability of the measurements compared to those made from the solar diffuser panels	Changes to the spectral response of the instrument are determined by inflight measurements of the solar diffuser panels, and coefficients used to scale the digital numbers of the instrument response to calibrated radiances can be adjusted
SNR measured at multiple radiance levels from the integrating sphere (or solar diffuser panel)	Requirements verification and characterization of radiometric performance	

	Purpose	How This is Used to Develop Calibration Parameters
Wide-field collimator measurements of fixed geometric test patterns	To build an optical map of the detectors	Enables construction of a Line of Sight (LOS) model from the focal plane to the Earth
Wide-field collimator measurements of fixed geometric test patterns with different reticle plates	To derive line spread functions, edge response, and modulation transfer function	
TIRS Preflight Activity		
Flood source-controlled heating of louvered plate	Temperatures across the surface of the plate are analyzed to characterize the uniformity of the radiometric response across the detectors within the focal plane and across the multiple SCAs	Known radiance levels of the flood source at different temperatures allow for linearity coefficients to be determined
Integration time sweeps of flood source	Establish linearity of detectors and focal plane electronics	Known effective radiance levels allow for linearity coefficient to be determined and compared to multiple flood source temperatures; these can be repeated on-orbit
A wide-field collimator and a set of fixed geometric patterns are scanned across the focal plane	To build an optical map of the detectors	Enables construction of a LOS model from the focal plane to the Earth
A wide-field collimator and a set of fixed geometric patterns are scanned across the focal plane at multiple temperature settings	To derive line spread functions, edge response, and modulation transfer function	
OLI On-Orbit Activities		
Integration time sweeps of solar diffuser	Characterize detector linearity	Potentially update linearization coefficients
Solar diffuser collects	Noise characterization including SNR, absolute radiometric accuracy characterization, uniformity characterization, radiometric stability characterization, relative gain calibration, absolute calibration (both radiance and reflectance)	The known reflectance of the diffuser panel is used to derive updated relative and absolute calibration coefficients
Long dark collects	Radiometric stability and noise (impulse noise, white noise, coherent noise and 1/f noise) characterization	
Extended solar diffuser collects	Monitor the detector stability (within-scene)	
Stimulation lamps data collects	Monitor the detector stability over days	
Side-slither maneuver	Characterize detector relative gains, in order to improve uniformity by reducing striping	Scanning the same target with detectors in line enables updated relative gains to be calculated

	Purpose	How This is Used to Develop Calibration Parameters
Focal Plane Module (FPM) overlap statistics	Normalize the gain of all the SCAs, to improve uniformity	Relative gain characterization
Cumulative histograms	Characterize striping in imagery	Relative gain characterization
Lunar data collection	Characterize stray light and characterize the absolute radiometric accuracy	
Characterization of Pseudo-Invariant Calibration Sites	Monitoring of temporal stability of OLI and TIRS instruments	Monitoring trends in Pseudo-Invariant Calibration Site (PICS) responses indicates a need for absolute radiometric calibration updates
TIRS On-Orbit Activities		
Integration time sweeps with blackbody and deep space	Monitor linearity of detectors and focal plane electronics	Determine calibration need to update linearity coefficients
Varying blackbody temperature over multiple orbits	Characterize detector linearity	
Blackbody and deep space collects	Noise (Noise Equivalent Detector Radiance ((NEdL))	Relative gain characterization
Long collects (over ocean)	Coherent noise, 1/f	Relative gain characterization
Vicarious calibration		Absolute radiometric calibration

Table 3-1. Summary of Calibration Activities, Their Purpose, and How Measurements are Used in Building Calibration Parameter Files

3.1.1 Instrument Characterization and Calibration

3.1.1.1 Description of Calibration Data Collections

A distinction is made between the calibration activities that measure, characterize, and evaluate instrument and system radiometric performance and those that are used to derive improved radiometric processing parameters contained in the L8 CPF for use by the Level 1 Product Generation System (LPGS). The measurement and evaluation activities are referred to as characterization operations, while the parameter estimation activities are referred to as calibration. Although both types of activities contribute to the "radiometric calibration" of the L8 OLI and TIRS instruments, the remainder of this document uses the term "characterization" to refer to radiometric assessment and evaluation operations and the term "calibration" to refer to those associated with estimating radiometric processing parameters.

Shutter Collects

Shutter collects provide the individual detector dark levels or biases, which are subtracted during ground processing from each detector's response in Earth images. This removes variations in detector dark current levels, reducing striping and other detector-to-detector uniformity issues in the imagery. These normal shutter collects are acquired before daylight imaging begins and after daylight imaging ends. An extended shutter collect is acquired about every three months and is about 36 minutes in duration. These longer shutter collects provide a measure of stability over typical Earth imaging intervals.

Stimulation Lamp Collects

The stimulation lamps are used to monitor the detector stability over days. While incandescent lamps tend to be poor absolute calibration sources, they excel at showing changes in detector response over relatively short periods. Three sets of stimulation lamps get used at three different frequencies: daily, bimonthly, and every six months. These different usages enable differentiation between detector changes and lamp changes.

Solar Diffuser Collects

The solar diffuser panels provide reflective references that were characterized prior to launch. Their regular use of the primary diffuser enables detector stability to be monitored and potential changes in calibration to be fed back into the ground processing system to maintain accuracy of the Earth imagery products. The second solar diffuser panel is used every six months as a check on stability of the primary (working) diffuser. Longer, 60-second collects of the working solar diffuser are used to monitor the within-scene detector response stability. Diffuser collects are also used to characterize the system noise, SNR performance, absolute radiometric accuracy, uniformity, and relative detector gains.

In an additional solar diffuser data collect, the integration time sweep, a series of collects at different detector integration times, is performed at a constant signal level. These collects allow an on-orbit assessment of the OLI detector electronics' linearity. Two extended (60-second) diffuser collects were performed during solar eclipses (November 3, 2013, and April 29, 2014) to better characterize the OLI's full detector-electronic chain linearity. Here, the uniform diffuser signal was obtained at a significantly lower radiance level than normal (about 40 percent and 10 percent), to allow evaluating and updating relative non-linearities between detectors.

Lunar Collects

Imaging the moon approximately every 28 days enables an independent measure of the OLI radiometric stability, as the moon is an extremely stable source. While the lunar surface is very stable, the viewing geometry can vary dramatically, so the lunar irradiance-based model, Robotic Lunar Observatory, is used to consider the viewing geometry. The lunar collects are also used to evaluate stray light effects and to find any other artifacts that might be visible. The moon is a good source for these artifacts because it is bright compared to the surrounding space.

Side Slither Collects

During a side slither data collect, the spacecraft is yawed 90°, so that the normally cross-track direction of the focal plane is turned along track. Here, each detector in an SCA tracks over nearly identical spots on the ground. By performing these side slither maneuvers over uniform regions of the Earth, individual detector calibration coefficients can be generated to improve the pixel-to-pixel uniformity. These maneuvers are performed over desert or snow/ice regions about every three months to monitor and potentially improve the pixel-to-pixel uniformity.

Examples of characterization activities include assessments of the following:

- Calibrating the detector response
- The detector's response to the solar diffusers and radiometric accuracy
- The 60-second radiometric stability, to evaluate the absolute radiometric uncertainty and detect changes in detector response
- The detector response to stimulation lamp, to evaluate and detect changes in gain
- Radiometric uniformity (Full FOV, banding 1, banding 2, and streaking as defined in the OLI Requirements Document), all artifacts affecting the radiometric accuracy of the data, and SCA discontinuity differences characterized by gathering statistics information in the overlap areas between the SCAs
- Deep space data and blackbody data to evaluate the absolute radiometric uncertainty of the TIRS instrument and detect changes in gains and biases to determine radiometric stability
- Dropped frames per interval, for trending the total number detected, excluding flagged dropped frames in all characterization algorithms

Examples of calibration activities include derivation of the following:

- Bias model parameters for each detector. The bias model for OLI is constructed using data from associated shutter images, video reference pixels, dark (masked) detectors, and associated telemetry (e.g., temperatures). The bias model for TIRS uses data from deep space images, dark (masked) detectors, and associated telemetry (e.g., temperatures). These bias model coefficients are used to derive the bias that needs to be subtracted from the detector during product generation.
- The relative gains for all active detectors, to correct the detector responses for "striping" artifacts.
- Gain determination to enable the conversion from DN to radiance and determine the accuracy of the radiometric product.
- The TIRS background response determination.

3.1.2 Pre-launch

OLI

Preflight instrument performance and data characterization proceeded from the subsystem level (e.g., focal plane module and electronics) to fully integrated instrument and Observatory testing and analysis. Instrument testing and performance requirements verification were performed at multiple stages of development to ensure the integrity of performance at the component, subsystem, and system levels.

For radiometric calibration of the OLI, an integrating sphere was used as the National Institute for Standards and Technology (NIST) traceable radiance source. The OLI was connected to the integrating sphere in a configuration that enabled the instrument to measure the output radiances from a prescribed set of illumination levels from xenon

and halogen lamps. In addition, integration time sweeps of full illumination at successively shorter detector exposure times were used to establish the linearity of the detectors and focal plane module electronics. Measurements of the integrating sphere at various radiance levels were also used to characterize the linearity. These and the integration time sweeps are used to determine the reciprocity between the two.

BATC, the manufacturer of the OLI, used a heliostat to facilitate the Sun as a calibration source for pre-launch testing. The heliostat captured and directed sunlight from the rooftop of the BATC facility to the solar diffuser panels of the instrument placed in a thermal vacuum chamber inside the facility.

The spectral reflectance and BRDF of the panels were characterized at the University of Arizona. A transfer spectroradiometer was used to measure the radiances from the integrating sphere and the solar diffuser panels at the same illumination levels as measured by the OLI to ensure traceability of the measurements compared to those made from the solar diffuser panels. On orbit, any changes to the spectral response of the instrument are determined by inflight measurements of the solar diffuser panels, and coefficients are used to scale the DNs of the instrument response so calibrated radiances can be adjusted.

The SNR for each of the OLI spectral bands is characterized at a prescribed radiance level, referred to as Ltypical. The SNR is defined as the mean of the measured radiances divided by their standard deviation. A curve is fit to the SNR at the measured radiance levels and is evaluated at the prescribed Ltypical. The SNR is measured at multiple stages of the instrument build, culminating the testing of the fully integrated instrument. The high SNR combined with the 12-bit quantization of the OLI radiometric response provides data that enhance our ability to measure and monitor subtle changes in the state and condition of the Earth’s surface.

The pre-launch verification of instrument and spacecraft radiometric performance specifications was carried out as part of the instrument and spacecraft manufacturers’ development, integration, and test programs. The radiometric characteristics of the OLI instrument were measured during instrument fabrication and testing at the BATC facility. Because the TIRS instrument is a NASA in-house development, pre-launch characterization and testing was carried out at the NASA GSFC. Additional measurements and tests were performed at Orbital Sciences Corporation (OSC) as the L8 spacecraft was being fabricated and integrated with the OLI and TIRS payloads.

A Horizontal Collimator Assembly (HCA) and a set of fixed geometric patterns are scanned across the focal plane to build an optical map of the detectors that enables construction of an LOS model from the focal plane to the Earth. A similar process is used with a different reticle plate to derive line spread functions. These measurements assist with characterizing the alignment of detectors within a given SCA as well as with aligning adjacent SCAs. These are fundamental parameters required for constructing the geometric models to achieve many of the geometric requirements.

TIRS

A louvered plate with stringently controlled heating was used as a flood source and placed within the TIRS FOV so that temperatures across the surface of the plate could be analyzed to characterize the uniformity of the radiometric response across the detectors within the focal plane and across the multiple SCAs. The flood source was measured at multiple temperature levels and at multiple integration time sweeps, in order to characterize the linearity of the detector responses.

A blackbody of known temperature was used as a calibration source to provide radiance to the detectors from which output voltages were converted to DNs. TIRS also measured a space-view port with a cold plate set at 170 K mounted on it, and the DNs output from the instrument were converted to radiance. The blackbody radiances were scaled by a “view factor” that was determined by viewing through the Earth-view (nadir) port.

Earth-view measurements were made at several temperature settings in order to establish a relationship among the temperature, DN levels, and radiance. These measurements were then combined with the blackbody and space-view measurements to derive a final set of coefficients for scaling DNs to radiances. Detector linearization was performed prior to the bias removal for TIRS because temperature contributions from instrument components were also being captured.

Similar to the approach taken with OLI, a wide-field collimator and a set of fixed geometric patterns were scanned across the focal plane to build an optical map of the detectors that enabled construction of an LOS model from the focal plane to the Earth. Instead of these targets being viewed under fixed illumination settings, these targets were presented and contrasted by controlled temperature settings. These measurements assisted with characterizing the alignment of detectors within a given SCA as well as with aligning adjacent SCAs. These were fundamental parameters required for constructing the geometric models to achieve many of the geometric requirements.

3.1.3 Post-launch

Radiometric characterization and calibration will be performed over the life of the mission using the software tools developed as part of the L8 Image Assessment System (IAS) and the Calibration Validation Toolkit (CVTK). The IAS provides the capability to perform radiometric characterization routinely, to verify and monitor system radiometric performance and estimate improved values for key radiometric calibration coefficients. On-orbit activities include those that occur during the OIV period characterization and calibration and post-OIV nominal operations.

Characterization activities include the following:

- Noise – characterizing the OLI response to shutter, lamp, diffuser, and lunar acquisitions, and the TIRS response to deep space views, On-Board Calibrator

(OBC) collects, and lunar acquisitions are used to assess various detector noise characteristics, including coherent, impulse, SNR, NEdL, and ghosting.
- Stability - characterizing the response of OLI to the solar diffusers, stim lamps, and lunar acquisition, and TIRS to the OBC for assessing the transfer-to-orbit response, the short-term (within-orbit) and long-term stability, diffuser and lunar acquisition reproducibility for OLI, and post-maneuver recovery reproducibility for TIRS.

Calibration activities include the following:

- Absolute Radiometric Response – characterizing the OLI solar diffuser, lunar irradiance, TIRS OBC, PICS, and underfly acquisitions with L7 in order to assess the absolute radiometric response and derive the initial on-orbit absolute gain CPF values.
- Relative Radiometric Response – characterizing the OLI diffuser, yaw, and PICS and TIRS OBC, yaw, and PICS sites for assessing the SCA-to-SCA and pixel-to-pixel relative response/uniformity. Special OLI diffuser and TIRS OBC integration time sweep collects are characterized to assess detector linearity and possible updates to the CPF linearity calibration coefficients.

Key radiometric CPF parameters that may need updates include absolute gains, relative gains, bias (default values), linearity Lookup Tables (LUTs), diffuser radiances (OLI), lamp radiances (OLI), OBC LUTs (TIRS), diffuser non-uniformity (OLI), OBC non-uniformity (TIRS), inoperable detectors, out-of-spec detectors, and detector select masks.

3.1.4 Operational Radiometric Tasks

The goals of these tasks are as follows:

- To demonstrate that the L8 mission meets or exceeds all radiometric requirements, particularly those that were deferred for formal verification on-orbit
- To perform an initial on-orbit radiometric calibration (relative and absolute) that makes it possible to achieve the previous goal and prepares the mission for routine operations
- To initialize and continue the process through nominal operations of evaluating OLI Key Performance Requirements (KPRs) by establishing an initial on-orbit performance baseline
- To trend radiometric characterization parameters throughout the mission

3.1.4.1 OLI Characterization Tasks

Several OLI characterizations and requirements verifications relate strictly to whether the instrument performance meets specifications, and therefore are not strongly tied to the coefficients stored in the CPF that require on-orbit updates. These requirements include stability (60-second, 16-day), noise (overall, impulse, coherent, 1/f), stray light, ghosting, bright target recovery, detector operability, and detectors out-of-specification.

Three lunar calibration acquisitions were made during the commissioning period; each acquisition comprises 15 individual image scans, performed over two consecutive orbits. Each OLI and TIRS SCA is scanned across the Moon, with one scan repeated in both orbits to provide a check on continuity of the observations. Lunar acquisitions are performed when the Earth-Sun-Moon configuration provides lunar phase angles in the -9 to -5 degree or the +5 to +9 degree ranges. The Moon traverses each phase angle range once per month, with the positive and negative angle ranges occurring approximately one day apart. In routine operations, one phase angle range is selected for all lunar acquisitions; during commissioning, both cases were collected. The timing of the commissioning period led to three pairs of nominal lunar acquisition opportunities: one in late March 2013 just before the under-fly of L7, one in late April 2013 after achieving the operational orbit, and one in late May 2013.

3.1.4.2 OLI Calibration Tasks

The OLI instrument was radiometrically calibrated before launch. The OLI viewed an integrating sphere monitored by a spectrometer that had been calibrated relative to a source that is traceable to a reference in the NIST Facility for Spectroradiometric Calibrations (FASCAL) facility. The gains (DN/radiance) from this calibration were stored in the CPF. The OLI's response to the diffuser panels was measured using the Sun as the source through a heliostat. Using the OLI gains, the radiance of the diffuser was measured and was corrected for the heliostat and the atmospheric transmittance to obtain a "predicted" TOA radiance for the diffuser. Additionally, the OLI diffuser's directional reflectance factors for the on-orbit illumination and view geometries were measured in the laboratory before launch, giving the diffuser a reflectance calibration. These data were used to derive "pre-launch" TOA radiance calibration coefficients. The first on-orbit measurements of the solar diffuser panel were compared to the "predicted" and "pre-launch" values to perform the transfer to orbit analysis.

A fundamental requirement of the Landsat Project is to provide a record of consistently calibrated image data. Therefore, OLI data need to be consistent with data from the previous Landsat sensors. Although the instruments are calibrated consistently before launch and monitored before launch through on-orbit commissioning, there is still a need to check the calibration relative to previous Landsat instruments and update the calibration parameters as necessary.

Procedures were developed to characterize any shift in calibration that may occur through launch and into orbit. Two methods of validating the absolute radiometric calibration include cross-calibration with L7 ETM+ via simultaneous observations and use of the PICS.

Although one of the goals of the Ground System is to generate OLI images as free of striping and banding as is practicable, it cannot be expected that OLI images over uniform areas will be completely free of banding or striping, especially when extreme contrast stretches are applied. There are a number of contributors to banding and striping: inadequately characterized differential non-linear responses among detectors;

inadequately characterized relative gain and bias parameters; instability in gain, bias, or non-linearity; and spectral differences across or between SCAs.

3.1.4.3 TIRS Characterization Tasks

A number of TIRS characterizations and requirements verifications relate strictly to whether the instrument meets performance specifications, and therefore are not strongly tied to the coefficients stored in the CPF that require on-orbit updates. These requirements include stability (60 second, 16-day), noise (overall, impulse, coherent, 1/f), stray light, ghosting, bright target recovery, detector operability, and detectors out-of-specification.

Three lunar acquisitions were performed during the commissioning period. Each acquisition comprises 15 individual image scans, performed over two consecutive orbits. Each TIRS SCA is scanned across the Moon, with one scan repeated in both orbits to provide a check on continuity of the observations. As with OLI, the TIRS lunar acquisitions are performed when the Earth-Sun-Moon configuration provides lunar phase angles in the -9 to -5 degree or the +5 to +9 degree ranges. During the operational mission lifetime, lunar acquisitions will be performed monthly as defined for the OLI.

3.1.4.4 TIRS Calibration Tasks

TIRS data need to be consistent with data from the previous sensors, so by extension, L8 TIRS data need to be cross-calibrated with L7 ETM+ data. At least two techniques will be used for this comparison and calibration (i.e., simultaneous data acquisitions collected during the under-fly of L7 and non-simultaneous observation of well-characterized targets). TIRS was carefully characterized and calibrated before launch, and procedures were developed to be able to characterize any shift in calibration that may occur during launch and insertion into orbit.

3.1.4.5 TIRS Relative Response - Uniformity Evaluation

As with the OLI, a number of factors may contribute to banding and striping in TIRS imagery: inadequately characterized differential non-linearity among detectors; inadequately characterized relative gain and bias; instability in gain, bias, or non-linearity; and spectral differences across or between SCAs.

3.2 Geometric Calibration Overview

This subsection describes the geometric characterization and calibration activities performed over the life of the L8 mission, using the software tools developed as part of the L8 IAS. The IAS provides the capability to perform four types of geometric characterization routinely to verify and monitor system geometric performance, and four types of geometric calibration to estimate improved values for key system geometric parameters. These are the parameters contained in the CPF for use in the Level 1 product generation. The measurement and evaluation activities are referred to as characterization operations, while the parameter estimation activities are referred to as calibration.

The geometric characterizations include the following:

1. Assessment of the absolute and relative geodetic accuracy of Level 1 data (Geodetic Characterization)
2. Assessment of the geometric accuracy of Level 1 products (Geometric Characterization)
3. Assessment of the accuracy of multitemporal OLI image-to-image registration (Image-to-Image Registration Characterization)
4. Assessment the accuracy of OLI and TIRS band-to-band registration (Band-to-Band Registration Characterization)

A fifth characterization algorithm will be used to evaluate OLI spatial performance on-orbit. This Modulation Transfer Function (MTF) bridge characterization algorithm uses images of selected ground targets (e.g., the Lake Pontchartrain Causeway) to estimate the OLI sensor edge response. The characterizations performed during the commissioning period were used to establish an OLI performance baseline to serve as a basis for comparison in evaluating the OLI KPRs throughout the life of the mission. The characterizations of primary interest as KPRs are OLI band registration accuracy and spatial performance.

The geometric calibrations include the following:

1. Determination of the alignment between the spacecraft navigation reference frame and the OLI payload LOS (Sensor Alignment Calibration)
2. Determination of corrections to the pre-launch OLI Pan band lines of sight, including relative alignment of the OLI sensor chip assemblies (OLI Focal Plane Calibration)
3. Determination of the alignment between the TIRS and OLI sensors, including the relative alignment of the TIRS sensor chip assemblies (TIRS Alignment Calibration)
4. Determination of corrections to the band location field angles for both OLI and TIRS (Band Alignment Calibration)

The most critical geometric calibration activities are: to measure and verify the L8 spacecraft, OLI, and TIRS system performance using the geodetic, geometric, band-to-band, image-to-image, and spatial characterization capabilities; to monitor the OLI sensor-to-spacecraft attitude control system alignment calibration; and to monitor the TIRS-to-OLI alignment calibration. This includes verifying and, if necessary, updating the OLI and TIRS focal plane (SCA-to-SCA) and band alignment calibrations. Monitoring and refining the OLI-to-spacecraft and TIRS-to-OLI alignment knowledge is critical to ensure that the Level 1 product accuracy specifications can be met. These calibration parameters were not expected to change greatly through launch, but they may require minor refinement on-orbit. The results of these calibration activities are used to verify that the system is performing within specifications and to create the CPFs used by the IAS and the LPGS to create Level 1 products that meet the L8 accuracy requirements. The calibration activities will continue throughout the life of the mission to

monitor the stability of the system's geometric and spatial performance and to identify and characterize any systematic variations in the system's geometric parameters as a function of time, temperature, and location. A longer sequence of calibration observations over a range of conditions will be needed to isolate, model, and characterize these higher-order behaviors. Table 3-2 summarizes these activities, along with the pre-launch activities.

	Purpose	How This is Used to Develop Calibration Parameters
OLI Preflight Activity		
Initial LOS directions for detectors using design locations	Establish nominal focal plane locations for individual detectors, bands, and SCAs	Gives nominal detector focal plane locations that can then be adjusted
Edge and line target analysis through thermal vacuum testing	Provide pre-launch adjustment to initial LOS of individual detectors	Allows refinement to initial LOS design model for detectors
TIRS Preflight Activity		
Initial LOS directions for detectors using design locations	Establish nominal focal plane locations for individual detectors, bands, and SCAs	Gives nominal detector focal plane locations that can then be adjusted
Edge and line target analysis through thermal vacuum testing	Provide pre-launch adjustment to initial LOS of individual detectors	Allows refinement to initial LOS design model for detectors
OLI On-Orbit Activities		
OLI Geodetic Accuracy Assessment	Ensure Level 1 Systematic imagery meets horizontal accuracy requirements and measures product accuracy prior to application of ground control	Folds into the OLI instrument to Attitude Control System alignment parameters
OLI to Attitude Control System Alignment	Improves in-flight knowledge of OLI to the Attitude Control System	OLI instrument to Attitude Control System alignment parameters
Geometric Accuracy Assessment	Evaluates the accuracy of the Level 1 Terrain-Precision corrected imagery and measures product accuracy after application of ground control	
Image-to-Image Registration Assessment	Ensures ability to co-register L1T imagery and measures OLI-to-OLI and OLI-to-reference ability	
OLI Focal Plane Calibration	Ensures accuracy between and within SCA geometry of the OLI Pan imagery and corrects for SCA-to-SCA misalignment	Allows for adjustment to OLI LOS parameters
Band-to-Band Registration Assessment	Measures the ability to align OLI and TIRS bands within a L1T image	Folds into the updating of the LOS parameters

	Purpose	How This is Used to Develop Calibration Parameters
Band Alignment Calibration	Adjusts OLI LOS parameters based on band-to-band registration assessment	Allows for adjustment of the OLI LOS parameters
OLI Spatial Characterization	Characterizes OLI system transfer function on orbit	
TIRS On-Orbit Activities		
TIRS Internal Geometric Characterization	Measures the ability to align the two TIRS bands within a L1T	Folds into updating of the TIRS LOS parameters
TIRS Internal Geometric Calibration	Adjusts TIRS LOS parameters based on TIRS internal geometric characterization	Allows for adjustment of the TIRS LOS parameters
TIRS Alignment Calibration	Measures the ability to align 3 SCAs of TIRS to the OLI instrument	Allows for adjustment of TIRS to OLI alignment parameters

Table 3-2. Summary of Geometric Characterization and Calibration Activities

3.2.1 Collection Types

Lunar Collects

Due to differences in the viewing geometry between lunar collects and nominal Earth collects, lunar collects are used only for measuring the alignment of the cirrus band with the other OLI bands.

Earth Collects

Geometric characterization and calibration are performed on nominal nadir-viewing Earth collects. The major difference associated with these collects and the type of characterization or calibration that is performed depends on the reference imagery for which it is characterized, and in some cases, eventually calibrated against. Three types of reference imagery are used for geometric characterization and calibration, including the Global Land Survey (GLS), Digital Orthophoto Quadrangle (DOQ) mosaics, and Satellite Pour l'Observation de la Terre (SPOT) mosaics.

3.2.2 Pre-launch

OLI Pre-launch

An initial OLI geometric model that defined the LOS for the detectors on the focal plane was calculated using the nominal design locations of the detectors and telescope optical system. This initial or nominal design was then updated using edge and line targets that were projected on to the focal plane through the optical system during prelaunch thermal vacuum testing. This model was then considered an as-built pre-launch set of LOSs for each detector for which each band for each SCA could be adjusted post-launch using the IAS geometric characterization and calibration processes.

TIRS Pre-launch

An initial TIRS geometric model, consisting of a detector and sensor chip assembly within the focal plane along with the optics of the telescope, was determined based on its assembly through instrument and component design and final integration to the

spacecraft. This included the focal plane and detector placement, the telescope and optical components, and the TIRS-to-spacecraft alignment measurements. These components were then updated during pre-launch using measurements taken during thermal vacuum testing. Targets were projected into the TIRS FOV at operator-selectable locations, allowing for careful identification of both the target within the focal plane and the origination of the target itself. This model was then considered an as-built pre-launch set of LOSs for each detector for which each band for each SCA could be adjusted post-launch using the IAS geometric characterization and calibration processes.

3.2.3 OLI Geodetic Accuracy Assessment

The purpose of the geodetic accuracy assessment is to ensure that the L8 Level 0R data can be successfully processed into Level 1 systematic products that meet the system requirement of 65 m at a circular error with 90 percent confidence (Circular Error 90 (CE90)) horizontal accuracy.

Predefined Ground Control Points (GCPs) (consisting of image chips with known geodetic positions) are automatically correlated with data from the OLI SWIR1 (for Global Land Survey 2000-based (GLS2000) control) or Pan bands (for DOQ control) to measure the discrepancy between the known ground location and the position predicted by the OLI geometric model.

The results of the control point mensuration are used for analysis by the IAS geodetic characterization software. The precision-correction software also combines the estimated attitude error from the precision solution with the current best estimate of OLI-to-spacecraft alignment from the CPF, to compute the adjusted alignment that would make the resulting attitude error zero. This apparent alignment is stored in the geometric trending database for subsequent use by the sensor alignment calibration procedures.

The geodetic accuracy characterization software processes the control point residuals (deleting those identified as outliers) to generate summary statistics and a geodetic accuracy analysis report each time the precision correction solution process is successfully completed. The geodetic accuracy results are stored in the geometric characterization trending database, with a flag to indicate the control type used (GLS or DOQ).

3.2.4 Sensor Alignment Calibration

The goal of the sensor alignment calibration is to improve the in-flight knowledge of the relationship between the OLI instrument and the spacecraft attitude control system reference frame. Sensor alignment calibration uses the results of the GCP processing conducted both as part of routine Level 1 product generation (using GLS2000 control) and as part of calibration/validation analysis activities over geometric calibration sites (using DOQ control). The end-to-end OLI geolocation accuracy error budget assumes that the IAS is able to estimate this alignment to an accuracy of 33 microradians (3-sigma) over periods as short as one 16-day WRS-2 cycle.

The potential need for sensor alignment calibration updates will be identified by monitoring the geodetic accuracy characterization results. If persistent geolocation accuracy biases are observed, then that would suggest the need for generating an updated sensor alignment matrix for inclusion in the CPF. Automated software tools are used to detect the existence of a new alignment calibration solution and to perform automated testing of the new and old calibration solutions against a set of test scenes extracted from the list of retrieved alignment calibration scenes. A new alignment matrix will be generated whenever a new version of the CPF is scheduled for release, nominally on a quarterly basis; therefore, any slowly varying seasonal alignment variations will be accounted for.

3.2.5 Geometric Accuracy Assessment

The purpose of the geometric accuracy assessment is to evaluate the accuracy of L1T image products using an independent set of GCPs. Although the geodetic accuracy characterization results report both the pre- and post-GCP correction scene accuracy statistics, the post-fit statistics are not an unbiased estimate of the actual accuracy of the corrected scene. An independent geometric accuracy assessment is performed by correlating the final Level 1 product with a separate set of GCPs that were withheld from the original precision correction solution. Scenes for which the number of available GCPs was too small to permit withholding some from the precision correction process do not have validation points. The geometric accuracy assessment procedure runs as a part of the standard Level 1 product generation flow.

3.2.6 OLI Internal Geometric Characterization and Calibration

OLI internal geometric accuracy refers to internal geometric distortions within the OLI images due to errors in the relative alignment of the 14 SCAs, also known as Focal Plane Modules (FPMs), on the OLI focal plane. If the OLI LOS model knowledge of the pointing for each SCA is slightly inaccurate, this will result in internal geometric distortions in the L1T products and, potentially, visible image discontinuities at SCA boundaries. Although the OLI LOS model is carefully characterized pre-launch, tools are available to detect and, if necessary, correct any SCA-to-SCA misalignment that may be observed by updating the OLI LOS model calibration. These tools are implemented in the IAS as the image-to-image registration accuracy characterization and the OLI focal plane calibration algorithms.

The OLI Pan band is used as the geometric reference for the entire instrument.

The image-to-image registration accuracy and the pattern of registration errors may indicate the presence of unwanted internal distortions in the OLI image that could be addressed by refining the OLI focal plane calibration. The following subsections describe the details of the image-to-image registration assessment and OLI focal plane calibration procedures individually.

3.2.6.1 Image-to-Image Registration Assessment

The goal of the image-to-image registration assessment is to verify the L8 requirement that multitemporal images of the same WRS scene can be successfully co-registered to an accuracy of 0.4 (LE90) multispectral pixels (i.e., 12 m). The image-to-image assessment procedure uses GCPs that have been extracted from a previously generated Level 1 image, or that match the points used to correct the pre-existing Level 1 product, in order to perform precision and terrain correction of a new acquisition to Level 1. It then performs a point-by-point comparison of the two images using automated image correlation.

Image-to-image registration assessment using the Pan band demonstrates the accuracy of the overall precision correction solution as well as the internal geometric fidelity of the images.

3.2.6.2 OLI Focal Plane Calibration

The OLI focal plane calibration is intended to detect and measure systematic deviations of the OLI LOS for each SCA from the model measured during pre-launch characterization. Any significant deviations detected will be folded back into the CPF as updates to the LOS model Legendre polynomial coefficients.

3.2.6.3 Band-to-Band Registration Assessment

The band-to-band registration assessment measures the relative alignment of the nine OLI and two TIRS spectral bands after processing to Level 1 to verify that the 4.5-meter (LE90) OLI, 18-meter (LE90) TIRS, and 30-meter (LE90) OLI-to-TIRS band-to-band registration requirements are met.

3.2.6.4 Band Alignment Calibration

The purpose of band placement calibration is to estimate improved values for the locations of the spectral bands on the OLI and TIRS focal planes for inclusion in the CPF. The band locations are embodied in the LOS model Legendre coefficients for each OLI and TIRS band/SCA. OLI and TIRS band alignment would use essentially the same algorithm but would process separately.

The Pan band is used as the reference for the OLI solution, because it is the band used to perform the sensor alignment and focal plane calibrations. TIRS Band 10 is used as the reference for TIRS band alignment since it is also used in TIRS alignment calibration. The OLI cirrus band is only used for lunar and high-altitude terrestrial targets.

3.2.7 TIRS Internal Geometric Characterization and Calibration

The TIRS geometric alignment calibration procedure accomplishes both internal and external geometric alignment calibration for the TIRS instrument. TIRS internal geometric accuracy can be degraded by internal geometric distortions within the TIRS images due to errors in the relative alignment of the three SCAs on the TIRS focal plane. If the TIRS LOS model knowledge of the pointing for each SCA is slightly

inaccurate, this will result in internal geometric distortions in the Level 1 product images and, potentially, visible image discontinuities at SCA boundaries.

TIRS external geometric accuracy refers to the accuracy with which TIRS data can be registered to corresponding OLI data and to an absolute ground coordinate system. This accuracy is dependent primarily on accurate knowledge of the alignment between the OLI and TIRS instruments.

The alignments of both the OLI and TIRS instruments relative to the spacecraft Attitude Control System (ACS) frame were measured during Observatory integration, but due to the accuracy limitations of these measurements and the likelihood of launch shift and zero-G release altering these alignments, on-orbit TIRS alignment estimation was updated to achieve the TIRS geometric accuracy requirements. Although the TIRS LOS model was also carefully characterized pre-launch, TIRS alignment calibration provides the tools needed to detect and, if necessary, correct any SCA-to-SCA misalignment that may be observed while updating the TIRS LOS model calibration.

The TIRS 10.8-micron band (Band 10) is used as the geometric reference for aligning the TIRS instrument to the OLI. Band 10 is also used as the reference band in TIRS band alignment calibration. As the TIRS geometric reference, internal SCA-to-SCA focal plane alignment is also performed using Band 10.

The following subsection describes the details of the TIRS alignment calibration procedure.

3.2.7.1 TIRS Alignment Calibration

The TIRS alignment calibration measures systematic deviations of the TIRS lines-of-sight for each SCA from the model measured during pre-launch characterization while simultaneously measuring the global misalignment of all three TIRS SCAs relative to the OLI. These measurements are used to compute updates to the TIRS-to-OLI and, indirectly, TIRS-to-ACS alignment matrices as well as updates to the TIRS LOS model Legendre polynomial coefficients, with the results being folded back into the CPF.

A control reference image of coincident OLI SWIR bands with good emissive-to-reflective band correlation is used for calibration. The TIRS alignment calibration procedure compares a precision- and terrain-corrected TIRS Band 10 SCA-separated image with a coincident OLI SWIR1 band SCA-combined reference image processed with the same spacecraft geometric model and scene-framing parameters. This enables measurement of the overall TIRS-to-OLI alignment, as well as the relative alignment of the individual TIRS SCAs.

3.2.8 OLI Spatial Performance Characterization

OLI spatial performance, expressed as the slope and width of the instrument’s response to a unit edge/step function, was carefully characterized during pre-launch testing. The experience of the L7 ETM+, which suffered from gradually degrading spatial fidelity over the first several years of on-orbit operations, led to the development of an algorithm to

measure and track on-orbit spatial performance. This was done by using long bridge targets to characterize the ETM+ MTF, which is the frequency domain representation of the instrument's spatial response. This algorithm was subsequently adapted for use with push-broom sensors using ALI data, and a variant of this adapted algorithm will be used for OLI spatial characterization. A method for using lunar scans to characterize ALI spatial performance was also developed, but the results were not sufficiently reliable for use in operational performance characterization.

No calibration activities are associated with spatial performance, although the OLI does have ground-commandable focus mechanisms, and TIRS focus can be adjusted by changing telescope temperatures. To support on-orbit focus verification, additional focus test sites have been identified to provide qualitative information about the state of OLI and TIRS focus during the commissioning period. These sites, listed in Appendix A, were selected to contain distinct targets that could be used for visual assessment as well as additional sites for quantitative analysis using the enhanced version of the spatial performance characterization algorithm. Combined with the quantitative results of the spatial performance characterization algorithm, visual inspection of the focus sites adds confidence that the OLI and TIRS are in proper focus. The derivation of any adjustments to the focus mechanism positions or TIRS telescope temperatures that may be required to improve on-orbit spatial performance would require additional analysis that is beyond the scope of this algorithm.

Spatial edge slope performance in all OLI bands (other than the cirrus band) is a KPR for OLI on-orbit performance. The derived spatial performance parameters can then be compared to the thresholds specified in the corresponding KPR to evaluate on-orbit performance. The precision of the on-orbit spatial performance estimates is such that repeated measurements are required to establish the validity of any suspicion that the standard performance level of a requirement is not being met.

3.2.9 OLI Bridge Target MTF Estimation

The purpose of the OLI bridge target MTF estimation procedure is to use OLI acquisitions of prescribed bridge targets to derive on-orbit estimates of the OLI System Transfer Function (STF) for each OLI spectral band other than the cirrus band. The STF estimates are then used to compute the corresponding point spread function and edge response slope performance for each spectral band. The OLI bridge target MTF estimation procedure applies a model of the OLI spatial response (in the form of the system transfer function) to pre-defined models of two bridges, shown in Figure 3-1, in the Lake Pontchartrain, Louisiana area, to simulate the OLI's response to each bridge in the direction transverse to the bridge. Comparing these models to oversampled bridge profiles constructed from actual OLI image data by interleaving samples from different points along the bridge allows for adjusted OLI STF parameters to be estimated.

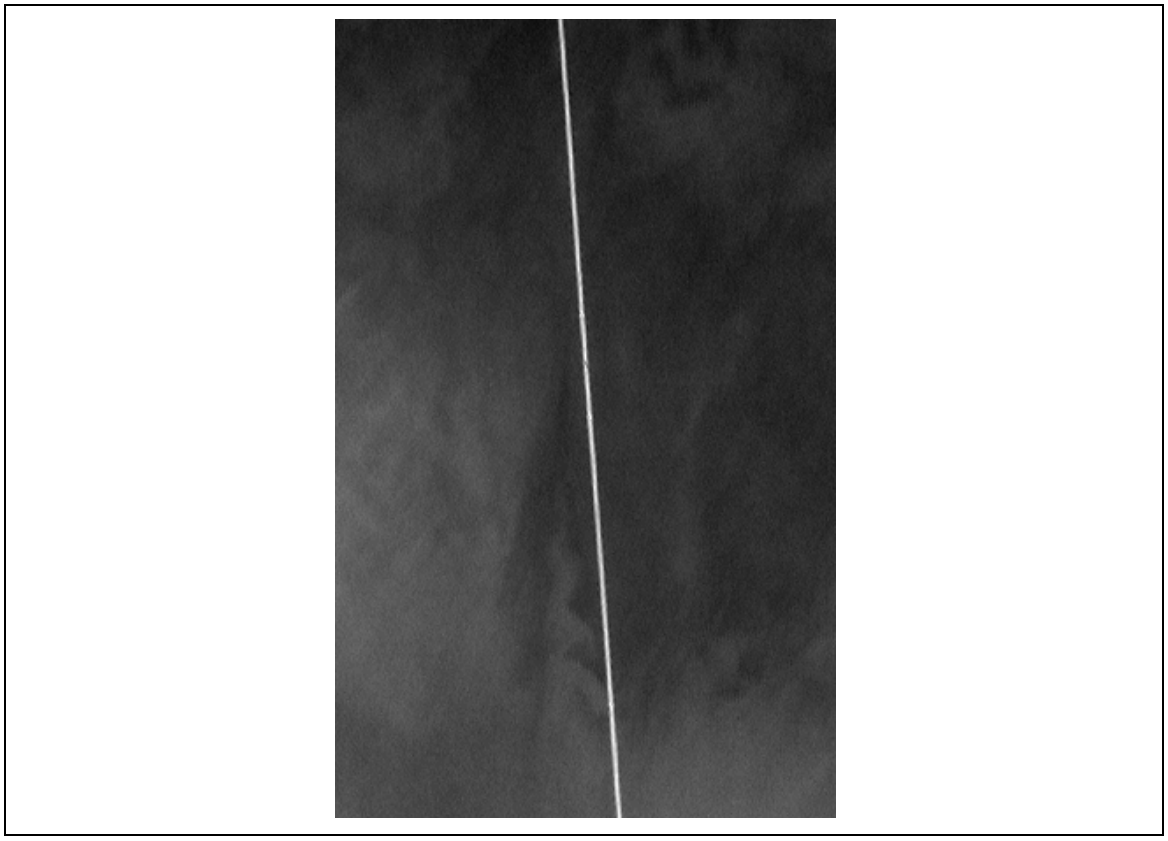

Figure 3-1. Simulated OLI Image of the Lake Pontchartrain Causeway

3.2.10 Geometric Calibration Data Requirements

The geometric characterization and calibration operations require three primary types of supporting information: GCPs, reference images, and digital terrain data. The following subsections describe the required characteristics, potential sources, and preprocessing requirements for each of these support data types.

3.2.10.1 Ground Control Points (GCPs)

The IAS uses GCPs for all geometric characterization and calibration activities. In all cases, the GCPs are used to perform a precision correction solution that will ensure accurate registration of the image data to a cartographic projection and use digital elevation data to correct for relief displacement in the process. The IAS and LPGS both access a database of GCPs. These points, adopted from the L7 mission, include both the global GCP set extracted from the GLS data and the higher precision control points extracted from geometric calibration reference data (e.g., DOQ mosaics, SPOT data). GCPs from either or both control sets can be extracted by control type: GLS or DOQ (DOQ is used as a generic type indicator for all GCPs extracted from geometric calibration sources).

The GLS control database covers essentially every land scene observed from the WRS-2 orbit. The control derived from the GLS is accurate to approximately 20 m Root Mean Square Error (RMSE) absolute, but since the goal is to make L8 products that are

consistent with the other products generated from the archive of historical data, GLS GCPs include image chips extracted from the ETM+ Band 5 at 30-meter Ground Sampling Distance (GSD). These have been automatically subdivided into separate CONTROL and VALIDATION subsets in scenes where a sufficient number of points were available.

The DOQ control database only covers scenes designated as geometric calibration sites. There are two main clusters of these sites. The first set is in the United States and was selected to provide at least one acquisition opportunity on every WRS-2 cycle day, including a group in the southwestern U.S. that is at approximately the same latitude to provide consistent acquisition conditions (position in orbit, ETM+ time-on). These contain control extracted from reduced-resolution DOQ data (panchromatic, 15-meter GSD). A second group of control scenes is in the eastern half of Australia. This control set is based on mosaics of SPOT panchromatic data provided by GeoScience Australia's National Earth Observation Group (NEOG). Being in the southern hemisphere, this set provides somewhat different orbital geometry and thermal conditions than the U.S. set. One of the primary purposes of the DOQ control set is to ensure accurate registration between L8 L1T products and the DOQ- and SPOT-derived reference imagery used for focal plane calibration.

The GLS control points were extracted from the GLS 2000 ETM+ images using an automated interest operator technique that selected points based on a local spatial operator that identified "interesting" points, and a spatial distribution test that decided which points provided the best distribution of control across the scene. A subsequent test was added to weed out points that contained only water. The GLS control has been in routine operational use for generating Landsat 5 and L7 standard L1T data products. An important note is that the GLS images themselves were generated based on a global block triangulation of L7 scenes with a sparse set of ground control provide by the National Geospatial Intelligence Agency (NGA). The scenes that contain NGA control are more accurate than those that were positioned solely through triangulation. The NGA-controlled scene subset will therefore be given special attention when mining the geodetic accuracy and sensor alignment data for systematic within-orbit effects.

The DOQ control points were extracted from the DOQ mosaic reference images (U.S. set) and the SPOT mosaic reference image (Australia). Therefore, they inherit the accuracy of those products. Because the primary purpose of these points is to ensure good OLI-to-reference image registration, the absolute accuracy of these points, though believed to be better than the GLS control, is of less interest. Appendix A includes the list of geodetic characterization sites where DOQ control points are available.

3.2.10.2 Reference Images

Two types of reference images are used by the geometric super-site calibration operations described above. The first type includes previously generated L8 Level 1 products used in the image-to-image registration assessment process. These reference images were generated by processing L0R data through the IAS Level 1 processing software after launch and are not discussed further here. The second type of reference

images were constructed pre-launch using a high-resolution image source. These images are used to provide the reference for OLI focal plane calibration as described above. These reference images are the subject of the remainder of this section.

The key characteristics of the focal plane calibration reference images are as follows:

1. High absolute geodetic accuracy (including removal of any terrain displacement effects)
2. Internal geometric integrity (no systematic internal distortions that could be confounded with OLI focal plane alignment effects)
3. Spectral similarity to the OLI Pan band
4. Resolution as good as or better than the OLI Pan band
5. Availability in areas of minimal seasonal change and low average cloud cover

Geodetic accuracy of one-half of a panchromatic pixel (7.5 m) should be sufficient, although higher accuracy is desirable. The internal geometric accuracy requirement disqualifies ETM+ data as a source of reference imagery, although in an emergency, ETM+ reference data (e.g., GLS) would be better than no data.

High-resolution panchromatic imagery from aerial photographs that meet the geodetic accuracy requirement have been available for years. Panchromatic satellite imagery is available from SPOT and a number of high resolution commercial missions, but the cost associated with acquiring the volume of data required to cover a Landsat scene has limited the application of these sources to a set of sites in Australia where GeoScience Australia's NEOG have provided full WRS-2 scene SPOT data coverage.

The preferred source of high-resolution reference imagery based on availability and cost are the DOQ produced under contract to the USGS. The DOQs are created by digitizing and orthorectifying panchromatic aerial photography. The DOQ products are distributed as 3.75 arc-minute quarter quads at 1-meter resolution. The DOQ geodetic accuracy is specified to meet National Map Accuracy Standards (NMAS) for 1:24,000-scale maps. This standard calls for a Circular Error (CE) of 40 feet at the 90 percent confidence level, which converts to approximately 6 m CE one sigma and meets the one-half OLI pixel requirement. DOQ data coverage has improved since the launch of L7, to the point where it is now possible to generate a DOQ reference image nearly everywhere in the conterminous U.S. Though still time-consuming to construct, this has made it possible to assemble sufficient DOQ reference sites to provide at least one acquisition opportunity on every WRS-2 cycle day.

SPOT data, though not quite as accurate as the DOQ data, are available globally. The primary drawback of using SPOT data is the cost. Fortunately, our colleagues at GeoScience Australia were good enough to provide several Landsat scene-sized mosaics of SPOT data in Australia for use in Landsat 5 and 7 bumper-mode calibrations. These reference images will continue to be used for OLI focal plane calibration, though they can be expected to become less useful over time as the imagery becomes outdated.

3.2.10.3 Terrain Data

Digital terrain data are needed to provide the elevation information used by the IAS (and LPGS) Level 1 terrain-correction process. Terrain-corrected images are used in all of the geometric calibration operations described in the previous subsections. The elevation information must completely cover the geometric calibration sites to support the terrain-correction process. The height values must be referenced to the World Geodetic System 1984 (WGS84) ellipsoid rather than mean sea level to be consistent with the ground control height values. Vertical accuracy better than 15 m (one sigma) is desirable. This keeps terrain-induced errors below 0.1 panchromatic pixels at the edges of the OLI FOV. An accuracy of 30 m (one sigma) is acceptable. For product generation purposes, it is also desirable that the elevation data used be consistent with the GLS 2000 reference dataset. The Digital Elevation Model (DEM) data used to generate the GLS datasets meet these requirements.

Assembling a global elevation dataset suitable for generating a global Landsat image base was a primary objective of the GeoCover (which evolved into the Global Land Survey) project. This resulted in a global DEM constructed from the best available source data, including the USGS Natural Elevation Data (NED) DEM data, the Canadian Digital Elevation Dataset (CDED), the NASA/NGA Shuttle Radar Topography Mission (SRTM) data, and NGA Digital Terrain Elevation Data (DTED) products. The GLS DEM provides a globally (mostly) consistent elevation dataset that corresponds to the GLS imagery that defines the L8 geometric reference. Tools were developed to retrieve any specified land area from the global DEM, so the elevation datasets required to process any given scene (nadir-viewing or off-nadir) are extracted and assembled on demand from the GLS archive. The digital terrain data for the desired output product area are extracted from the GLS DEM archive, as noted above, and then preprocessed into the output space used for the calibration test scene. This DEM resampling step is part of the normal Level 1 processing sequence.

3.3 Calibration Parameters

The Calibration and Validation Team (CVT) is responsible for the sustained radiometric and geometric calibration of the L8 satellite and the TIRS and OLI sensors. To achieve this, the team assesses new imagery on a daily basis, performs both radiometric and geometric calibration when needed, and develops new processing parameters for creating Level 1 products. Processing parameters are stored in the CPF, the Response Linearity Look-Up Table (RLUT), and the Bias Parameter File (BPF), which are stamped with effectivity dates and bundled with L0R products.

3.3.1 Calibration Parameter File

The CVT updates the CPF at least every three months. Updates were more frequent during early orbit checkout and will occur between the regular three-month cycles whenever necessary. Irregular updates will not affect the regular schedule. The timed release of a new CPF must be maintained because of the Universal Time Code (UTC) Corrected (UT1) time corrections and pole wander predictions included in the file. These parameters span 180 days and include approximately 45 days before and 45 days after

the effective start date of each CPF. The IAS maintains an archive of CPFs, which can be accessed at https://www.usgs.gov/land-resources/nli/landsat/calibration-validation.

The CPF is time-stamped with an effective date range. The parameters in the file—Effective_Date_Begin and Effective_Date_End—designate the range of valid acquisition dates and are in YYYY-MM-DDThh:mm:ss format (ISO 8601). The parameter file used in processing an image requires an effective date range that includes the acquisition date of the ordered image.

Through the course of the mission, a serial collection of CPFs is generated and made available for download. CPFs are replaced when improved calibration parameters for a given period are developed. The need for unique file sequence numbers becomes necessary as file contents change. Version numbers for all effective date ranges after the launch begin with 01.

The following is an example of the file-naming procedure:

L8CPFyyyy[1]mm[1]dd[1]_yyyy[2]mm[2] dd[2]_cc.nn	
L	Constant for Landsat
C	Sensor (C = combined for OLI and TIRS)
08	Satellite numerical representation
CPF	Three-letter CPF designator
_	CPF designator / starting date separator
yyyy[1]	Four-digit effective starting year
mm[1]	Two-digit effective starting month
dd[1]	Two-digit effective starting day
_	Effective starting/ending date separator
yyyy[2]	Four-digit effective ending year
mm[2]	Two-digit effective ending month
dd[2]	Two-digit effective ending day
_	Ending date / collection number separator
Cc	Collection number (starts with 01)
.	Collection number / version number separator
nn	Version number for this file (starts with 00)

Table 3-3. Calibration Parameter File Naming Convention

For example, if the IAS created four CPFs at three-month intervals, and updated the first file twice and the second and third files once in 2012, the assigned file names would be as follows:

File 1
LC08CPF_20120101_20120331_01.01
LC08CPF_20120101_20120331_01.02
LC08CPF_20120101_20120331_01.03
File 2
LC08CPF_20120401_20120630_01.01
LC08CPF_20120401_20120630_01.02

File 3
LC08CPF_20120701_20120930_01.01
LC08CPF_20120701_20120930_01.02
File 4
LC08CPF_20121001_20121231_01.01

This example assumes that the effective date ranges do not change. The effective date range for a file can change if a specific problem (e.g., detector outage) is discovered within the nominal effective range. Assuming this scenario, two CPFs with new names and effective date ranges are created for the period under consideration. The Effective_Date_End for a new pre-problem CPF would change to the day before the problem occurred, while the Effective_Date_Begin remains unchanged.

A post-problem CPF with a new file name would be created with the Effective_Date_Begin corresponding to the imaging date when the problem occurred and the Effective_Date_End corresponding to the original Effective_Date_End for the period under consideration. New versions of all other CPFs affected by the updated parameters also would be created.

For example, assume a detector stopped responding on July 25, 2012. Two new CPFs need to be created that supersede the period represented by file number three, version two, and a new version of file number four. The new file names and version numbers become the following:

File 3
LC08CPF_20120701_20120930_01.01
LC08CPF_20120701_20120930_01.02
LC08CPF_20120701_20120724_01.03
LC08CPF_20120725_20120930_01.03
File 4
LC08CPF_20121001_20121231_01.01

3.3.1.1 LC08CPF_20121001_20121231_01.01 File Structure

All calibration parameters are stored as American Standard Code for Information Interchange (ASCII) text using the Object Definition Language (ODL) syntax developed by the NASA Jet Propulsion Laboratory (JPL). ODL is a tagged keyword language developed to provide a human-readable data structure to encode data for simplified interchange. The body of the file is composed of the following statement types:

1. Attribute assignment statement used to assign values to parameters.
2. Group statements used to aid in file organization and enhance parsing granularity of parameter sets.

To illustrate, consider the first nine parameters in the file. These nine parameters form their own group, which is called FILE_ATTRIBUTES. The syntax employed for this collection of parameters in the CPF appears as follows:

```
GROUP = FILE_ATTRIBUTES
  Spacecraft_Name = "Landsat_8"
  Sensor_Name = "Operational Land Imager"
  Effective_Date_Begin = "2013-01-01T00:00:00"
  Effective_Date_End = "2013-03-31T23:59:59"
  Baseline_Date = "2013-02-13T00:01:00"
  File_Name = "LC08CPF_20130101_20130331_01.05"
  File_Source = "LC08CPF_20130101_20130331_01.00"
  Description = "Updates to the TIRS Focal Plane, Attitude
parameters, TIRS detector offsets, and UT1 time parameters"
  Version = 5
END_GROUP = FILE_ATTRIBUTES
```

3.3.2 Bias Parameter Files

The bias model calibration algorithms operate on each OLI shutter collect and each TIRS deep space collect to generate bias model parameters for each imaging band, SCA, and detector for a given time interval. The BPFs are time-stamped the same way the CPFs are time-stamped. The BPFs are generated automatically about every half orbit, or 50 minutes. Level 1 processing must wait for these BPFs to be generated prior to processing to ensure radiometric quality of the products. The file name contains the file identifier, sensor, effective date range, and version number.

LS8BPFyyyy[1]mm[1]dd[1]HH[1]MM[1]SS[1]_yyyy[2]mm[2]dd[2]HH[2]MM[2]SS[2].nn	
L	Constant representing Landsat
S	Sensor (O for OLI or T for TIRS)
8	Satellite numerical representation
BPF	Bias Parameter File
yyyy[1]	Four-digit effective starting year
mm[1]	Two-digit effective starting month
dd[1]	Two-digit effective starting day
HH[1]	Two-digit effective starting hours
MM[1]	Two-digit effective starting minutes
SS[1]	Two-digit effective starting seconds
_	Effective starting/ending date separator
yyyy[2]	Four-digit effective ending year
mm[2]	Two-digit effective ending month
dd[2]	Two-digit effective ending day
HH[2]	Two-digit effective ending hours
MM[2]	Two-digit effective ending minutes
SS[2]	Two-digit effective ending seconds
.	File name/extension separator
Nn	Version Number for this file (starts with 01)

Table 3-4. Bias Parameter File Naming Convention

3.3.3 Response Linearization Lookup Table (RLUT) File

The RLUT file provides the parameters used to linearize the detector response for the OLI and TIRS instruments. Multiple methods of linearizing the response are supported.

The parameters are organized into groups of detectors for each band/SCA. The file is very large and stored in Hierarchical Data Format (HDF). This document provides a high-level overview of how the RLUT is applied to linearize the detector response, but for full details, refer to the Calibration and Validation (Cal/Val) Algorithm Description Document (ADD).

Each RLUT file covers an effective date range. The parameters in the file, “Effective Begin Date” and “Effective End Date”, designate the range of valid acquisition dates and are in YYYY-MM-DDThh:mm:ss format (ISO 8601). The parameter file used in processing an image should have an effective date range that includes the acquisition date of the ordered image. The detector linearity is not expected to change often; therefore, the effective date range is typically very large.

Throughout the mission, the file change history is maintained by means of effective begin and end dates plus the assignment of a version number to deal with changes that occur during the effective date period.

The file name contains the file identifier, effective date range, and version number.

LCNNRLUT_yyyy^{1}mm^{1}dd^1_yyyy^{2}mm^{2}dd^2_cc_nn.h5	
L	Constant representing Landsat
C	Sensor (C = Combined OLI and TIRS)
NN	Satellite numerical representation (08 = Landsat 8, 09 = Landsat 09)
RLUT	Response Linearization Look Up Table
_	RLUT / starting date separator
yyyy^1	Four-digit effective starting year
mm^1	Two-digit effective starting month
dd^1	Two-digit effective starting day
_	Effective starting/ending date separator
yyyy^2	Four-digit effective ending year
mm^2	Two-digit effective ending month
dd^2	Two-digit effective ending day
_	Date / collection number separator
cc	Collection number (starts with 01)
_	Collection/version number separator
nn	Version number for this file (starts with 01)
.	File name/extension separator
h5	HDF file extension

Table 3-5. Response Linearization Look-Up Table File Naming Convention

Section 4 Level 1 Products

4.1 Level 1 Product Generation

4.1.1 Overview

The geometric algorithms used by LPGS at EROS were originally developed for the L8 IAS. The overall purpose of the IAS geometric algorithms is to use Earth ellipsoid and terrain surface information in conjunction with spacecraft ephemeris and attitude data, in addition to knowledge of the OLI and TIRS instruments and L8 satellite geometry, to relate locations in image space (band, detector, sample) to geodetic object space (latitude, longitude, and elevation).

These algorithms are used to create accurate Level 1 output products, characterize the OLI and TIRS absolute and relative geometric accuracy, and derive improved estimates of geometric calibration parameters, such as the sensor to spacecraft alignment.

4.1.2 Level 1 Processing System

The Level 1 processing algorithms include the following:

- Ancillary data processing
- L8 sensor/platform geometric model creation
- Sensor LOS generation and projection
- Output space / input space correction grid generation
- Systematic, terrain-corrected image resampling
- Geometric model precision correction using ground control
- Precision, terrain-corrected image resampling

Figure 4-1 shows the LPGS Standard Product Data Flow, which includes radiometric and geometric processing.

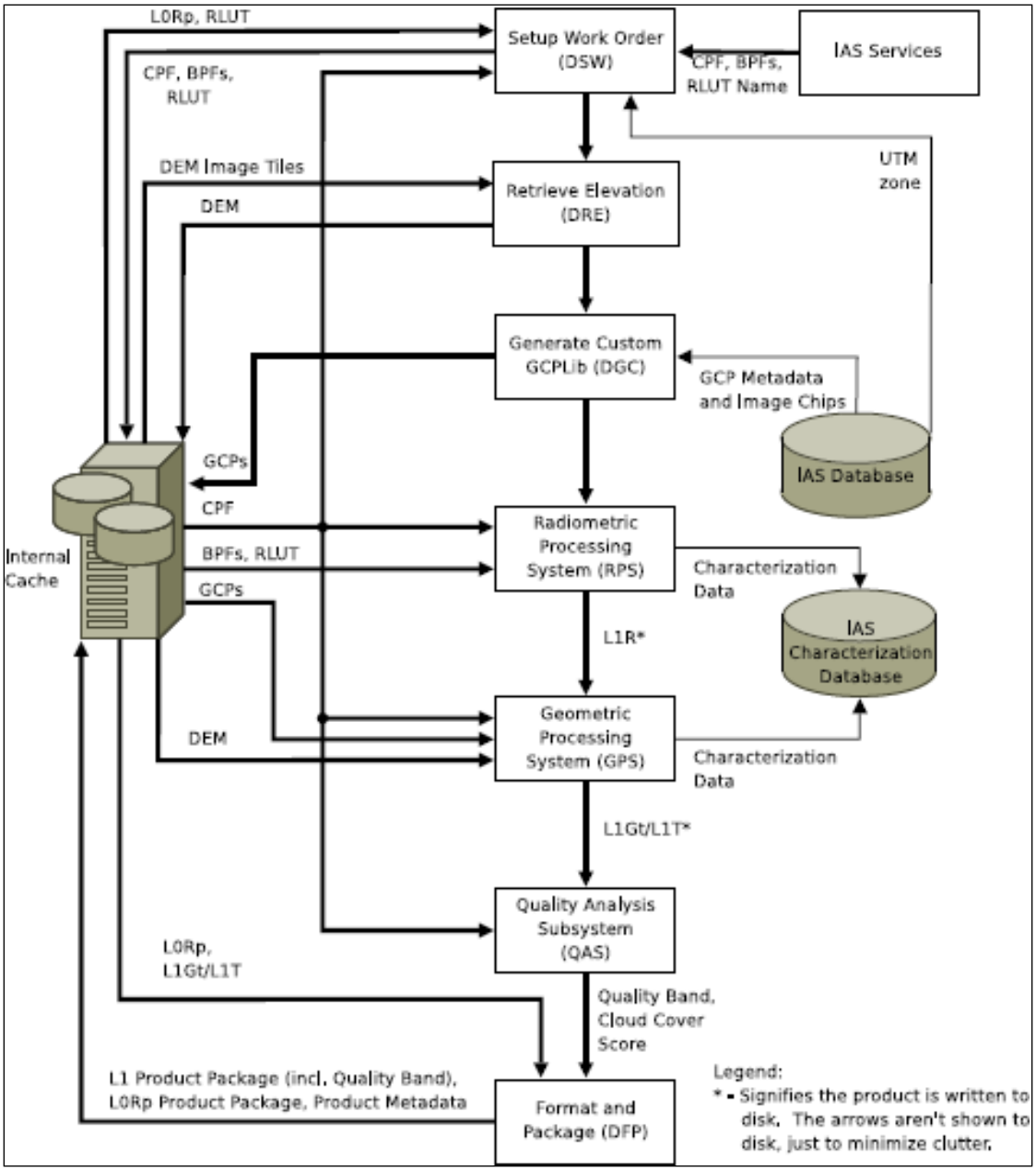

Figure 4-1. LPGS Standard Product Data Flow

The following paragraphs describe the purpose and function of each of the major LPGS Subsystems. Complete detailed designs for each Subsystem are presented in subsequent sections.

- Process Control Subsystem (PCS) – The PCS controls work order scheduling and processing. The PCS manages and monitors LPGS resources and provides processing status in response to Operator requests.
- Data Management Subsystem (DMS) – The DMS provides data management services for the LPGS and handles the external interfaces for the System. It

provides tools for formatting and packaging products. The DMS also maintains LPGS disk space and populates temporary storage with data from ingested files.

- Radiometric Processing Subsystem (RPS) – The RPS converts the brightness of the L0R image pixels to absolute radiance in preparation for geometric correction. The RPS performs radiometric characterization of L0R images by locating radiometric artifacts in images. The RPS provides the results of characterizations performed to the IAS characterization database. The RPS corrects radiometric artifacts and converts the image to radiance.
- Geometric Processing Subsystem (GPS) – The GPS creates Level 1 geometrically corrected imagery (Level 1 Geometric Systematic (L1Gs) from L1R products. The geometrically corrected products can be systematic terrain-corrected (L1Gt) or precision terrain-corrected products (L1TP). The GPS provides the results of characterizations performed to the IAS characterization database. The GPS generates a satellite model, prepares a resampling grid, and resamples the data to create an L1Gt or L1T product. The GPS performs sophisticated satellite geometric correction to create the image according to the map projection and orientation specified for the Level 1 standard product.
- Quality Assessment Subsystem (QAS) – The QAS performs cloud cover assessment and generates the product quality band. The QAS provides tools for visual inspection of images where a problem has been encountered while creating the product.
- User Interface (UI) – The UI provides the Graphical User Interface (GUI) for the LPGS Operator and the Anomaly Analysis Subsystem (AAS). It allows the Operator to monitor the status of work orders and track processing anomalies.

4.1.3 Ancillary Data

The L8 OLI and TIRS geometric correction algorithms are applied to the wideband (data contained in Level 0R (raw) or 1R (radiometrically corrected)) products. Some of these algorithms also require additional ancillary input datasets. These include the following:

- Ancillary data from the spacecraft and Scalable Inertial Reference Unit (SIRU) provides attitude information for the spacecraft.
- Ground control / reference images for geometric test sites - used in precision correction, geodetic accuracy assessment, and geometric calibration algorithms.
- Digital elevation data for geometric test sites - used in terrain correction and geometric calibration.
- Pre-launch ground calibration results, including band/detector placement and timing, and attitude sensor characteristics.
- Earth parameters, including static Earth model parameters (e.g., ellipsoid axes, gravity constants) and dynamic Earth model parameters (e.g., polar wander offsets, UT1-UTC time corrections) - used in systematic model creation and incorporated into the CPF.

4.1.4 Data Products

One of the goals of L8 is the provision of high-quality, standard data products. About 650 scenes per day are imaged globally and returned to the United States archive. All of

these scenes are processed to a Level 1 standard product and made available for download over the Internet at no cost to users.

The Level 1 data available to users is a radiometrically and geometrically corrected image. Inputs from both the sensors and the spacecraft are used, as well as GCPs and DEMs. The result is a geometrically rectified product free from distortions related to the sensor (e.g., view angle effects), satellite (e.g., attitude deviations from nominal), and Earth (e.g., rotation, curvature, relief). The image is also radiometrically corrected to remove relative detector differences, dark current bias, and some artifacts. The Level 1 image is presented in units of DNs, which can be easily rescaled to spectral radiance or TOA reflectance.

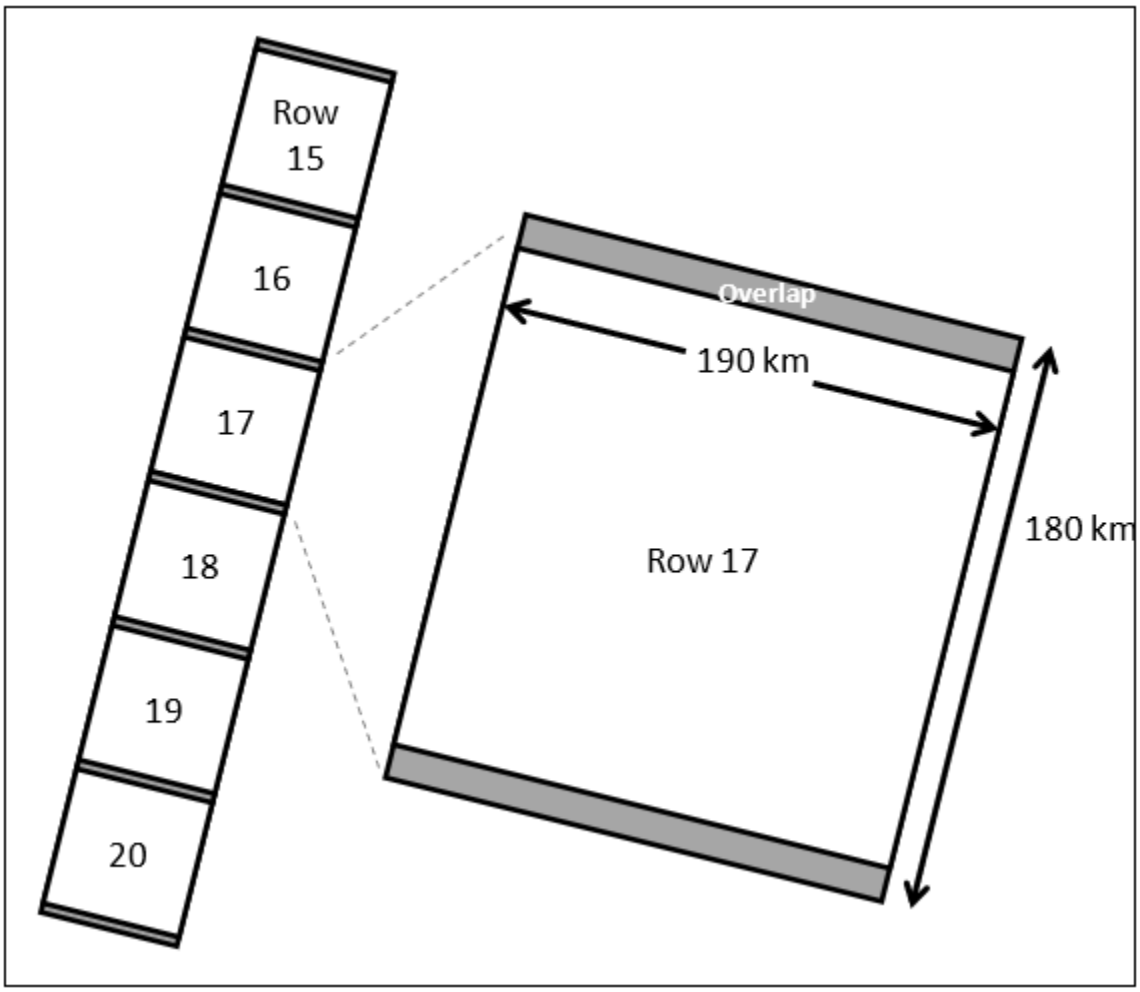

Figure 4-2. Level 1 Product Ground Swath and Scene Size

4.1.4.1 Product Components

A complete Level 1 product consists of 13 files, including the 11 band images, a product-specific metadata file, and a Quality Assessment (QA) image. The image files

are all 16-bit GeoTIFF images. The OLI bands are Bands 1-9. The TIRS bands are designated as Bands 10 and 11.

The QA image is a 16-bit mask, which marks clouds, fill data, and some land cover types. Section 5.4 gives a full description of the L8 QA mask.

The Level 1 metadata (MTL) file contains identifying parameters for the scene, along with the spatial extent of the scene and the processing parameters used to generate the Level 1 product. This file is a human-readable text file in ODL format.

4.1.4.2 Product Format

The L8 data product delivered to users is packaged as Georeferenced Tagged Image File Format (GeoTIFF) (a standard, public-domain image format based on Adobe's TIFF), which is a self-describing format developed to exchange raster images. The GeoTIFF format includes geographic or cartographic information embedded within the imagery that can be used to position the image in a geographic information display. Each L8 band is presented as a 16-bit grayscale image. Specifically, GeoTIFF defines a set of TIFF tags, which describes cartographic and geodetic information associated with geographic TIFF imagery. GeoTIFF is a means for tying a raster image to a known model space or map projection and for describing those projections. A metadata format provides geographic information to associate with the image data. However, the TIFF file structure allows both the metadata and the image data to be encoded into the same file.

For details on GeoTIFF format, please download the GeoTIFF Format Specification (PDF) or visit http://trac.osgeo.org/geotiff/.

4.1.4.3 Cloud Cover Assessment (CCA)

The L8 CCA system uses the C Function of Mask (CFMask) algorithm to identify fill, cloud, cloud confidence, cloud shadow, and snow/ice in Landsat 8 scenes for representation in the QA band as bit-mapped values. CFMask derives from the Function of Mask (FMask), an algorithm written at Boston University.

CFMask is a multi-pass algorithm that uses decision trees to prospectively label pixels in the scene; it then validates or discards those labels according to scene-wide statistics. It also creates a cloud shadow mask by iteratively estimating cloud heights and projecting them onto the ground.

Users should be aware that, like other cloud algorithms, CFMask may have difficulties over bright targets, such as building tops, beaches, snow/ice, sand dunes, and salt lakes. Optically, thin clouds will always be challenging to identify and have a higher probability of being omitted by the algorithm. In addition, the algorithm performance has only been validated for cloud detection, and to a lesser extent for cloud shadows. No rigorous evaluation of the snow/ice detection has been performed.

NOTE: Comparison of the various cloud detection algorithms used for Landsat data products has been performed. (Foga, S.)

Landsat CCA validation data can be accessed from the Landsat Cloud Cover Assessment Validation Datasets web page.

4.1.5 Calculation of Scene Quality

The quality algorithm is calculated by the following two formulas:

SIQS = 9 - [SNF/ANF * (NDF / DFBP + NCF / CFBP)]
IIQS = 9 - [(NDF/DFBP + NCF/CFBP)

Where:

SIQS = Scene Image Quality Score
IIQS = Interval Image Quality Score
SNF = Standard number of video frames in a scene [7001 for OLI, 2621 for TIRS]
ANF = Actual number of frames in the scene/interval
NDF = Number of dropped frames in the scene/interval
DFBP = Dropped Frame Break Point: dropped frame count at which the quality score drops by one point [2]
NCF = Number of video frame CRC failures in the scene/interval
CFBP = CRC Failures Break Point: Video frame CRC failure count at which the quality score drops by one point [100]

Numbers in brackets are configurable. If changed, the quality algorithm version is updated, and the new values documented.

Image_Quality_OLI

Values: 0–9, where
9 = Best
0 = Worst
-1 = quality not calculated or assessed

Image_Quality_TIRS

Values: 0–9, where
9 = Best
0 = Worst
-1 = quality not calculated or assessed

4.2 Level 1 Product Description

4.2.1 Science Data Content and Format

The L8 instruments represent an evolutionary advance in technology. OLI builds upon Landsat heritage and technologies demonstrated by the ALI. As such, OLI is a push-broom sensor with a four-mirror telescope and uses 12-bit quantization. The OLI collects 30-meter data for visible, near infrared, and shortwave infrared spectral bands and provides for a 15-meter Pan band. New with OLI is the addition of a 30-meter deep blue Coastal Aerosol band (Band 1) for coastal water and aerosol studies and a 30-meter Cirrus band (Band 9) for cirrus cloud detection. Additionally, the bandwidth has been refined (narrowed) for six of the heritage bands.

The TIRS instrument collects data for two narrow spectral bands in the thermal region, formerly covered on previous Landsat instruments by one wide spectral band. Although TIRS is a separate instrument, the 100-meter TIRS data are registered to the OLI data in order to create radiometrically, geometrically, and terrain-corrected 12-bit data products.

These sensors both provide improved SNR radiometric performance quantized over a 12-bit dynamic range. This translates into 4096 potential grey levels in an image compared with only 256 grey levels in previous 8-bit instruments. Additionally, improved SNR performance enables better characterization of land cover state and condition.

4.2.1.1 Science Data Content

In addition to Table 2-1 in Section 2, Figure 4-3 compares L8 spectral bands and wavelength to that of L7 ETM+.

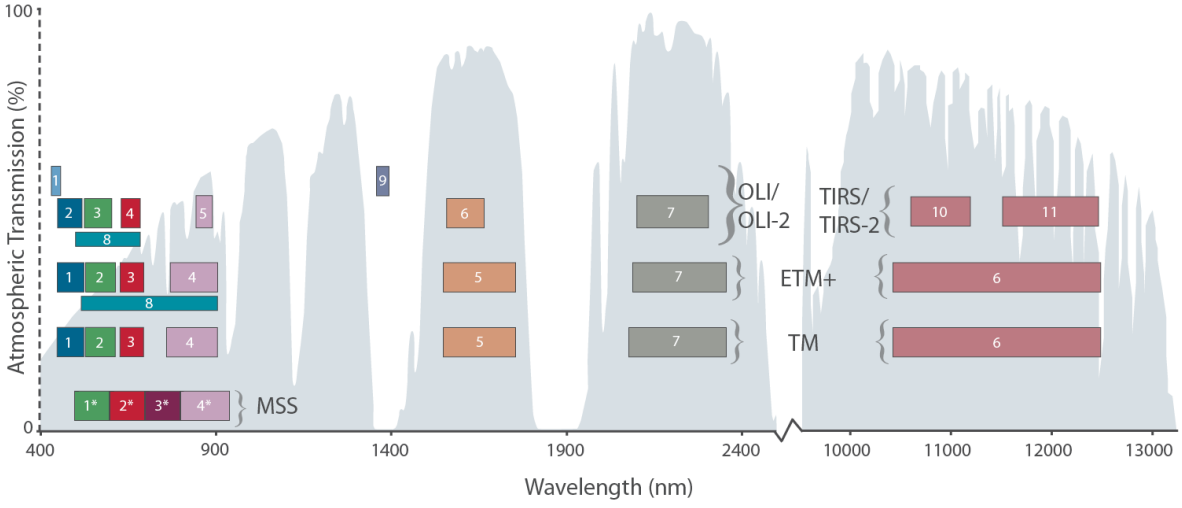

Figure 4-3. Spectral Bands and Wavelengths for Landsat Sensors

4.2.1.2 Science Data Format

L8 acquires high-quality, well-calibrated multispectral data over the Earth's land surfaces. On average, over 650 unique scenes are acquired per day across the globe and sent to the USGS EROS Center for storage, archive, and processing. All of these scenes are processed to a standard Level 1 product. The highest available product derivative is made available for download at no cost to users. A complete standard Level 1 product consists of 13 files, including OLI Bands 1-9 (one file per band), TIR Bands 10 & 11 (one file per band), a product-specific metadata file, and a QA file.

LSDS-809 Landsat 8 (L8) Level 1 (L1) Data Format Control Book (DFCB) is an excellent reference for L8 product format and information. The following paragraphs summarize the Level 1 data format.

For details on GeoTIFF format, please refer to the GeoTIFF Format Specification (PDF) or visit http://trac.osgeo.org/geotiff/.

In addition to GeoTIFF, the data incorporate cubic convolution resampling, North Up (Map) image orientation, and Universal Transverse Mercator (UTM) map projection (Polar Stereographic projection for scenes with a center latitude greater than or equal to -63.0 degrees) using the WGS84 datum.

The format of the final output product is a tar.gz file. Specifically, the files are written to a tar file format and then compressed with the gzip application. Of note, the tar file does not contain any subdirectory information. Therefore, uncompressing the file places all of the files directly into the current directory location.

Table 4-1 displays the standard file-naming convention for L8 Level 1 products.

Landsat 8 File Naming Convention	
LXSS_LLLL_PPPRRR_YYYYMMDD_yyyymmdd_CC_TX	
L	Landsat
X	Sensor ("C" = OLI/TIRS combined, "O" = OLI-only, "T" = TIRS-only)
SS	Satellite ("08" = Landsat 8)
LLLL	Processing correction level (L1TP/L1Gt/L1Gs)
PPP	WRS path
RRR	WRS row
YYYYMMDD	Acquisition year (YYYY)/Month(MM)/Day(DD)
yyyymmdd	Processing year (yyyy)/ Month (mm)/ Day (dd)
CC	Collection number (01, 02…)
TX	Collection category ("RT" = Real-Time, "T1" = Tier 1, "T2" = Tier 2)
Example:	**LC08_L1GT_029030_20151209_20160131_01_T1**

Table 4-1. Landsat 8 File Naming Convention

4.2.2 Metadata Content and Format

The MTL file is created during product generation and contains information specific to the Level 1 product ordered. The MTL file contains identifying parameters for the scene, along with the spatial extent of the scene and the processing parameters used to

generate the Level 1 product. This file is a human-readable text file in ODL format. An example of the MTL file is listed in Appendix C.

In general, the MTL file includes the following parameters:

- Unique Landsat scene identifier
- WRS path and row information
- Scene Center Time of the date the image was acquired
- Corner longitude and latitude in degrees and map projection values in meters
- Reflective, thermal, and Pan band lines and samples
- File names included
- Image attributes including cloud cover, sun azimuth and elevation, and number of GCPs used
- Band minimum and maximum reflectance and radiance rescaling

4.2.3 Quality Assessment Band

The QA Band contains quality statistics gathered from the image data and cloud mask information for the scene. The QA file is a 16-bit image with the same dimensions as the standard L1T scene. Bits are allocated for some artifacts that are distinguishable after the systematic correction (Level 1Gs) stage of processing. The first bit (bit 0) is the least significant. Section 5.4 provides a full description of the L8 QA band.

Used effectively, QA bits improve the integrity of science investigations by indicating which pixels might be affected by instrument artifacts or be subject to cloud contamination. For example, Normalized Difference Vegetation Index (NDVI) calculated over pixels containing clouds will show anomalous values. If such pixels were included in a phenology study, the results might not show the true characteristics of seasonal vegetation growth. Cloud-contaminated pixels will lower NDVI values and measurements, such as the timing of ‘green up’ or peak maturity, would appear later than they actually occurred. A worse consequence would be that the reported reduction of vegetation growth would be taken as an indicator of environmental change, potentially prompting unnecessary land management policies or practices.

Rigorous science applications seeking to optimize the value of pixels used in a study will find QA bits useful as a first-level indicator of certain conditions. Otherwise, users are advised that this file contains information that can be easily misinterpreted, and it is not recommended for general use. Robust image processing software capable of handling 16-bit data is necessary to compute statistics of the number of pixels containing each of the designated bits.

Figure 4-4 displays the Quality Band for Landsat 8 Sample Data (Path 45 Row 30) Acquired April 23, 2013.

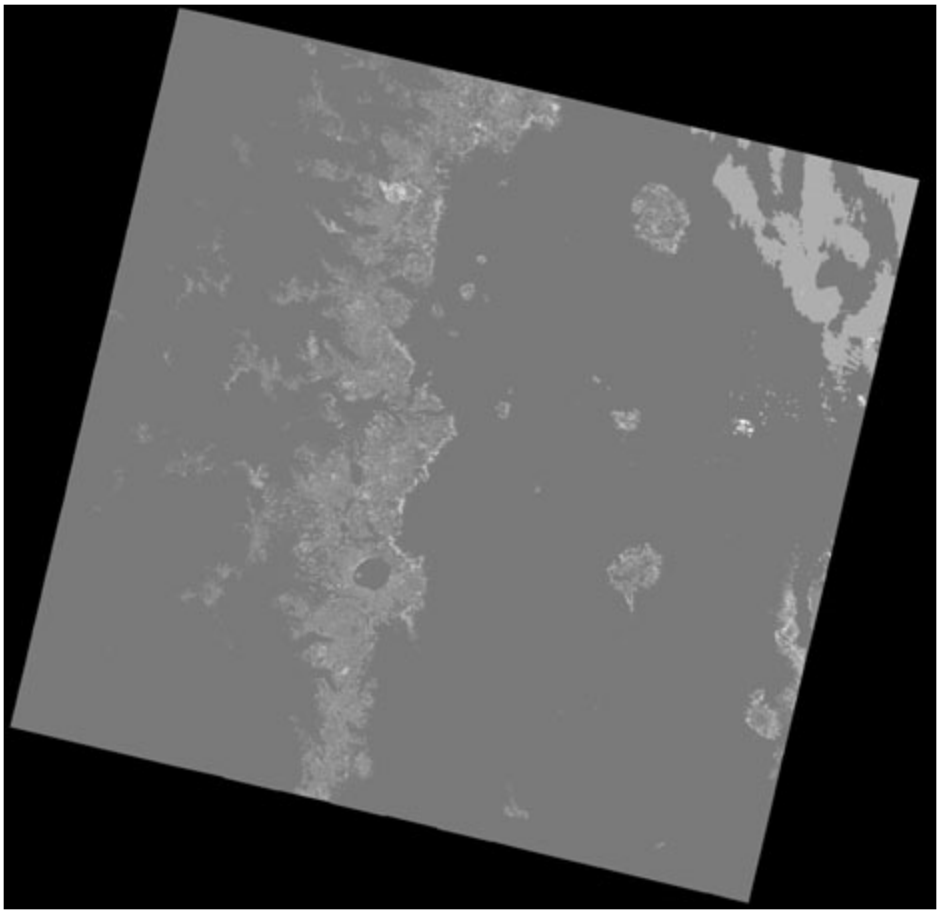

Figure 4-4. Landsat 8 Quality Band

The QA image can be stretched to emphasize the light ("1") and dark ("0") pixels for a quick view of general quality conditions. In the image above, the lighter pixels are likely to be affected by snow or clouds.

Section 5 Conversion of DNs to Physical Units

5.1 OLI and TIRS at Sensor Spectral Radiance

Images are processed in units of absolute radiance using 32-bit floating-point calculations. These values are converted to 16-bit integer values in the finished Level 1 product. They can then be converted to spectral radiance using the radiance scaling factors provided in the metadata file:

$$L_\lambda = ML * Q_{cal} + A_L$$

where:

L_λ = Spectral radiance ($W/(m^2 * sr * \mu m)$)
M_L = Radiance multiplicative scaling factor for the band (RADIANCE_MULT_BAND_n from the metadata)
A_L = Radiance additive scaling factor for the band (RADIANCE_ADD_BAND_n from the metadata)
Q_{cal} = Level 1 pixel value in DN

5.2 OLI Top of Atmosphere Reflectance

Similar to the conversion to radiance, the 16-bit integer values in the Level 1 product can also be converted to TOA reflectance. The following equation is used to convert Level 1 DN values to TOA reflectance:

$$\rho\lambda' = M_\rho * Q_{cal} + A_\rho$$

where:

ρ_λ' = TOA Planetary Spectral Reflectance, without correction for solar angle. (Unitless)
M_ρ = Reflectance multiplicative scaling factor for the band (REFLECTANCEW_MULT_BAND_n from the metadata).
A_ρ = Reflectance additive scaling factor for the band (REFLECTANCE_ADD_BAND_N from the metadata).
Q_{cal} = Level 1 pixel value in DN

Note that ρ_λ' is not true TOA Reflectance, because it does not contain a correction for the solar elevation angle. This correction factor is left out of the Level 1 scaling at the users' request; some users are content with the scene-center solar elevation angle in the metadata, while others prefer to calculate their own per-pixel solar elevation angle across the entire scene. Once a solar elevation angle is chosen, the conversion to true TOA Reflectance is as follows:

$$\rho_\lambda = \frac{\rho_\lambda'}{\cos(\theta_{SZ})} = \frac{\rho_\lambda'}{\sin(\theta_{SE})}$$

where:

ρ_λ	=	TOA planetary reflectance
$\boldsymbol{\theta_{SE}}$	=	Local sun elevation angle; the scene center sun elevation angle in degrees is provided in the metadata
$\boldsymbol{\theta_{SZ}}$	=	Local solar zenith angle; θSZ = 90° - θSE

5.3 TIRS Top of Atmosphere Brightness Temperature

TIRS data can also be converted from spectral radiance (as described above) to brightness temperature, which is the effective temperature viewed by the satellite under an assumption of unity emissivity. The conversion formula is as follows:

$$T = \frac{K_2}{\ln\left(\frac{K_1}{L_\lambda}+1\right)}$$

where:

$\boldsymbol{T}$	=	Top of atmosphere brightness temperature (K) where:
$\boldsymbol{L_\lambda}$	=	TOA spectral radiance (Watts/(m2 * srad * μm))
$\boldsymbol{K_1}$	=	Band-specific thermal conversion constant from the metadata (K1_CONSTANT_BAND_x, where x is the thermal band number)
$\boldsymbol{K_2}$	=	Band-specific thermal conversion constant from the metadata (K2_CONSTANT_BAND_x, where x is the thermal band number)

5.4 Unpacking Quality Assessment Band Bits

The pixel values in the QA band file must be translated to 16-bit binary form to be used effectively. The gray shaded areas in Table 5-1 show the bits that are currently being populated in the Level 1 QA Band and the conditions each describe.

Landsat 8 OLI, OLI/TIRS Collection 1 QA band bits; Read from RIGHT to LEFT, starting with Bit 0																
Cumulative Sum																
	65553	32767	16383	8191	4095	2047	1023	511	255	127	63	31	15	7	3	1
BIT	15	14	13	12	11	10	9	8	7	6	5	4	3	2	1	0
Description				Cirrus Confidence		Snow/Ice Confidence		Cloud Shadow Confidence		Cloud Confidence		Cloud	Radiometric Saturation		Terrain Occlusion	Designated Fill

Table 5-1. Bits Populated in Level 1 QA Band

For the single bits (0, 1, and 4):

- 0 = “No” = this condition does not exist
- 1 = “Yes” = this condition exists

For radiometric saturation bits (2-3), read from left to right, represent how many bands contain saturation:

- 00 - No bands contain saturation
- 01 - 1-2 bands contain saturation
- 10 - 3-4 bands contain saturation
- 11 - 5 or more bands contain saturation

For the remaining double bits (5-6, 7-8, 9-10, 11-12), read from left to right, represent levels of confidence that a condition exists:

- 00 = “Not Determined” = Algorithm did not determine the status of this condition / "No" = This condition does not exist
- 01 = “Low” = Algorithm has low to no confidence that this condition exists (0-33 percent confidence)
- 10 = “Medium” = Algorithm has medium confidence that this condition exists (34-66 percent confidence)
- 11 = “High” = Algorithm has high confidence that this condition exists (67-100 percent confidence

Certain values occur regularly and can be interpreted without unpacking them into 16-bit strings and using Table 5-1 as a reference. Table 5-2 displays QA band attributes and pixel values. Table 5-3 displays QA Value Interpretations.

A no-cost tool is available for user download that will extract the bit-packed information in the OLI QA band for easy interpretation. Details are provided at https://www.usgs.gov/land-resources/nli/landsat/landsat-quality-assessment-tools.

Attribute	Pixel Value
Fill	1
Terrain Occlusion	2, 2722
Clear	2720, 2724, 2728, 2732
Radiometric Saturation - 1-2 bands	2724, 2756, 2804, 2980, 3012, 3748, 3780, 6820, 6852, 6900, 7076, 7108, 7844, 7876
Radiometric Saturation - 3-4 bands	2728, 2760, 2808, 2984, 3016, 3752, 3784, 6824, 6856, 6904, 7080, 7112, 7848, 7880
Radiometric Saturation - 5+ bands	2732, 2764, 2812, 2988, 3020, 3756, 3788, 6828, 6860, 6908, 7084, 7116, 7852, 7884
Cloud	2800, 2804, 2808, 2812, 6896, 6900, 6904, 6908
Cloud Confidence - Low	2720, 2722, 2724, 2728, 2732, 2976, 2980, 2984, 2988, 3744, 3748, 3752, 3756, 6816, 6820, 6824, 6828, 7072, 7076, 7080, 7084, 7840, 7844, 7848, 7852

Attribute	Pixel Value
Cloud Confidence - Medium	2752, 2756, 2760, 2764, 3008, 3012, 3016, 3020, 3776, 3780, 3784, 3788, 6848, 6852, 6856, 6860, 7104, 7108, 7112, 7116, 7872, 7876, 7880, 7884
Cloud Confidence - High	2800, 2804, 2808, 2812, 6896, 6900, 6904, 6908
Cloud Shadow - High	2976, 2980, 2984, 2988, 3008, 3012, 3016, 3020, 7072, 7076, 7080, 7084, 7104, 7108, 7112, 7116
Snow/Ice - High	3744, 3748, 3752, 3756, 3776, 3780, 3784, 3788, 7840, 7844, 7848, 7852, 7872, 7876, 7880, 7884
Cirrus Confidence - Low	2720, 2722, 2724, 2728, 2732, 2752, 2756, 2760, 2764, 2800, 2804, 2804, 2808, 2812, 2976, 2980, 2984, 2988, 3008, 3012, 3016, 3020, 3744, 3748, 3752, 3756, 3780, 3784, 3788
Cirrus Confidence - High	6816, 6820, 6824, 6828, 6848, 6852, 6856, 6860, 6896, 6900, 6904, 6908, 7072, 7076, 7080, 7084, 7104, 7108, 7112, 7116, 7840, 7844, 7848, 7852, 7872, 7876, 7880, 7884

Table 5-2. Landsat 8 Possible Attributes and Pixel Values

[N/D, not determined; Conf., confidence]

Pixel Value	Cirrus Conf.	Snow/ Ice Conf.	Cloud Shadow Conf.	Cloud Conf.	Cloud	Radiometric Saturation	Terrain Occlusion	Fill	Pixel Description
0	ND	ND	ND	ND	ND	ND	ND	ND	ND
1	ND	ND	ND	ND	ND	ND	ND	Yes	Fill
2	ND	ND	ND	ND	ND	ND	Yes	No	Terrain occlusion
2720	Low	Low	Low	Low	No	No	No	No	Clear terrain
2804	Low	Low	Low	High	Yes	1-2 bands	No	No	High confidence cloud with some saturation
2988	Low	Low	High	Low	No	5+ bands	No	No	Cloud shadow with frequent saturation
3744	Low	High	Low	Low	No	No	No	No	Snow/ice
3748	Low	High	Low	Low	No	1-2 bands	No	No	Snow/ice with some saturation
7072	High	Low	High	Low	No	No	No	No	Cirrus cloud, cloud shadow
7076	High	Low	High	Low	No	1-2 bands	No	No	Cirrus cloud, cloud shadow with some saturation
7116	High	Low	High	Medium	No	5+ bands	No	No	Cirrus cloud, cloud shadow, medium cloud confidence with frequent saturation

Table 5-3. Landsat 8 Collection 1 Level 1 QA Value Interpretations

5.5 LandsatLook Quality Image (.jpg)

The 8-bit LandsatLook Quality Image is available to download when downloading L8 data products. This file provides a quick view of the quality of the pixels to determine which scene would work best for each user's application. Only the highest confidence conditions are used to create the LandsatLook Quality image.

NOTE: This image may not be useful to all users.

For information on LandsatLook Images visit https://www.usgs.gov/land-resources/nli/landsat/landsatlook-images.

Table 5-4 displays the bits and colors associated with the LandsatLook Quality Image. Figure 5-1 is the Landsat Look Quality Image for Landsat 8 Path 45 Row 30 Acquired April 23, 2013.

Landsat 8 LandsatLook 8-bit Quality Designations		
Bit	**Description**	**Color**
0	Designated Fill	
1	Terrain Occlusion	
2	Radiometric Saturation	
3	Cloud	
4	Cloud Shadow	
5	Snow/Ice	
6	Cirrus	
7	Unused	Unused

Table 5-4. Bits and Colors Associated with LandsatLook Quality Image

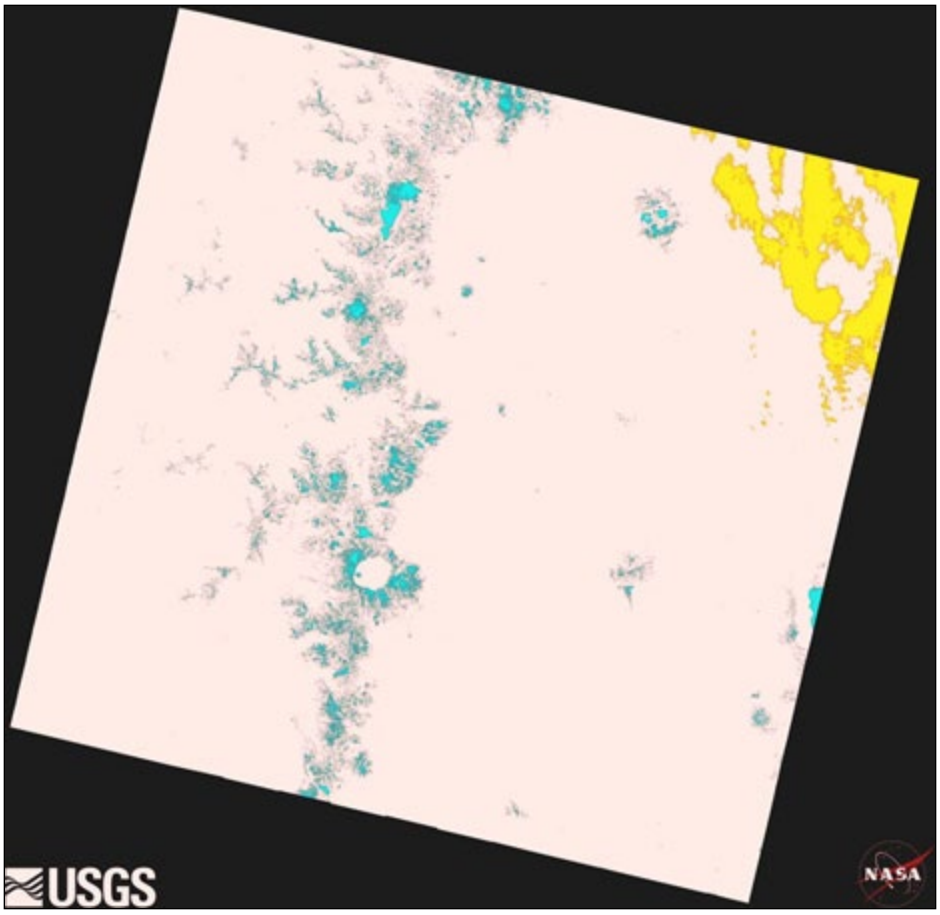

Figure 5-1. Landsat Look Quality Image

Section 6 Landsat 8 Data Search and Access

The USGS archive holds data collected by the Landsat suite of satellites, beginning with Landsat 1 in 1972. Over 500 L8 scenes are added to the USGS archives each day and become available to all users for download at no charge using the sites described in this section. All Landsat data products are distributed via HTTPS access. Current L8 products available include the following:

- LandsatLook “Natural Color” Image - a full-resolution, 3-band .jpg image (approximate size: 4.5 MB)
- LandsatLook “Thermal” Image - a full-resolution, thermal band 10 .jpg image (approximate size: 2.5 MB)
- LandsatLook “Quality” Image - a full-resolution Quality Assessment band .jpg image (Approximate size: 2.5 MB)
- LandsatLook Images with Geographic Reference - a bundle including the “Natural”, “Thermal”, and “Quality” full-resolution images, along with .wld and .xml files with geographic reference information (Approximate size: 9.0 MB)
- Level 1 Data Product - a compressed file including all individual multispectral and/or thermal band and metadata files (Approximate size: 950 MB)

Visit the Landsat Collections webpage for more details about the Landsat data products.

The interfaces outlined in the following subsections allow users to search and download L8 data held in the USGS Archives. The functionality of each differs; however, the data products are all delivered from the same location. Each interface includes a Help section to provide more details about step-by-step processes.

6.1 EarthExplorer (EE)

EE is the primary search interface accessing aerial, mapping, elevation, and satellite data held in the USGS archives, including Landsat data products. Before downloading data products, users must complete the user registration at https://ers.cr.usgs.gov/register/. Some functions of the website will work only after a successful login.

https://earthexplorer.usgs.gov

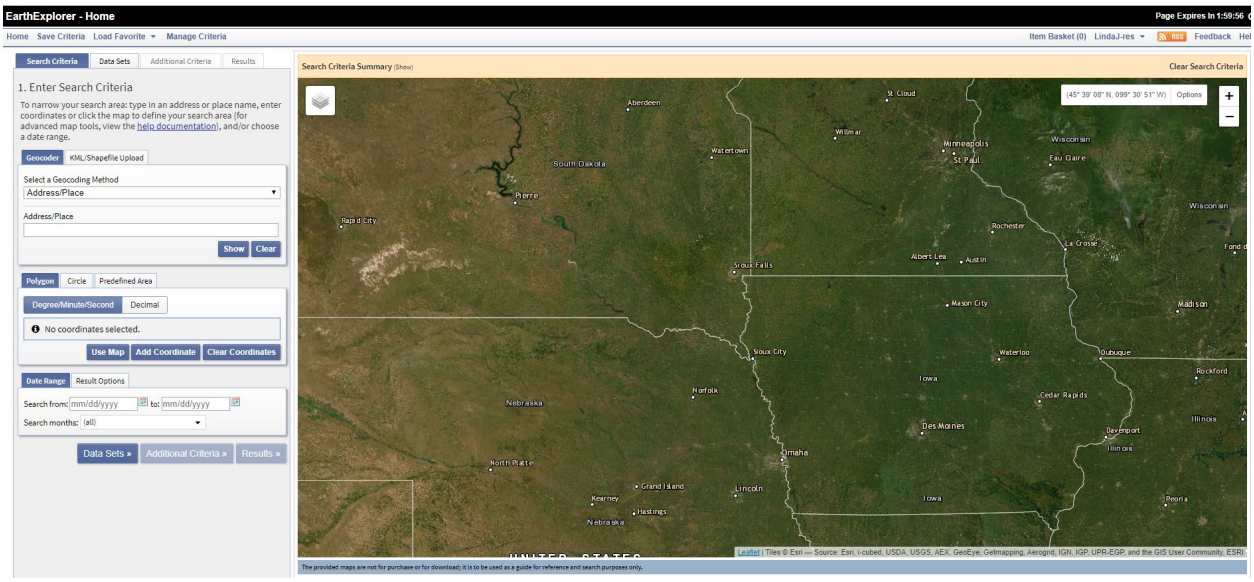

Figure 6-1. EarthExplorer Interface

The Search Criteria tab options allow users to select the geographic area of interest by typing a place name, latitude/longitude coordinates, path/row, a shape file, or a .kml file. The user can also specify the date range and number of results.

The Data Set tab lists all categories of data held in the USGS EROS Archives. The Landsat section of this tab lists all Landsat datasets, which are organized by collection and processing level (see Figure 6-2).

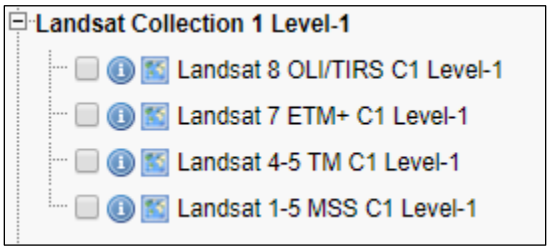

Figure 6-2. EarthExplorer Landsat Level 1 Datasets

Each dataset displays an Information button preceding the name that users can click to view more details about the dataset.

After selecting the dataset(s), the Additional Search Criteria button is active. The user can click this button to view the Additional Criteria (Optional) tab. This tab allows users to search by specific scene ID or path/row and set cloud cover limits. Users interested in searching nighttime imagery can select that option on this tab as well. After making their selection(s), users click the Results button, located on the bottom right side of the Additional Criteria (Optional) tab.

After a successful search, results are presented in a manner that allows users to view a browse image of the scene, a subset of the metadata file, or the footprint of a scene on the map. To view the available data products, the user clicks the Download Options icon (a green arrow) near each scene. A gold icon indicates scenes can be added to a bulk download order.

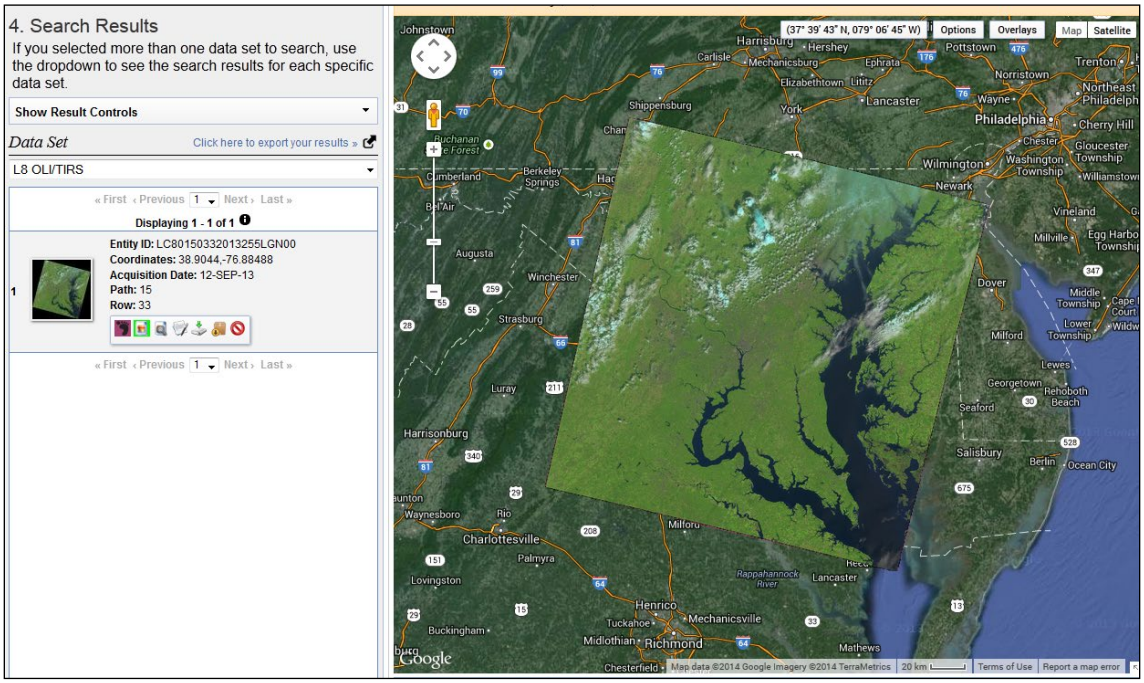

Figure 6-3. EarthExplorer Results - Browse Image Display

The Show Result Controls section (located above the results listing) allows users to view the footprints or browse of all results or add them all to a bulk download order (see Figure 6-4).

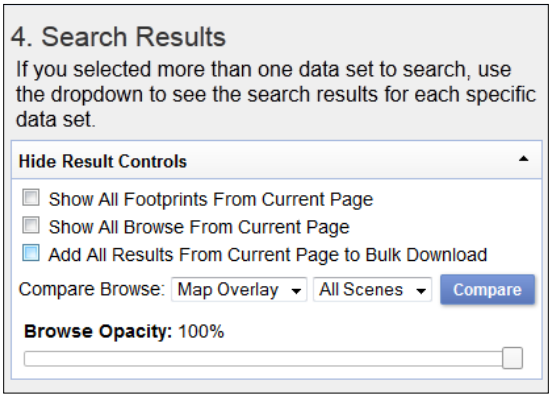

Figure 6-4. EarthExplorer Results Controls

6.2 Global Visualization Viewer (GloVis)

The GloVis Viewer is a browse-based tool that displays all available Landsat scenes held in the USGS archives.

https://glovis.usgs.gov

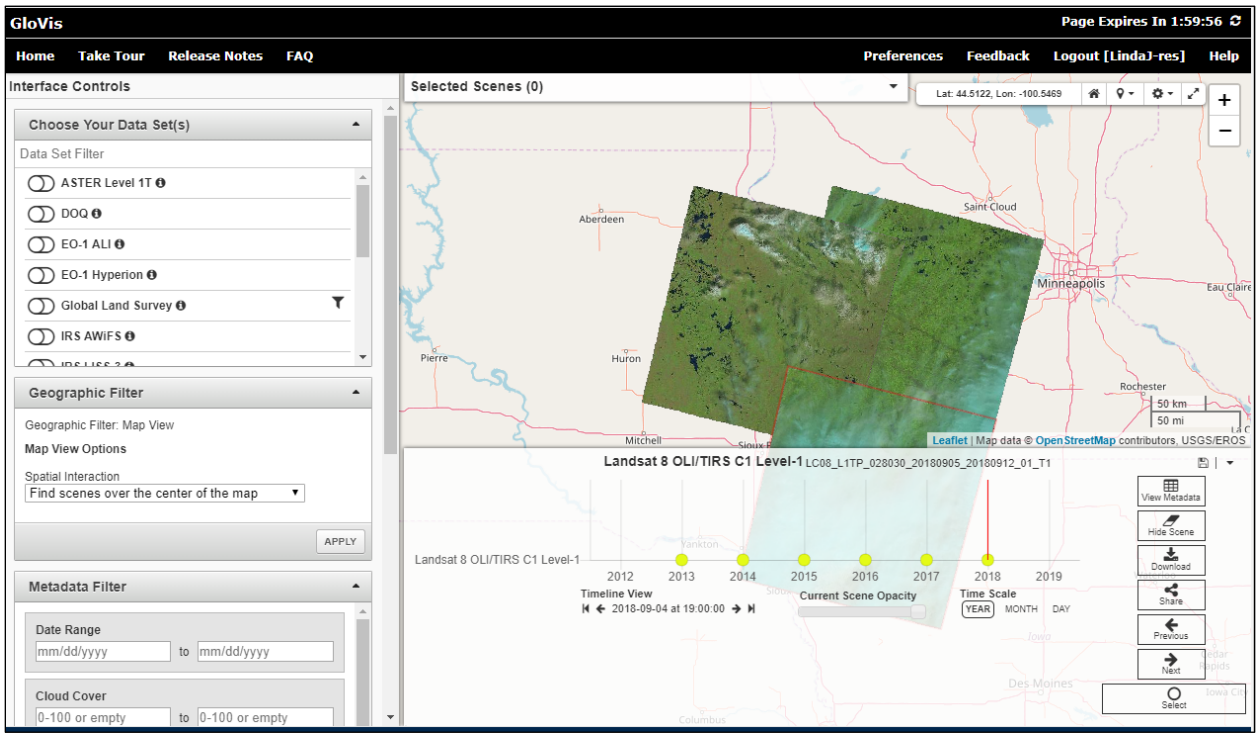

Figure 6-5. Global Visualization Viewer (GloVis) Interface

Upon opening, the viewer displays the most recent, least cloudy image of Path 29 Row 30 (southeast South Dakota). Use the Interface Controls to select Data Sets, and to filter for dates and cloud cover.

Scenes added to the Scene List are sent to the Cart, which forwards the request to EarthExplorer and prompts users to login. The data can then be downloaded individually or added to a bulk download order.

6.3 LandsatLook Viewer

The LandsatLook Viewer interface allows users move around the globe and zoom into the area of interest. Like GloVis, selected scenes are forwarded to EarthExplorer for login and download.

https://landsatlook.usgs.gov/viewer.html

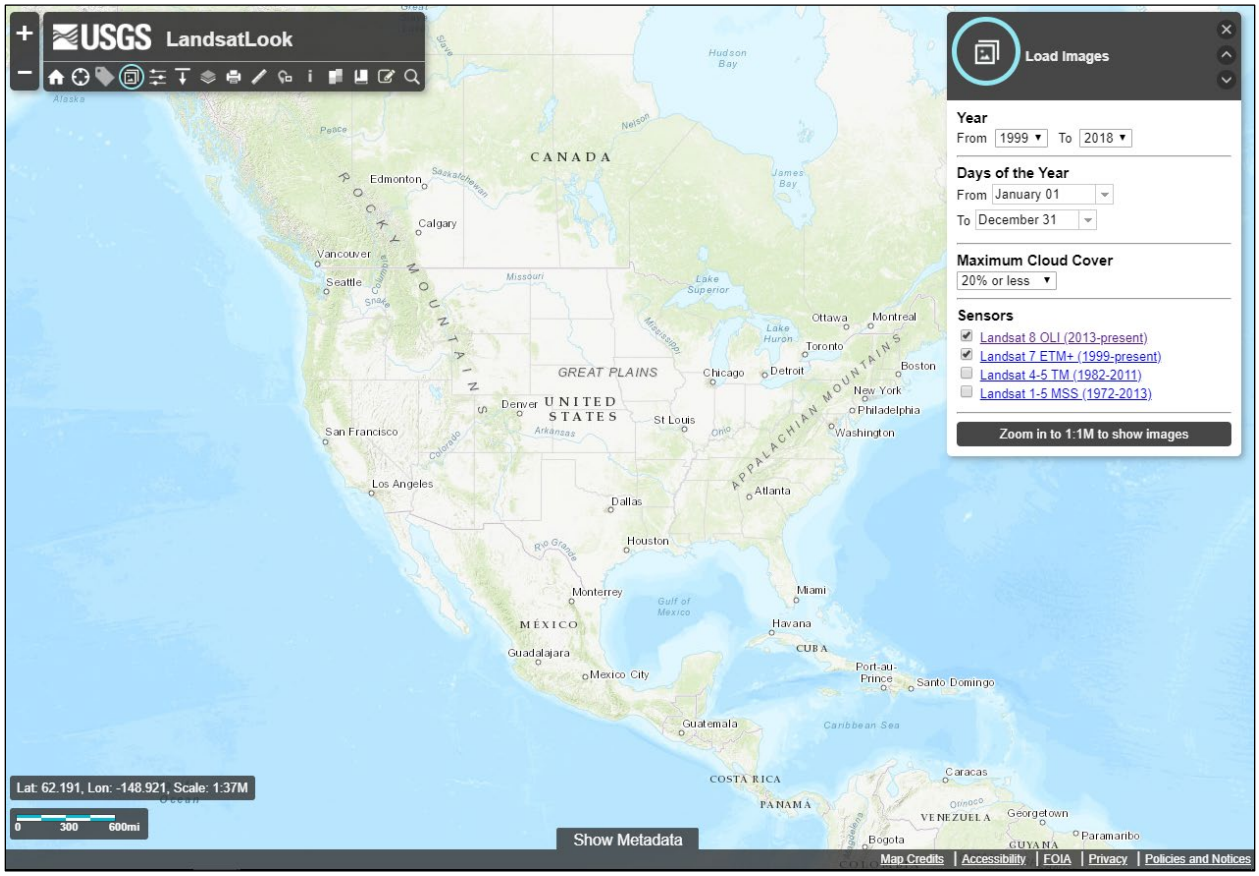

Figure 6-6. The LandsatLook Viewer

Appendix A Landsat 8 Known Issues

Certain artifacts are expected in all satellite-borne sensors, and Landsat is no exception. However, moving to a push-broom sensor configuration with few moving parts, along with thorough testing, has dramatically reduced the number of issues and artifacts that have been observed on L8. Of note, several artifacts that existed on previous Landsat instruments, including cross-track banding, scan correlated shift, and dropped scan lines, are not possible on the OLI and TIRS instruments. Other artifacts such as coherent noise and memory effect exist only at very low levels and are virtually undetectable.

USGS maintains a list of L8 OLI and TIRS calibration notices that describe new or temporary artifacts and how they are addressed and corrected. Please refer to https://www.usgs.gov/land-resources/nli/landsat/calibration-validation for up-to-date information and details regarding known issues and current artifacts. In general, the known OLI and TIRS instrument image artifacts consist of stray light (TIRS only), striping, oversaturation (OLI only), and Single Event Upsets (SEUs).

A.1 TIRS Stray Light

The TIRS instrument is well within requirements for noise and stability, as determined using its onboard calibration systems. Comparisons of L8 calibrated data to surface buoy-based predictions, however, indicated a significant overestimation of radiance (TIRS results are too hot) and high variability in these comparison results. Differences between the ground-based results and TIRS results ranged up 5 K in the TIRS Band 10 and up to 10 K in TIRS Band 11. Some of this variation is related to the time of year (i.e., the temperature differences were larger during the summer, when the land surrounding the calibration sites was warmer). Additionally, some TIRS data are affected by significant banding, a low frequency variation in signal across the FOV, particularly over the three focal plane sensor chip assembly boundaries, even when viewing uniform regions. In addition, the banding may vary within a given scene in the along-track direction.

The banding that occurs in some measurements, but not in others, was hypothesized to be caused by stray light entering the optical path from outside the direct FOV. In these cases, the out-of-field light introduced additional incident energy on the detectors that was not uniform across the detector arrays. For example, during on-orbit check out, the image in Figure A-1 was acquired over Lake Superior. The image shows that the uniformity appeared to change as the TIRS instrument scanned along track from northeast to southwest across the lake. This banding change is indicated in Figure A-1 by red arrows.

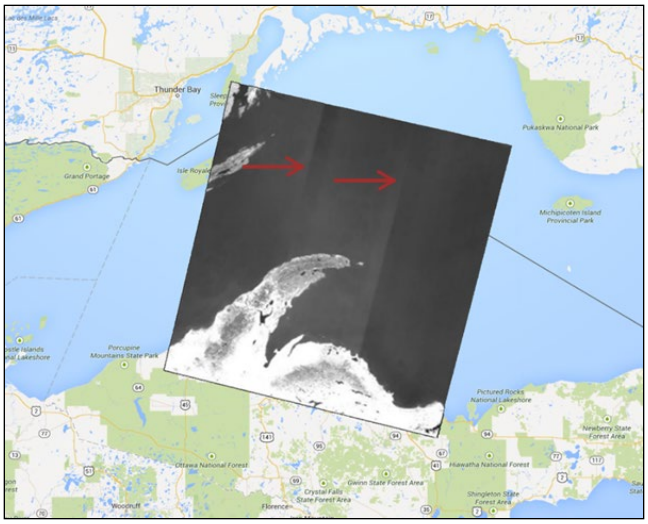

Figure A-1. TIRS Image of Lake Superior Showing Apparent Time-Varying Errors

Several scans from the Earth to the Moon were acquired to investigate the potential stray light in the optical system. The analysis of these lunar scans, along with subsequent optical modeling efforts, confirmed that radiance from outside the instrument's FOV was adding a non-uniform signal across the detectors and causing the observed banding. Additional scans of the Moon were acquired to better quantify the amount and location of stray light affecting TIRS imagery. Figure A-2 shows the results of this lunar scanning. The gray lines indicate the angle between the TIRS boresight and the Moon where there was no ghost visible in any of the TIRS detectors. The blue lines indicate where a lunar ghost was observed by at least one detector within the TIRS focal plane.

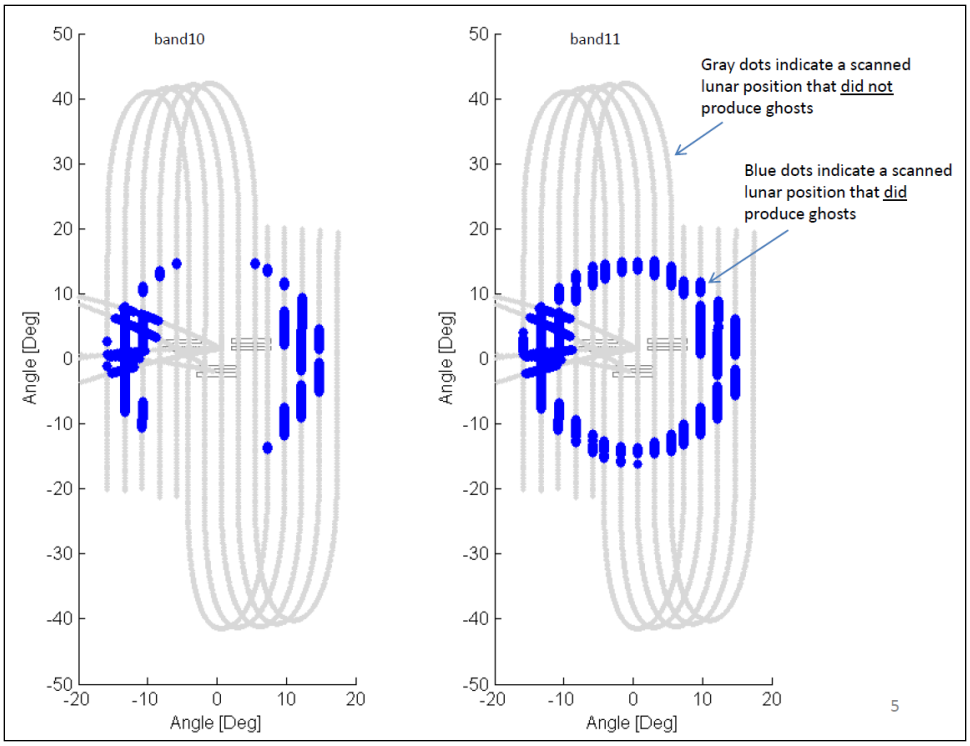

Figure A-2. TIRS Special Lunar Scan to Characterize the Stray Light Issue

The larger amount of stray light observed in Band 11 is consistent with previous observations of variation in the accuracy of the imagery based on ground measurements and the larger amount of banding. Therefore, there is little doubt that the errors observed in the current thermal band data are caused by stray light.

The Landsat CVT adjusted the TIRS band's radiometric bias to improve (but not fully eliminate) the absolute radiometric error for typical Earth scenes during the growing season. The bias corrections were implemented when the L8 data were reprocessed in February 2014. These corrections minimized the bias in temperatures derived from TIRS instrument data for typical Earth scenes. An uncertainty of ± 1 K (1 sigma) remains in temperatures derived from Band 10 data and an uncertainty of ± 2 K (1 sigma) remains in temperatures derived from Band 11 data for the test dataset.

Specifically, this stray light error was estimated to be 0.29 W/m2/sr/μm for Band 10 and 0.51 W/m2/sr/μm for Band 11. Investigations showed the TIRS instrument reported a higher radiance than the water buoy measurements, as shown in the left graph of Figure A-3. The graph on the right of Figure A-3 shows the results after accounting for this average radiance error, which is the calibration adjustment that was implemented for reprocessing in February 2014. As described above, this adjustment minimizes the apparent bias, but does not change the variance in the data resulting from stray light. Additionally, colder scenes tend to be overcorrected due to this bias adjustment. The variability in the offset, as shown in Table A-1, is about twice as large in Band 11 as Band 10, and Band 10 is about twice as large as Landsat 7 ETM+ thermal band

uncertainty. Due to the larger calibration uncertainty associated with Band 11, it is recommended that users refrain from relying on Band 11 data in quantitative analysis of the TIRS data, such as the use of split window techniques for atmospheric correction and retrieval of surface temperature values. Users should note the errors from this stray light effect are dependent on the surrounding area temperatures (including clouds), so 1-sigma variances may be misleading. Correction for the TIRS stray light requires knowledge of the temperature of the areas surrounding TIRS scenes.

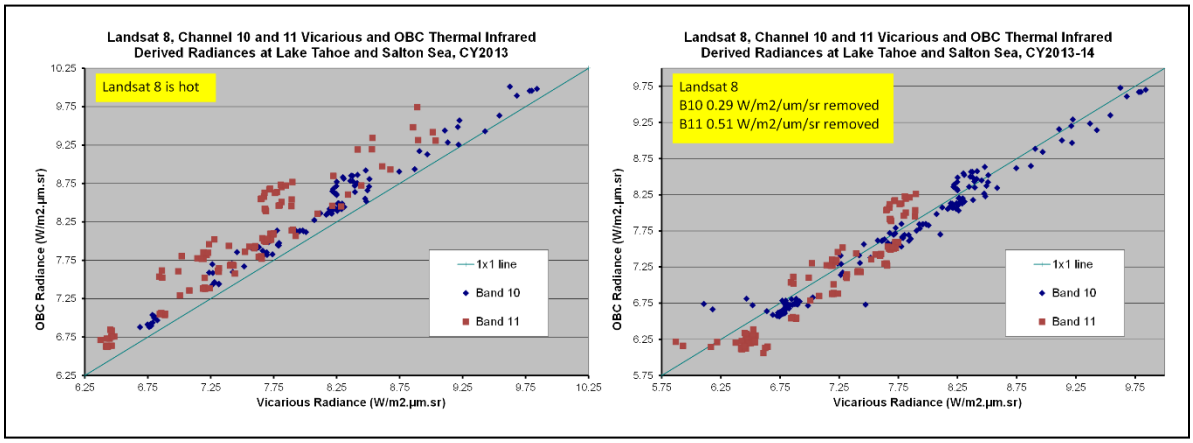

Figure A-3. Thermal Band Errors (left group) Prior to Calibration Adjustment and (right group) After Calibration Adjustment

TIRS Bands	Radiance Offset [W/m2/sr/um]	Temperature Offset [K @ 300K]
10	-0.29 +/- 0.12	-2.1 +/- 0.8
11	-0.51 +/- 0.2	-4.4 +/- 1.75

Table A-1. TIRS Band Variability

The out-of-field source of the stray light was determined based on scans of the moon and tests of a spare telescope in the lab. In general, light was impinging on the detectors from a ring about 13 degrees outside of the field of view. Each TIRS detector is affected differently, so a stray light source model was generated for every TIRS detector. On-orbit, the source of the stray light from all locations is not known, but the stray light correction algorithm uses the radiance at the edge of the image as an approximation for what might be out of view. (see Figure A-4)

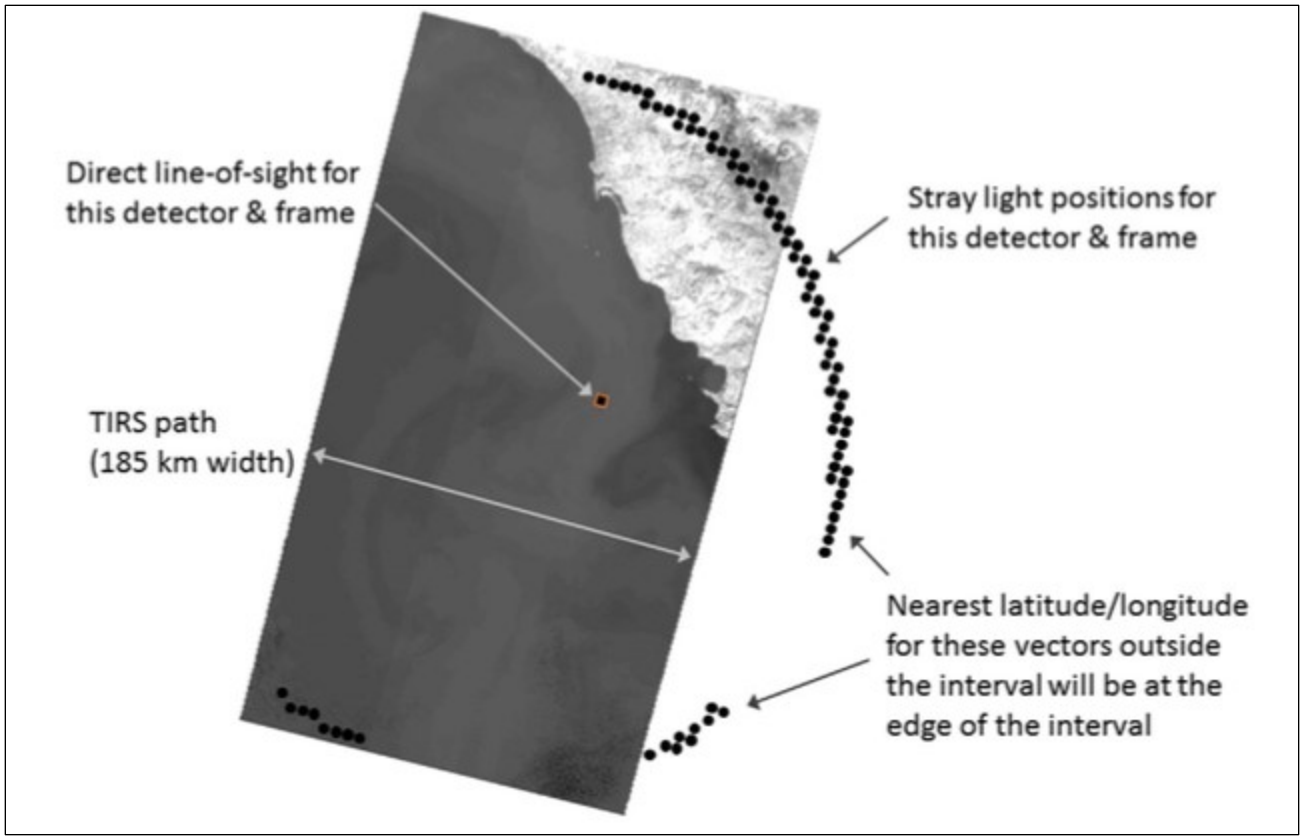

Figure A-4. Stray Light Source of a Single TIRS Detector Illustration

The source of the stray light is within the TIRS interval to the north and south of the detector, but to the east the stray light originates from outside the sensor's field-of-view (also to the west, though this detector is not affected by stray light to the west). For the locations that fall within the FOV, the TIRS scene radiance is used as the stray light radiance. For the locations that fall outside the FOV, the radiances at the edge of the scene are used as a surrogate for the actual source. This assumes that the radiances at the scene edges are roughly correlated to the radiance field outside the FOV. (Gerace and Montanaro, 2017)

Vicarious calibration data over large water bodies were used to assess the stray light corrected image data. Initial results indicate significant improvement in the absolute accuracy of both TIRS bands. Errors were reduced from 2.1K @ 300K with no correction to 0.3K with the stray light correction for Band 10 and from 4.4K to 0.19K for Band 11. Variability of these errors is reduced as well, from 0.87K to 0.52K at 300K for Band 10 and from 1.67K to 0.91K at 300K for Band 11.

An algorithm was developed and implemented into the processing system in February 2017. This change corrected the stray light and reduced the errors. (The amount of stray light in the scenes is estimated using scenes acquired before and after the target scene, as well as the edge pixels of the target scene. The stray light estimate is then subtracted from the target scene.)

A.2 TIRS Scene Select Mechanism (SSM) Encoder Current Anomaly

The TIRS SSM encoder converts angular positions to digital codes representing the orientation of the SSM. The angular position of the SSM is used to point the mirror precisely to any of three primary SSM positions: Earth imaging, blackbody calibration, and deep space calibration. The angular position of the SSM is used also during data processing to properly position TIRS pixels onto the Earth's surface. Operationally, the angular position of the SSM is provided as ancillary data to the TIRS Level 0 data processing stream (see Figure A-5).

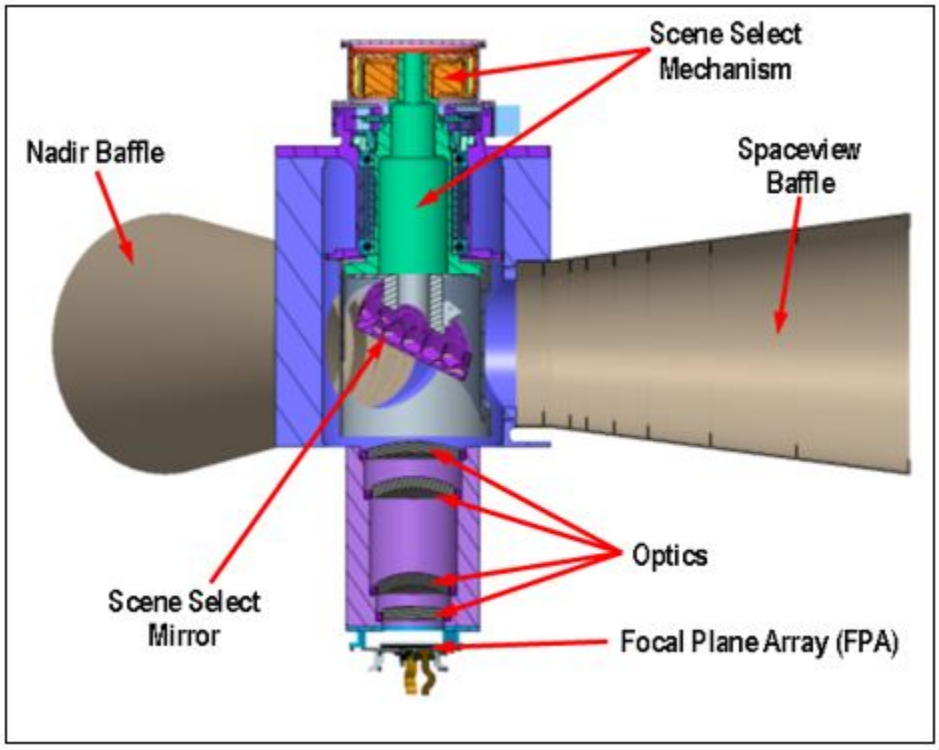

Figure A-5. Cutaway of TIRS SSM in Sensor

Anomalous current levels associated with the SSM encoder electronics have affected the acquisition and processing of L8 TIRS Level 1 data products. First discovered on December 19, 2014, activities to resolve the SSM anomaly started, and by March 2015, data was considered nominal, until a similar event happened on November 1, 2015. This section describes the background, activities, and resolutions for each of the events.

First instance – December 19, 2014

Initially detected in the fall of 2014, the telemetry data for the TIRS SSM position encoder -12V supply showed increased current. Examination of the data indicated that the current may have begun rising as early as July 2013, one month after commissioning was complete (however, performance of the SSM encoder was not affected at that time). In December 2014, the encoder current reached the "yellow limit"

threshold, set by the Flight Operations Team (FOT) as a trigger to power off the encoder (see Figure A-6). The far right side of the plot shows when the encoder was powered off and tested.

Figure A-6. Increase of -12V Current during SSM Anomaly

On December 19, 2014, the FOT suspended nominal calibration collections and suspended processing of newly acquired TIRS data while a team from the USGS and NASA established an Anomaly Review Board (ARB) to analyze the problem, determine the root cause, and conduct on-orbit tests.

The TIRS was developed with a redundant set of electronics that allow it to be switched from side A (primary) and side B (redundant/backup) if the primary electronics became inoperable. Therefore, when the encoder current reached the “yellow limit” threshold, operations on the side A electronics were stopped.

From that point forward, standard Level 1 data products contained valid OLI data (even though cloud cover assessment scores and associated attributes in the quality assurance band were of degraded quality). While TIRS data continued to be acquired, the Level 1 data product was configured to include invalid (zero-fill) data for the TIRS bands until the anomalies associated with the SSM encoder electronics could be investigated and resolved. The processing of TIRS data with gain values of “zero” was considered the most expedient fix to ground processing with minimal impact on OLI processing and Level 1 data product generation. The CVT continued to investigate whether accurate SSM pointing estimates could be derived in the absence of the normal SSM encoder measurements.

In January 2015, the FOT and subject matter experts conducted numerous tests in an effort to determine the cause of the SSM encoder current anomaly. A number of options were evaluated, with two being the best options: 1) Remaining on the A-side electronics and using a new but not fully tested operations concept for the sensor; or 2) Switching to the redundant B-side electronics and continuing with the existing pre-anomaly operations concept. Switching to the redundant electronics provides the quickest path to a full return to normal operations with minimal risk, providing the best quality science data along with the potential for an extended mission life.

After extensive investigations and testing, the TIRS electronics were switched from the primary A-side to redundant B-side on March 2, 2015. OLI imaging was suspended for 2 orbits while the switch was performed. TIRS imaging was suspended while TIRS B-side commissioning and checkout activities were completed. On March 9, 2015, TIRS resumed normal operational imaging using the B-side electronics (with a fully functional SSM encoder). On March 13, 2015, processing of TIRS data resumed, with revised CPF files established following the switch to the B-side electronics.

On April 30, 2015, reprocessing started for L8 scenes acquired from December 19, 2014, to March 13, 2015, to repopulate the TIRS data using SSM position estimates derived from image measurements where necessary. Some TIRS data for a number of scenes were not processed due to non-nominal instrument configuration. There were several intervals identified for which the data was good for a portion of the interval, but where the SSM was commanded to rotate off nadir, making the TIRS data unusable for the remaining duration of the interval. Scenes acquired when TIRS was well outside the field of view of OLI (due to an off nadir SSM) were produced as OLI-only products. The reprocessing effort completed on May 18, 2015.

The table below shows the reprocessing periods for L8 data affected by the 2014 TIRS SSM anomaly.

Acquisition Date Range	Sensor Imagery Acquired	Provisional TIRS Product Availability	Reprocessing Period	Nominal TIRS Data Product Availability	Notes
December 19, 2014 – March 1, 2015 (23:57:34 UTC)	OLI & TIRS	N/A	April 30, 2015 - May 18, 2015	May 18,2015	Several lost TIRS scenes in the period; TIRS imaging stopped in preparation for TIRS side-swap
January 30, 2015	OLI & TIRS (see notes)	N/A	N/A	N/A	Path 14 Rows 40-121 SSM off-nadir; OLI only data products
February 2, 2015	OLI & TIRS (see notes)	N/A	N/A	N/A	Path 35 Rows 13-43 SSM off-nadir; OLI only data products

Acquisition Date Range	Sensor Imagery Acquired	Provisional TIRS Product Availability	Reprocessing Period	Nominal TIRS Data Product Availability	Notes
December 19, 2014 – March 1, 2015 (23:57:34 UTC)	OLI & TIRS	N/A	April 30, 2015 - May 18, 2015	May 18,2015	Several lost TIRS scenes in the period; TIRS imaging stopped in preparation for TIRS side-swap
February 10, 2015	OLI & TIRS (see notes)	N/A	N/A	N/A	Paths 11, 27, 43, 59, 75, 91 SSM off-nadir; OLI only data products
February 11, 2015	OLI & TIRS (see notes)	N/A	N/A	N/A	Paths 2, 6, 18, 34, 50, 82, 107, 123, 139, 155, 171, 187, 203, 219 SSM off-nadir; OLI only data products
February 19, 2015	OLI & TIRS (see notes)	N/A	N/A	N/A	Path 21 Rows 28-50 SSM off-nadir; OLI-only data products
March 2, 2015 (13:53:23 UTC) - March 3, 2015 (00:40:35 UTC)	None	N/A	N/A	N/A	No TIRS or OLI data acquired due to TIRS side-swap activities
March 3, 2015 (00:40:35 UTC) - March 4, 2015 (00:02:18 UTC)	OLI	N/A	N/A	N/A	OLI-only imaging resumes
March 4, 2015 (00:02:18 UTC) - March 4, 2015 (16:20 UTC)	OLI & TIRS (see notes)	N/A	N/A	N/A	B-Side; Paths 5, 94, 110, 126, 142, 158, 174, 190, 206, 222 SSM off-nadir; OLI-only data products
March 4 (16:20:00 UTC) - March 7 (00:00:00 UTC)	OLI & TIRS	N/A	April 13, 2015 - April 20, 2015	April 20,2015	B-side, nominal SSM; without TIRS calibration parameters
March 7 (00:00:00 UTC) - April 13, 2015	OLI & TIRS	March 16, 2015	April 13, 2015 - April 20, 2015	April 20,2015	Nominal TIRS that includes regular Blackbody and

Acquisition Date Range	Sensor Imagery Acquired	Provisional TIRS Product Availability	Reprocessing Period	Nominal TIRS Data Product Availability	Notes
December 19, 2014 – March 1, 2015 (23:57:34 UTC)	OLI & TIRS	N/A	April 30, 2015 - May 18, 2015	May 18,2015	Several lost TIRS scenes in the period; TIRS imaging stopped in preparation for TIRS side-swap
(23:59:59 UTC)					Deep space calibration collects

Table A-2. Reprocessing Schedule for SSM Anomaly

CPF File Changes Required to Support SSM Anomaly

CPF files for the December 19, 2014, to March 4, 2015 anomaly period have updated Earth-orientation parameters, which may cause a slight change (< 3 m) in the geometry of OLI and TIRS bands within L1Gt products.

From December 19, 2014, to March 7, 2015, there were no TIRS calibration collections; therefore, TIRS data for that period were processed using nominal pre-anomaly calibration parameters. This caused a slight degradation in thermal measurements, but worst-case errors are estimated at 0.2 Kelvin (K) when viewing a 300 K target. The errors introduced by not having calibration collects for this period of time are much smaller than the errors introduced by TIRS stray light, which can reach up to 2 to 4 K. Several intervals were identified as having a single event which could cause an anomaly within the imagery. During the acquisition of these intervals, the Mission Operations Center issued commands to switch modes of operation on the SSM and a movement of the SSM occurred.

These data were processed as nominal; however, the TIRS quality scores were lowered from the nominal “9” to “8”, to indicate lower quality. The images below are examples where the mode of operations was changed within a scene, causing a small anomaly visible in the TIRS data. Figure A-7 displays the anomaly for Landsat 8 Path 75 Row 17 acquired February 26, 2015.

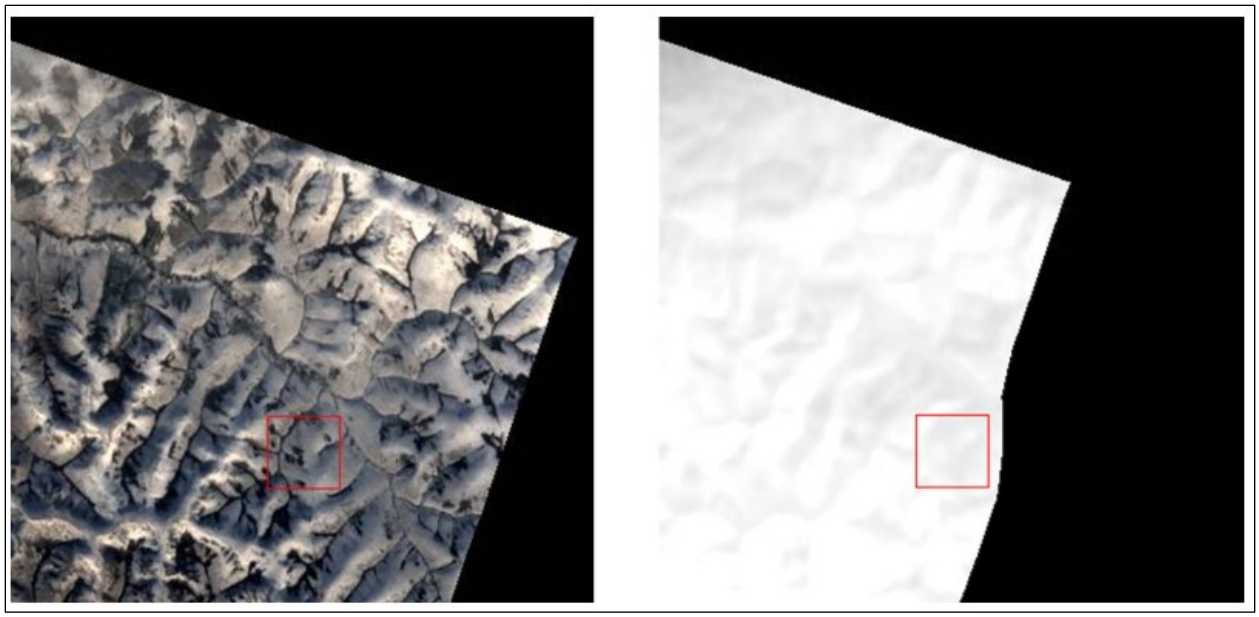

Figure A-7. OLI (left) and TIRS (right) Images Showing Mode Change Anomaly

Second Instance – November 1, 2015

In late October 2015, the L8 Flight Operations Team (FOT) noticed an increasing trend in the B-side encoder electronics current, and on November 1, 2015, the TIRS instrument experienced another anomalous condition related to the instrument's ability to accurately measure the location of the SSM. The anomaly caused the upper bits of the encoder counts in the ancillary data to be corrupt, resulting in the TIRS bands becoming mis-registered by approximately 500 m (18 pixels). The encoder was powered off during a morning pass on Monday, November 2, 2015.

OLI data was not affected, and as before, TIRS data continued to be collected, but the it the Level 1 products contained TIRS bands temporarily zero-filled until the conditions of this anomaly could be investigated and categorized.

The L8 Flight Operations Team (FOT) monitored current levels within the TIRS SSM encoder electronics, the CVT analyzed instrument telemetry, and the TIRS image data in order to accurately measure the position of the SSM. This information was needed for the development of a model of SSM motion that could be used to process TIRS data collected under an alternative operations concept without active SSM control and with only limited encoder measurements.

TIRS data continued to be collected with the scene select mirror encoder electronics disabled (mode 0). While in this mode, the TIRS LOS model was regularly updated using SSM position estimates derived from image measurements. An updated geometric modelling approach was finalized, and the algorithms and code were placed into the LPGS and then tested and verified.

In February 2016, L8 data acquired from November 1 to December 31, 2015, were reprocessed into nominal Level 1 products containing valid TIRS data.

On April 25, 2016, a new LPGS release was implemented to restore the ability to produce valid thermal data for L8 scenes from this date forward, as well as L8 data acquired from January 1 to April 25, 2016.

Newly processed L8 data use preliminary estimated position information for the SSM encoder. To compensate for not having SSM encoder information to indicate where the TIRS sensor is pointing, a new algorithm was developed to provide estimates for the TIRS SSM encoder position.

A new parameter in the Landsat 8 metadata (MTL.txt) file provides the result of the algorithm: **"TIRS_SSM_MODEL"**. This parameter contains one of three labels:

- **Preliminary.** Most of new acquisitions are processed and labeled as Preliminary because the estimated SSM position information used to process the data is predicted from the SSM movement trend. These scenes have a higher uncertainty in the OLI/TIRS band alignment, which likely results in OLI/TIRS band misregistration: starting at ~60-90 m, Linear Error 90 percent (LE90) confidence level follows each twice-per-lunar-cycle TIRS radiometric calibration event and improves to ~30 m LE90 within one to two days following each event.

  When the TIRS_SSM_MODEL parameter is "Preliminary", the "IMAGE_QUALITY_TIRS" parameter in the MTL file is set to a lower value to provide an additional indication that the TIRS quality is not normal.

  After 12 to 16 days (coinciding with both the full moon and midway between full moons of each month), the data are reprocessed using the refined final estimated SSM position. After the data is reprocessed, it is re-labeled "Final".

- **Final.** Scenes that display this label contain TIRS data that have been reprocessed using all available SSM encoder telemetry information and refined TIRS LOS model parameters. These data should align properly with the OLI bands, and the quality closely approximates the "Actual" encoder values. The registration of the TIRS bands in scenes with the "Final" TIRS_SSM_MODEL should be as good as the "Actual" scenes: ~20 m, LE90.

- **Actual.** Scenes displaying this label contain TIRS data processed using actual measured SSM positions determined from the SSM encoder telemetry. Level 1 data products labeled "Actual" contain the best TIRS quality available, resulting in TIRS bands aligning properly with OLI bands.

TIRS data with the metadata parameter TIRS_SSM_MODEL of "Final" or "Actual" are geometrically accurate enough for normal use; however, the TIRS Stray Light anomaly has not been addressed, so these data are not precise enough for use in a split-window algorithm.

A.3 Lower Truncation Acquisitions

The detectors of the Landsat 8 OLI can register 14 bits of data. However, only the upper or lower 12 bits are transmitted from the spacecraft to the ground. During normal operations, the upper 12 bits are transmitted to the USGS ground station to maximize the dynamic range.

On occasion, USGS and NASA calibration and validation engineers submit special requests to acquire some path/rows in the lower truncation mode — meaning that the spacecraft only transmits data to the ground station from the instruments lower 12 bits. Landsat 8 lower truncation acquisitions were made in 2013, 2015, and in 2019 (details are listed below).

During lower truncation mode acquisitions, regions of high brightness within a scene exceed the lower 12-bit range of 4096 (digital number values per detector), causing the count to begin again using the 13th and 14th bits, which are beyond the lower 12-bit range reported. This causes the numeric values to "roll over" and start counting from zero again. Pixels affected by ‘roll over’ do not correctly reflect the brightness of the Earth’s surface and will visually take on an apparently random value (See Figure A-8).

These roll over values are not differentiated from valid values elsewhere in the image. More so, the cloud information in the Landsat 8 OLI Quality Assessment Band is unreliable.

NOTE: Data acquired in lower truncation mode are available for download from EarthExplorer, and while most cloud free acquisitions will not be affected by the lower truncation mode setting, users should use caution if using these images for operational activities. The metadata field SENSOR_MODE indicates "TRUNCATION_OLI = "LOWER" for these scenes.

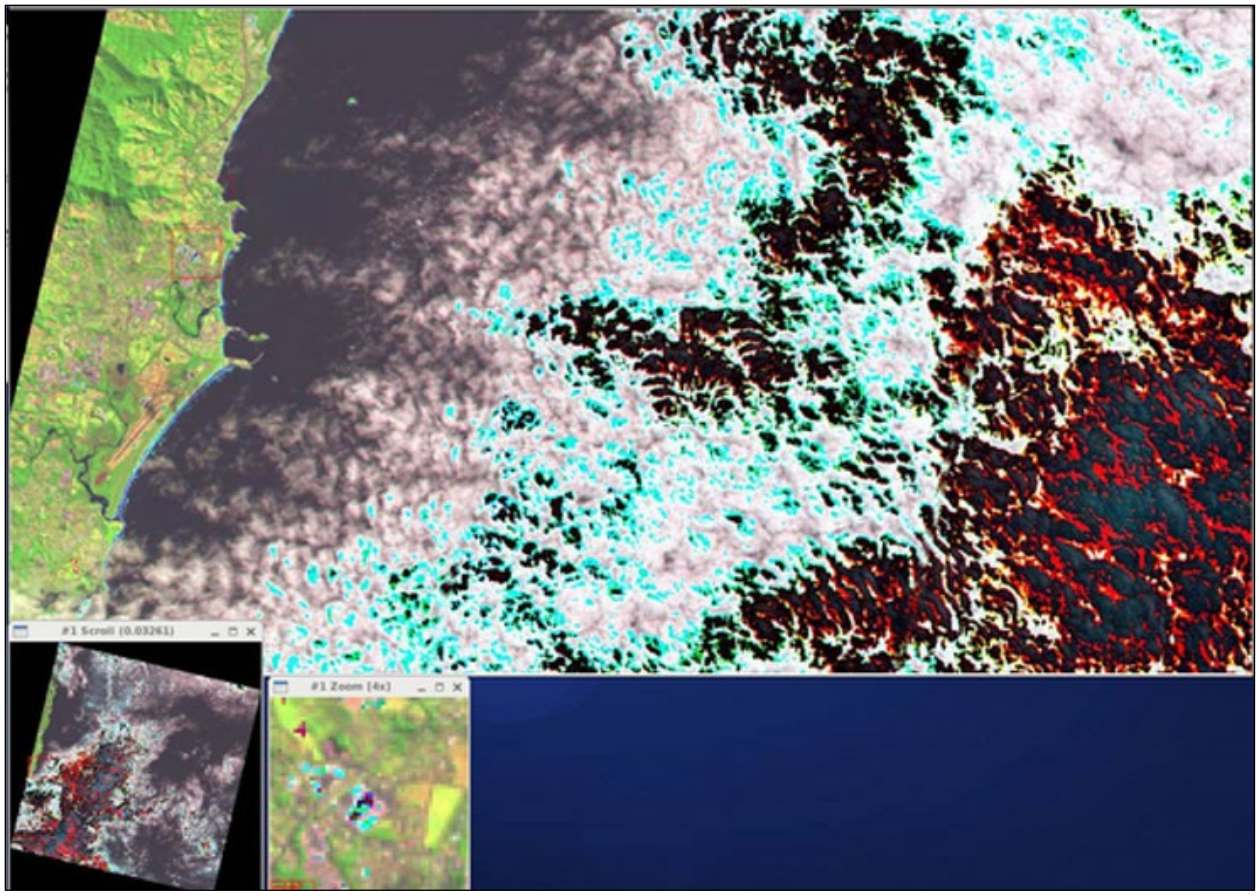

Figure A-8. Landsat 8 Oversaturated Pixels Acquired with Lower 12 Bits

The 2013 scenes were acquired during the on-orbit checkout period, prior to data becoming available to all users. This file lists the 2013 scenes acquired in lower truncation mode.

Scenes acquired in 2015 were used to investigate the value of the lower two bits and support the possibility of downloading all 14 bits of data for Landsat 9. Data to support two studies were acquired: 1) a night interval through the western United States over fires and urban areas, and 2) a day interval off the coast of eastern Australia over dark water. The artifacts are most noticeable over fires in the night data, and over clouds in the day data.

The dates and locations affected by 2015 Landsat 8 12-bit lower truncation studies are listed below.

Western United States (nighttime acquisitions)
Path 139, Rows 202 to 2017
August 22, 2015 (DOY 234)
September 7, 2015 (DOY 250)
September 23, 2015 (DOY 266)

Features include: San Diego (row 207), Los Angeles (row 208), Lake Tahoe (row 211), Portland, Mount St Helens, Mount Hood (row 216), Mount Adams, Mount Adams Wildfire (row 216), and Seattle, Mount Rainer (row 217).

Eastern Australia dark water coastal (daytime acquisitions)
Path 88, Rows 75 to 84
September 1, 2015 (DOY 244)
September 17, 2015 (DOY 260)
October 3, 2015 (DOY 276)
Features include: Coastal Australia (rows 80-82), Cato Reef (row 76)
From September to December 2019, a number of scenes are being acquired in lower truncation mode. The dates and affected paths are listed on the Landsat 8 Lower Truncation webpage.

The dates and path/rows affected by 2019 Landsat 8 12-bit lower truncation studies are listed below. Typically, only the first row "001" is affected. However, affected additional rows are listed below. Visit the Landsat 8 Lower Truncation webpage for more details.

September 2019

9/12-DOY 255: Path 24 Rows 244-248, Path 40 Rows 001-002
9/17-DOY 260: Path 27 Rows 246-248, Path 43 Rows 001-036
9/19-DOY 262: Path 25 Rows 247-248, Path 41 Rows 001-038
9/26-DOY 269: Path 42 Rows 001-037
9/28-DOY 271: Path 40 Rows 001-003

October 2019

10/3-DOY 276: Path 43 Rows 001-036
10/5-DOY 278: Path 41 Rows 001-038
10/12-DOY 285: Path 42
10/14-DOY 287: Path 40
10/19-DOY 292: Path 43
10/21-DOY 294: Path 41
10/28-DOY 301: Path 42
10/30-DOY 303: Path 40

November 2019

11/4-DOY 308: Path 43
11/6-DOY 310: Path 41
11/13-DOY 317: Path 42
11/15-DOY 319: Path 40
11/20-DOY 324; Path 43
11/22-DOY 326: Path 41
11/29-DOY 333: Path 42

December 2019

12/1-DOY 335: Path 40
12/6-DOY 340: Path 43
12/8-DOY 342: Path 41
12/15-DOY 349: Path 42
12/17-DOY 351: Path 40
12/22-DOY 356: Path 43
12/24-DOY 358: Path 41
12/31-DOY 365: Path 42

A.4 Striping and Banding

Striping is a phenomenon that appears as columns of consistently lighter or darker pixels in a single band of radiometrically corrected data. Banding is a similar phenomenon, but it occurs across multiple contiguous columns. Both are often caused by incorrect calibration of detectors with respect to one another. These effects in OLI imagery are less than 4 DN in its 12-bit dynamic range, or less than 0.5 percent of the radiance of a typical Earth image and are generally seen in OLI Bands 1 (CA), 2 (Blue), and 9 (Cirrus). This low level of non-uniformity is typically not visible to most users of L8 data. Figure A-9 and Figure A-10 are examples of striping and banding.

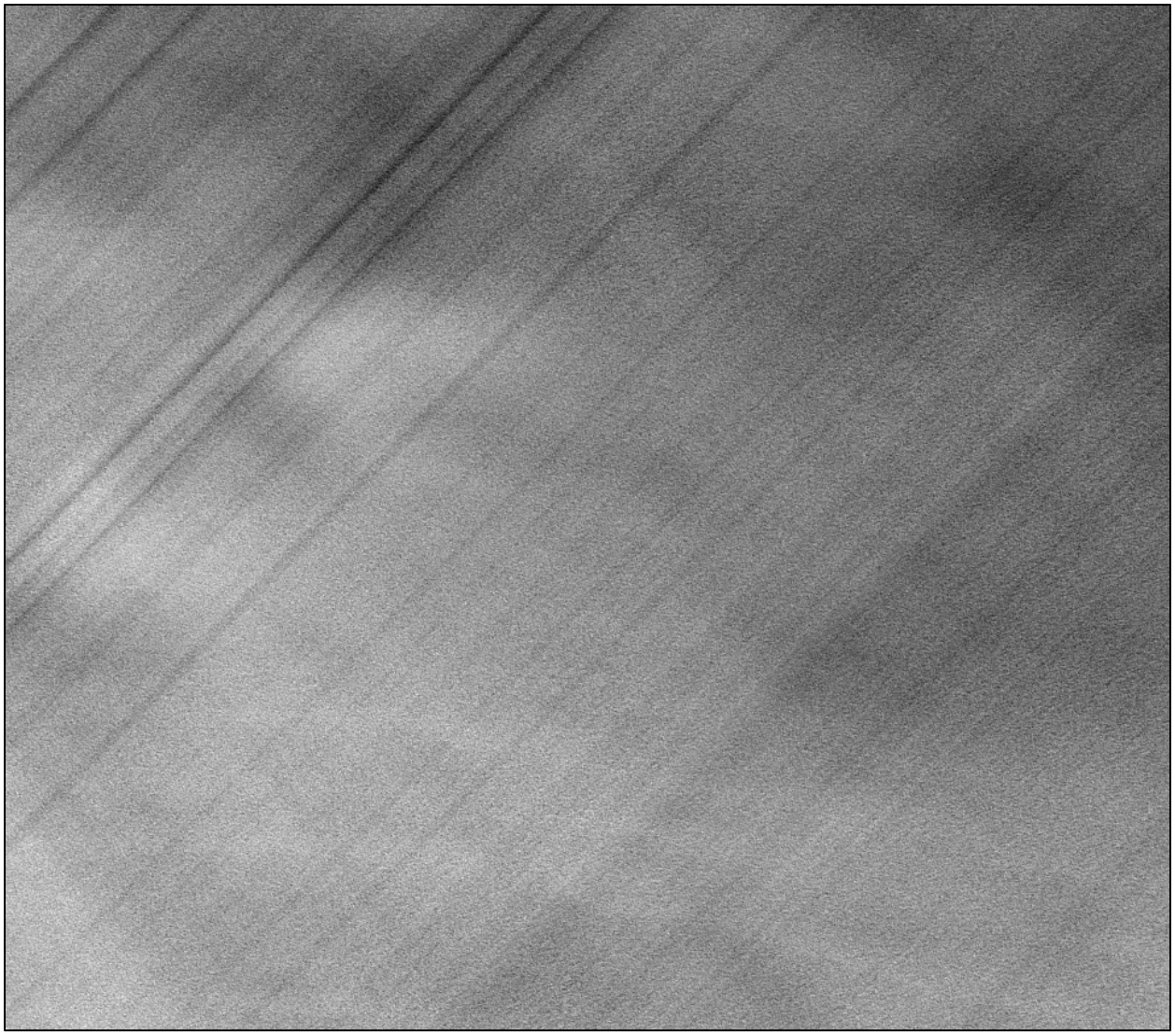

Figure A-9. Striping and Banding Observed in Band 1

Figure A-9 displays the striping and banding observed in Band 1 (Coastal Aerosol) in Landsat 8 Path 16 Row 4 (acquired April 28, 2013), which is over a very homogenous region of the Greenland ice sheet. Single-pixel wide columns are considered striping; the thicker columns are banding.

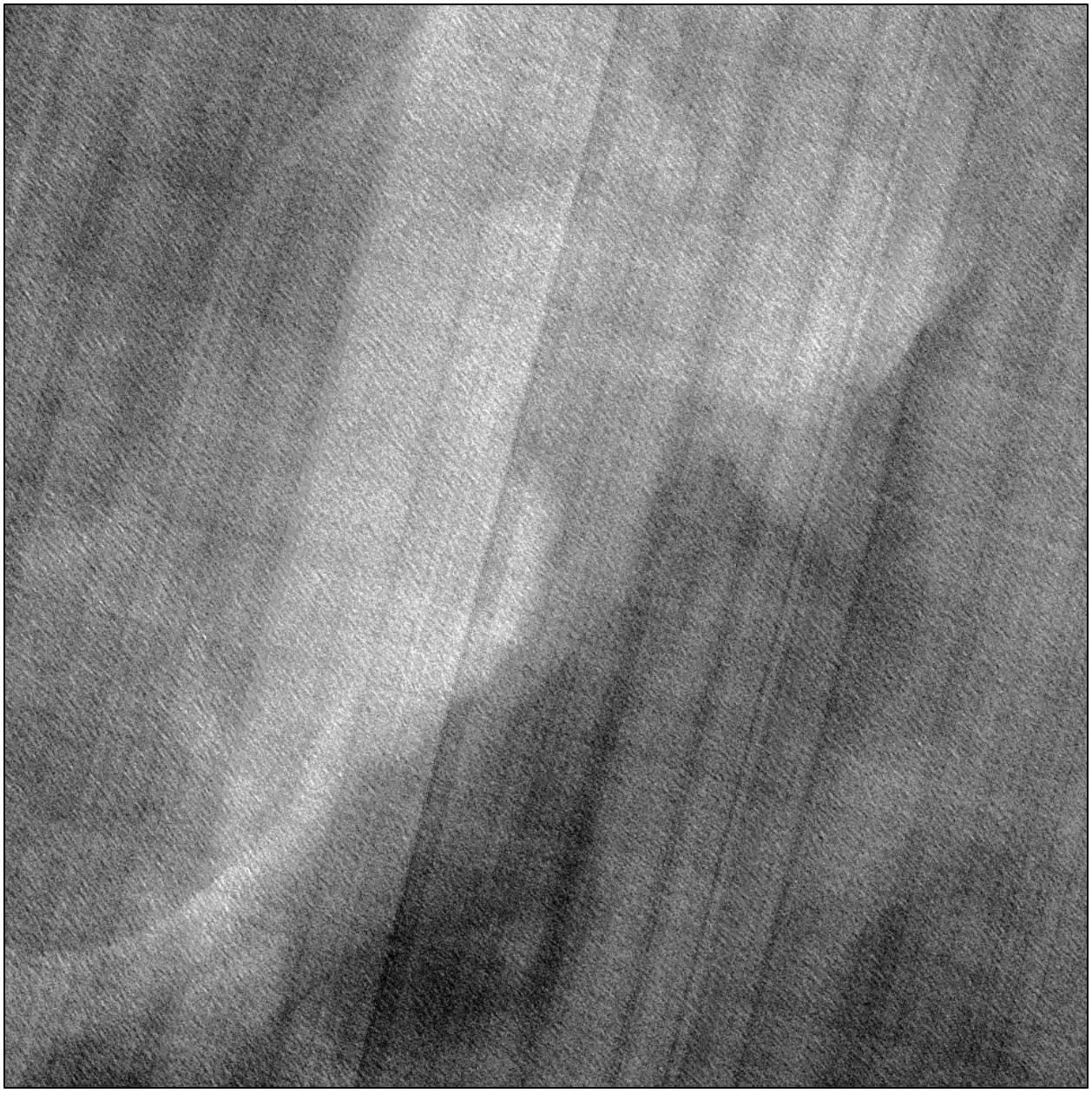

Figure A-10. Striping and Banding Observed in Band 2

Figure A-10 displays the striping and banding observed in Band 2 (Blue band) in Landsat 8 Path 75 Row 88 (acquired May 11, 2013), which is over clear, calm ocean water.

Striping and Banding also affect TIRS imagery, as seen in Figure A-11.

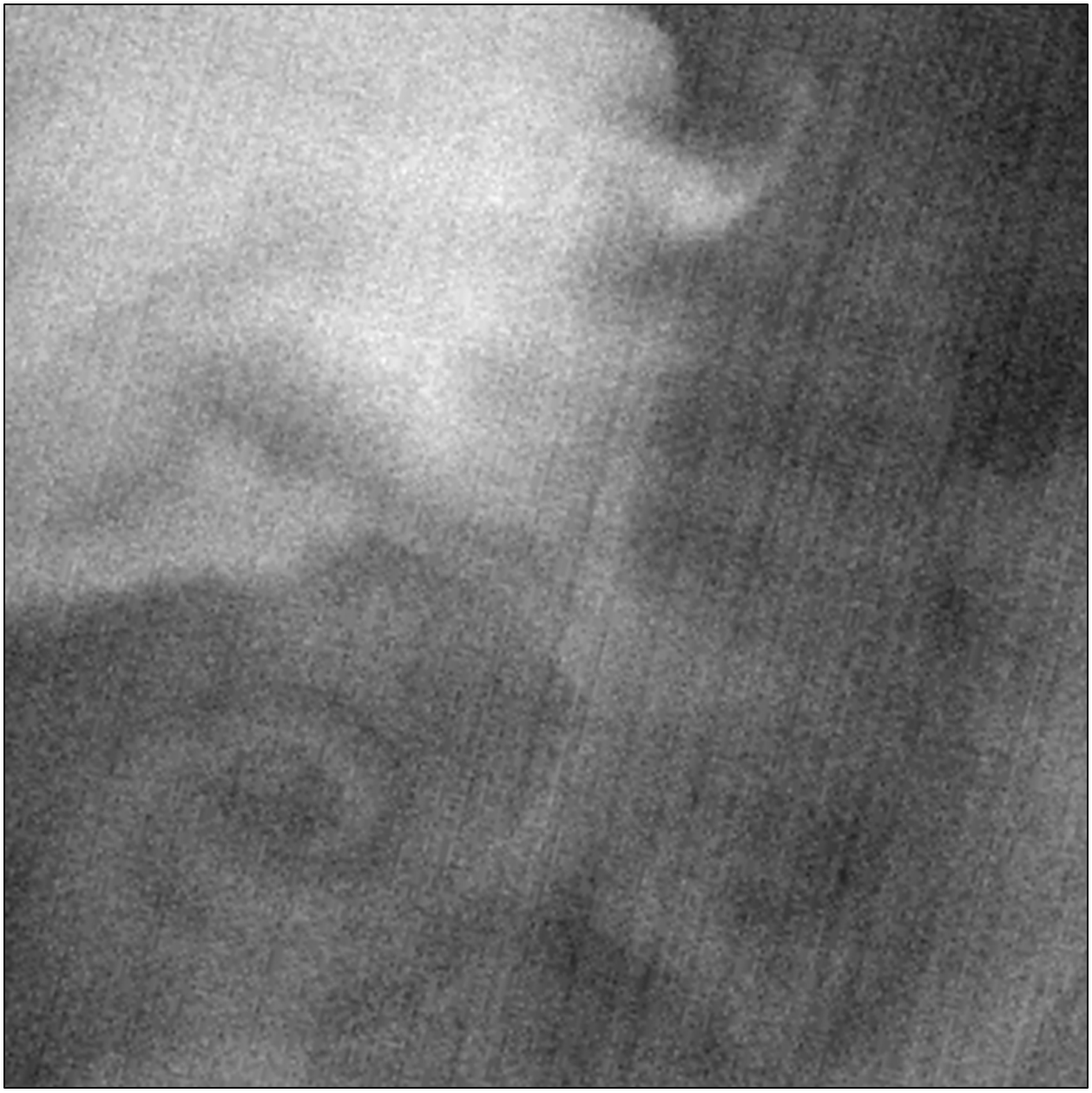

Figure A-11. Striping and Banding observed in TIRS Band 10

Figure A-11 displays the striping and banding observed in TIRS Band 10 in Landsat 8 Path 75 Row 88 (acquired May 11, 2013), which is over clear, calm ocean water. This low level of non-uniformity is typically not visible to most users of L8 data.

Normal radiometric processing removes most of the banding and striping in OLI and TIRS imagery. The CPF used during Level 1 processing provides the parameters for corrections. However, minor responsivity changes in individual detectors cannot be accounted for, so some non-uniformity will remain in the data. Some of this striping may be corrected with future calibrations.

A.5 SCA Overlaps

Both OLI and TIRS are designed with discrete SCAs, which have some detectors overlapping the adjacent SCAs. This causes a small region between each SCA to be viewed by multiple detectors. The imagery for this region is created by averaging over the detectors viewing each pixel. In some situations, this can cause an artifact that resembles banding, but it is in fixed locations and often transient, depending on the underlying terrain.

SCA overlap artifacts are most visible over high clouds, as the detectors on each SCA view a slightly different area of each cloud. Figure A-12 shows an example of this.

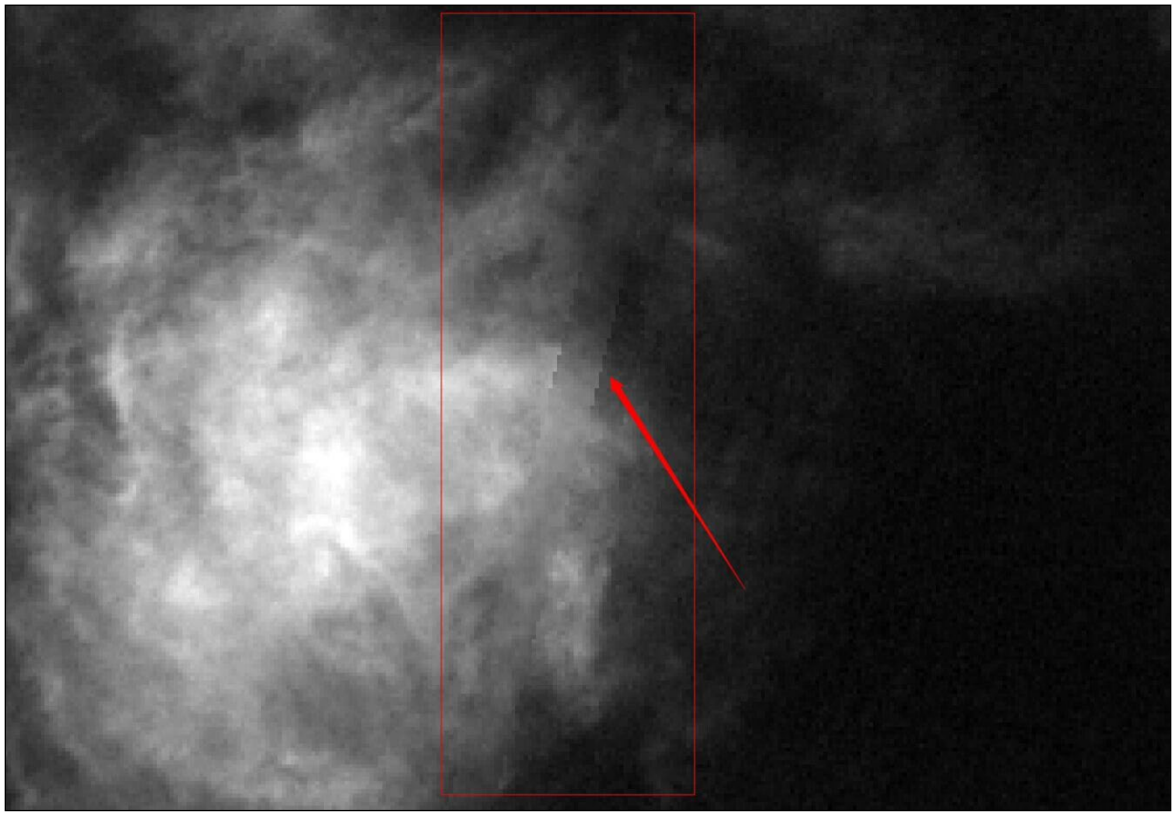

Figure A-12. SCA Overlap Visible in Band 9

Figure A-12 displays the SCA overlap artifact observed in Band 9 (cirrus band) in Landsat 8 Path 14 Row 36 (acquired April 1, 2014), where high clouds were visible at the boundary between two SCAs.

SCA overlaps are commonly seen in TIRS imagery because of contributions from the stray light artifact.

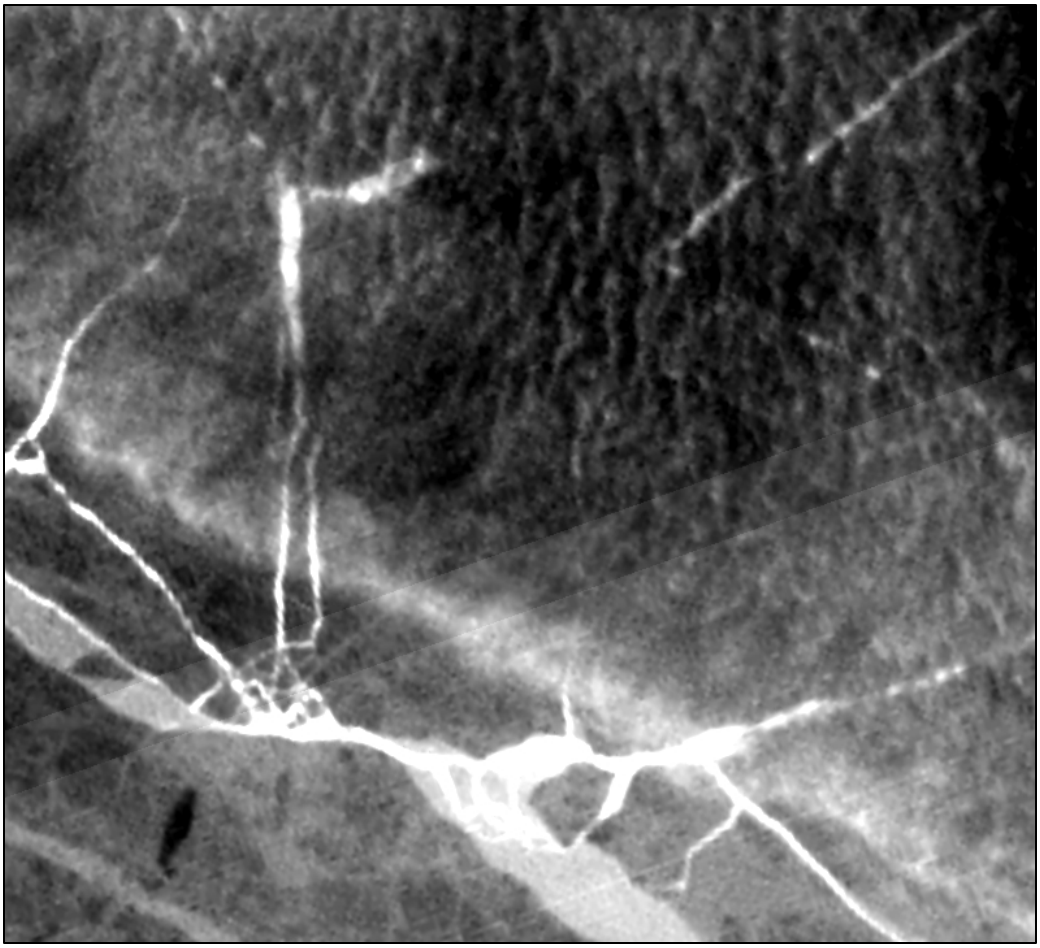

Figure A-13. SCA Overlap Visible in TIRS Band 10

Figure A-13 displays the SCA overlap artifact observed in TIRS Band 10 in Landsat 8 Path 37 Row 248 (acquired May 17, 2013) at the boundary between two SCAs. In this image, stray light has shifted the calibration of two adjacent SCAs, making the overlap region visible.

A.6 Oversaturation

Oversaturation occurs when a detector views an object that is much brighter than the maximum radiance the instrument was designed to handle. This causes the detector to deliver a voltage that is larger than expected by the 12-bit electronics, so the detector's value rolls over the 12-bit limit and records as a very small integer. Therefore, this artifact appears as dark spots in the middle of very bright objects. Figure A-14 represents an oversaturation example in Landsat 8 SWIR Bands 6 and 7, in Path 188 Row 34 (acquired October 26, 2013).

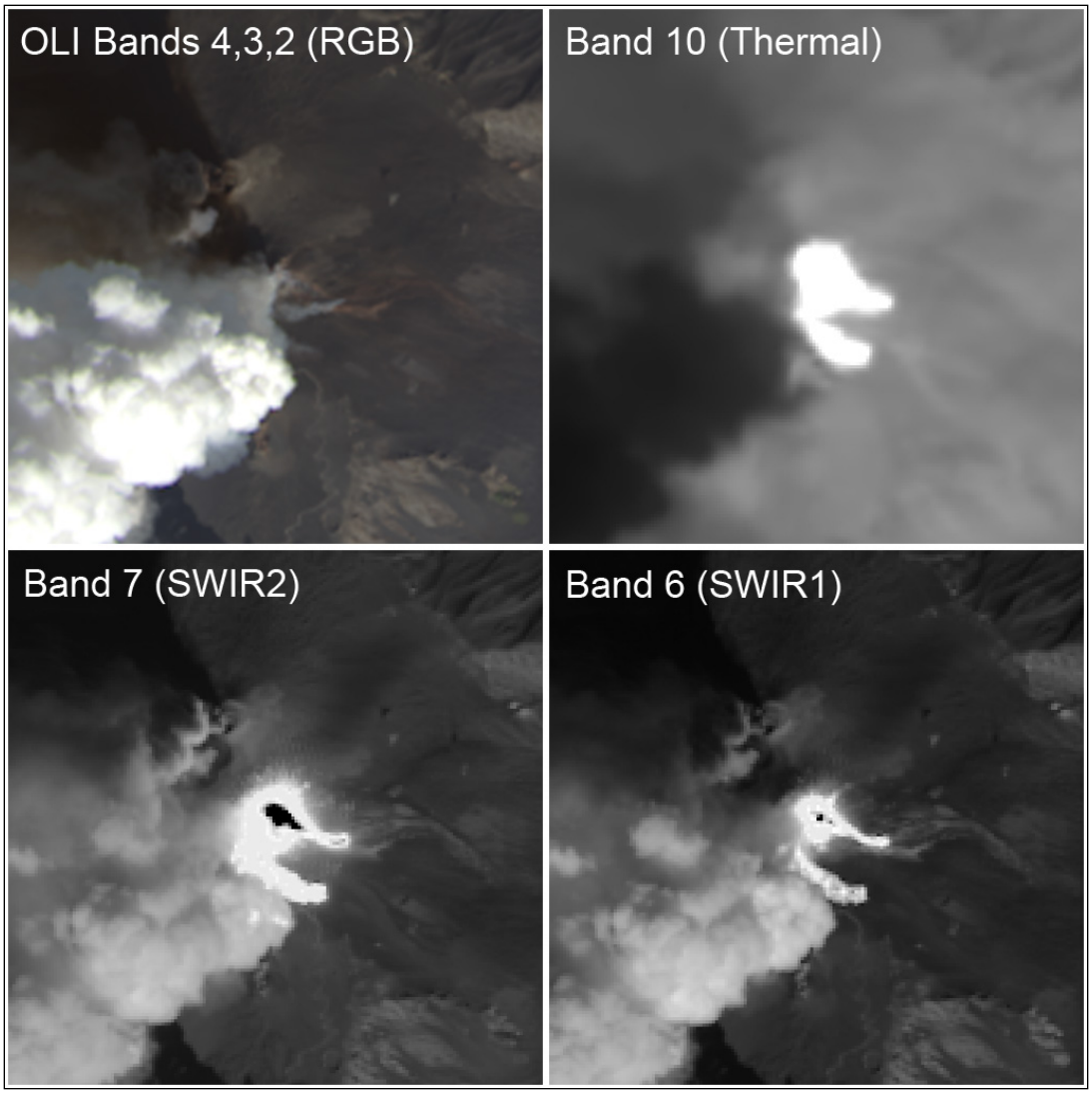

Figure A-14. Oversaturation Example in OLI SWIR Bands 6 & 7

Oversaturation artifacts are typically rare but are repeatable artifacts that normally occur in OLI Bands 7 and 6 over large fires or volcanic events. Additionally, oversaturation may occur in other OLI bands over land surface objects that are very bright or exhibit strong specular reflectance. Oversaturation does not cause permanent harm to the instrument, and the detectors recover immediately with no visible memory effect.

A.7 Single Event Upsets (SEUs)

An SEU is a “catch-all” term used for any electronic fault that causes brief, instantaneous artifacts in the imagery. Usually, SEUs are caused by charged particles from the Earth's radiation belts striking the detectors or instrument electronics. These particle hits are relatively rare but are seen more commonly over the poles and over the South Atlantic Anomaly – a region where the Earth's magnetic field is weakest, and the radiation belt is at its lowest altitude. Transmission errors can also cause SEUs, but due to the design of L8, these errors are not possible with OLI or TIRS imagery.

SEUs appear in OLI as single-frame bright spots that may affect several detectors in a line. The electronics design is such that SEUs often affect only odd or even detectors, but as seen in the lower portion of Figure A-15, can affect both odd and even detectors with a two-pixel gap between the odd and even detectors. Users may never notice an SEU because they are rare, typically only a single pixel, and geometric resampling distorts or erases these small artifacts in Level 1 products. They are most visible in Level 1 Radiometric (Corrected) (L1R) or Level 0 imagery. Figure A-15 is an example of a couple SEU events measured by OLI. As noted above, the SEU clearly manifests as a line of single-frame bright spots.

Figure A-15. Example of OLI SEU Event

SEUs occur at random. They cannot be corrected, but their effect on the imagery is minor. They do not cause permanent harm to the instrument detectors.

Appendix B Observatory Component Reference Systems

B.1 Observatory Component Reference Systems

The L8 IAS geometry algorithms use ten coordinate systems. These coordinate systems are referred to frequently in the remainder of this document and are briefly defined here to provide context for the subsequent discussion. They are presented in the order in which they would be used to transform a detector and sample time into a ground position.

B.2 OLI Instrument Line-of-Sight (LOS) Coordinate System

The OLI LOS coordinate system is used to define the band and detector pointing directions relative to the instrument axes. These pointing directions are used to construct LOS vectors for individual detector samples. This coordinate system is defined so that the Z-axis is parallel to the telescope boresight axis and is positive toward the OLI aperture. The origin is where this axis intersects the OLI focal plane.

The X-axis is parallel to the along-track direction, with the positive direction toward the leading, odd numbered SCAs (see Figure B-1). The Y-axis is in the across-track direction with the positive direction toward SCA01. This definition makes the OLI coordinate system nominally parallel to the spacecraft coordinate system, with the difference being due to residual misalignment between the OLI and the spacecraft body.

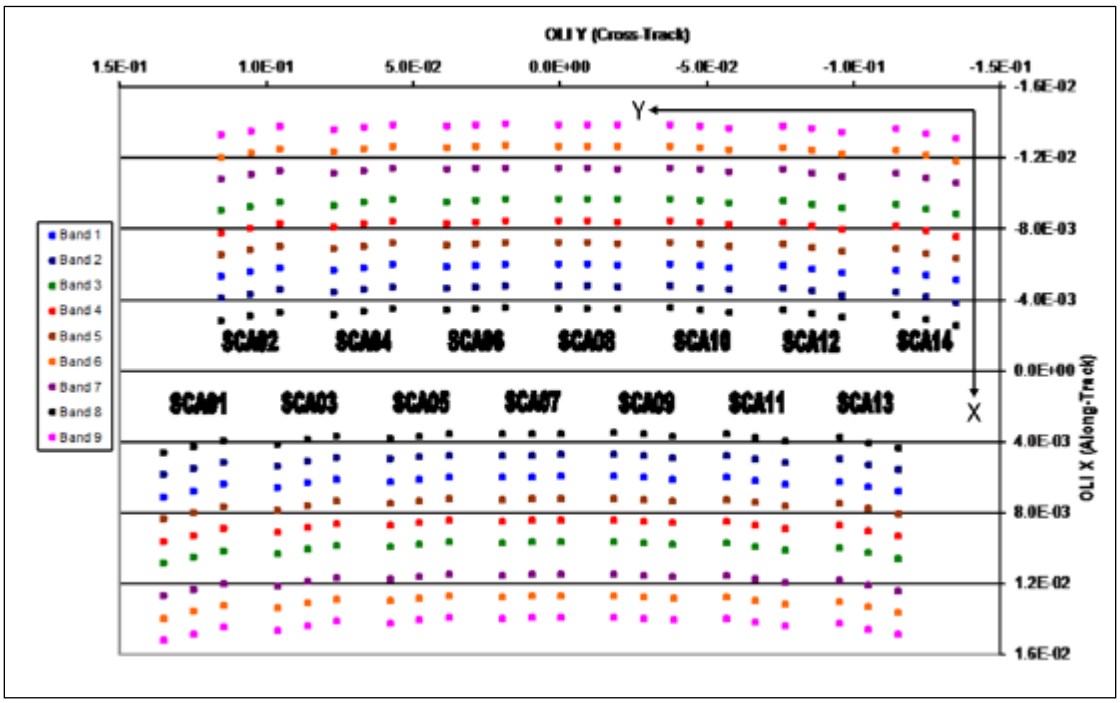

Figure B-1. OLI Line-of-Sight (LOS) Coordinate System

B.3 TIRS Instrument Coordinate System

The orientations of the TIRS detector LOS directions and of the TIRS Scene Select Mirror (SSM) are both defined within the TIRS instrument coordinate system. TIRS LOS coordinates define the band and detector-pointing directions relative to the instrument axes. These pointing directions are used to construct LOS vectors for individual detector samples. The vectors are then reflected off the SSM to direct them out of the TIRS aperture for Earth viewing. The TIRS LOS model is formulated so that the effect of a nominally pointed SSM is included in the definition of the detector lines-of-sight, with departures from nominal SSM pointing causing perturbations to these lines-of-sight. This formulation allows TIRS LOS construction to be very similar to OLI. This is described in detail below, in the TIRS LOS Model Creation algorithm.

The TIRS coordinate system is defined so that the Z-axis is parallel to the TIRS boresight axis and is positive toward the TIRS aperture. The origin is where this axis intersects the TIRS focal plane. The X-axis is parallel to the along-track direction, with the positive direction toward the leading SCA (SCA02 in Figure B-2). The Y-axis is in the across-track direction with the positive direction toward SCA03. This definition makes the TIRS coordinate system nominally parallel to the spacecraft coordinate system, with the difference being due to residual misalignment between the TIRS and the spacecraft body.

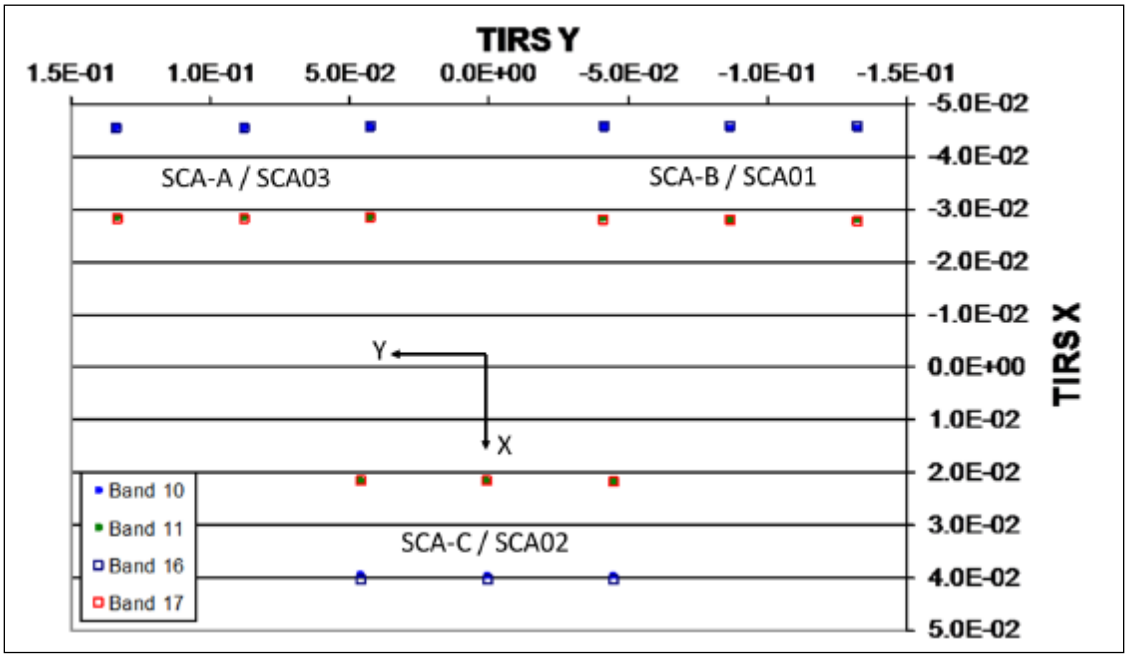

Figure B-2. TIRS Line-of-Sight (LOS) Coordinates

B.4 Spacecraft Coordinate System

The spacecraft coordinate system is the spacecraft-body-fixed coordinate system used to relate the locations and orientations of the various spacecraft components to one another and to the OLI and TIRS instruments. It is defined with the +Z axis in the Earth-

facing direction, the +X axis in the nominal direction of flight, and the +Y axis toward the cold side of the spacecraft (opposite the solar array). This coordinate system is used during Observatory integration and pre-launch testing to determine the pre-launch positions, alignments of the attitude control sensors (star trackers and SIRU), and instrument payloads (OLI and TIRS). The spacecraft coordinate system is nominally the same as the navigation reference system (see below) used for spacecraft attitude determination and control. However, for reasons explained below, these two coordinate systems are treated separately.

B.5 Navigation Reference Coordinate System

The navigation reference frame (a.k.a., the attitude control system reference) is the spacecraft-body-fixed coordinate system used for spacecraft attitude determination and control. The coordinate axes are defined by the spacecraft ACS, which attempts to keep the navigation reference frame aligned with the (yaw-steered) orbital coordinate system (for nominal nadir pointing) so that the OLI and TIRS boresight axes are always pointing toward the center of the Earth. The orientation of this coordinate system relative to the inertial coordinate system is captured in spacecraft attitude data.

Ideally, the navigation reference frame is the same as the spacecraft coordinate system. In practice, the navigation frame is based on the orientation of the absolute attitude sensor (i.e., star tracker) being used for attitude determination. Any errors in the orientation knowledge for this tracker with respect to the spacecraft body frame will lead to differences between the spacecraft and navigation coordinate systems. This becomes important if the absolute attitude sensor is changed, for example, by switching from the primary to the redundant star tracker during on-orbit operations. Such an event would effectively redefine the navigation frame to be based on the redundant tracker, with the difference between the spacecraft and navigation frames now resulting from redundant tracker alignment knowledge errors, rather than from primary tracker alignment knowledge errors. This redefinition would require updates to the on-orbit instrument-to-ACS alignment calibrations. Therefore, the spacecraft and navigation reference coordinate systems are different because the spacecraft coordinate system is fixed but the navigation reference can change.

B.6 SIRU Coordinate System

The spacecraft orientation rate data provided by the spacecraft attitude control system's inertial measurement unit are referenced to the SIRU coordinate system. The SIRU consists of four rotation-sensitive axes. This configuration provides redundancy to protect against the failure of any one axis. The four SIRU axis directions are determined relative to the SIRU coordinate system, the orientation of which is itself measured relative to the spacecraft coordinate system both pre-launch and on-orbit, as part of the ACS calibration procedure. The IAS uses this alignment transformation to convert the SIRU data contained in the L8 spacecraft ancillary data to the navigation reference coordinate system for blending with the ACS quaternions.

B.7 Orbital Coordinate System

The orbital coordinate system is centered at the spacecraft, and its orientation is based on the spacecraft position in inertial space (see Figure B-3). The origin is the spacecraft's center of mass, with the Z-axis pointing from the spacecraft's center of mass to the Earth's center of mass. The Y-axis is the normalized cross product of the Z-axis and the instantaneous (inertial) velocity vector and corresponds to the negative of the instantaneous angular momentum vector direction. The X-axis is the cross product of the Y- and Z-axes. The orbital coordinate system is used to convert spacecraft attitude, expressed as Earth-Centered Inertial (ECI) quaternions, to roll-pitch-yaw Euler angles.

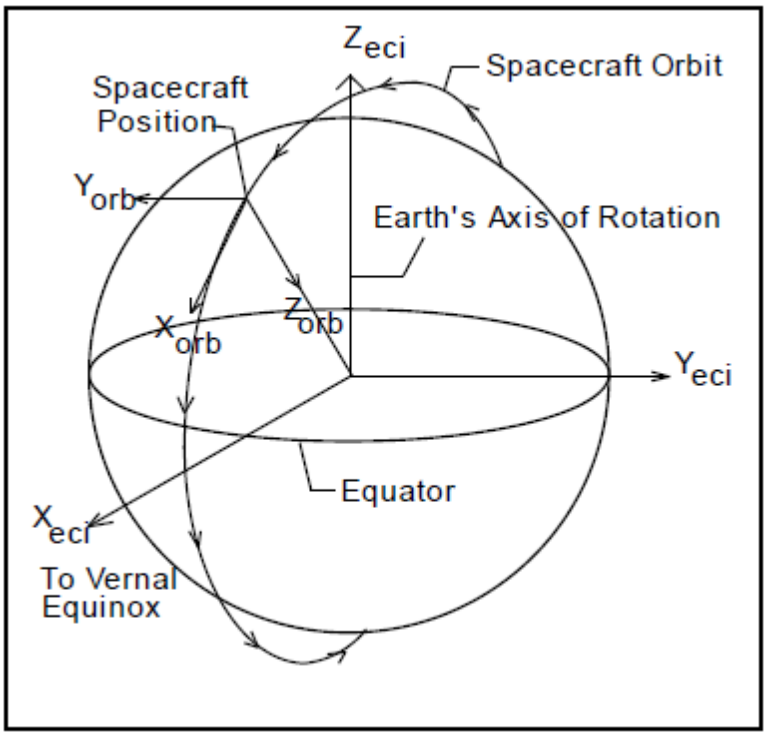

Figure B-3. Orbital Coordinate System

B.8 ECI J2000 Coordinate System

The ECI coordinate system of epoch J2000 is space-fixed with its origin at the Earth's center of mass (see Figure B-4). The Z-axis corresponds to the mean north celestial pole of epoch J2000.0. The X-axis is based on the mean vernal equinox of epoch J2000.0. The Y-axis is the cross product of the Z and X axes. This coordinate system is described in detail in the Explanatory Supplement to the Astronomical Almanac published by the U.S. Naval Observatory. Data in the ECI coordinate system are present in the L8 spacecraft ancillary data form of attitude quaternions that relate the navigation frame to the ECI J2000 coordinate system.

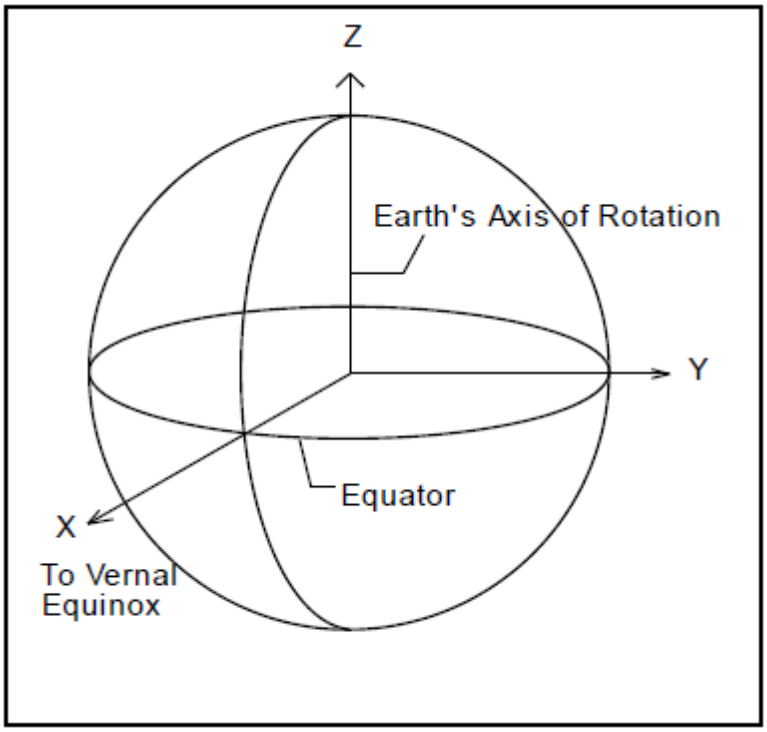

Figure B-4. Earth-Centered Inertial (ECI) Coordinate System

B.9 ECEF Coordinate System

The Earth-Centered, Earth-Fixed (ECEF) coordinate system is Earth-fixed with its origin at the Earth's center of mass (see Figure B-5). It corresponds to the Conventional Terrestrial System defined by the Bureau International de l'Heure (BIH), which is the same as the WGS84 geocentric reference system. This coordinate system is described in the Supplement to Department of Defense World Geodetic System 1984 Technical Report, Part 1: Methods, Techniques, and Data Used in WGS84 Development, TR 8350.2-A, published by the NGA.

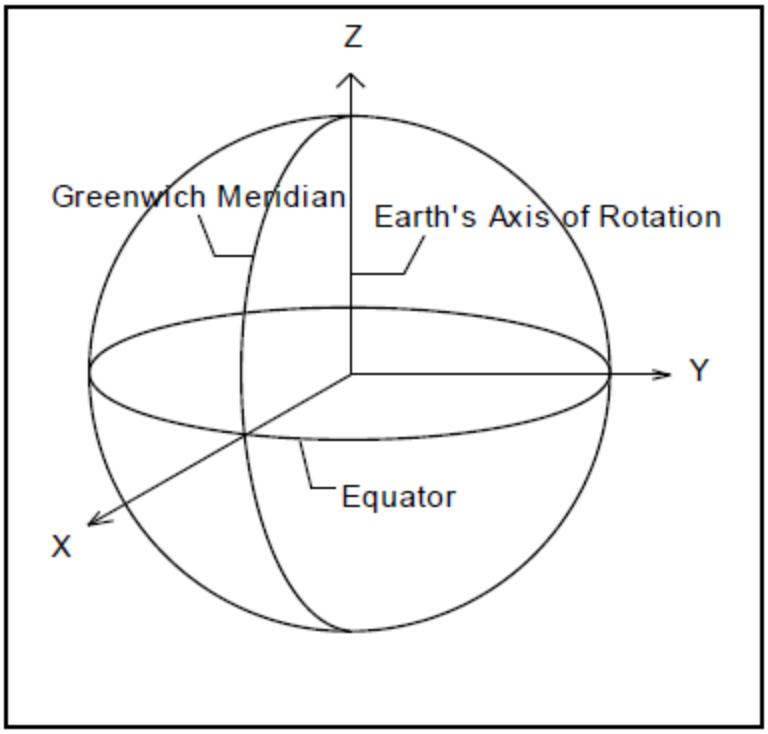

Figure B-5. Earth-Centered, Earth-Fixed (ECEF) Coordinate System

B.10 Geodetic Coordinate System

The geodetic coordinate system is based on the WGS84 reference frame, with coordinates expressed in latitude, longitude, and height above the reference Earth ellipsoid (see Figure B-6). No ellipsoid is required by the definition of the ECEF coordinate system, but the geodetic coordinate system depends on the selection of an Earth ellipsoid. Latitude and longitude are defined as the angle between the ellipsoid normal and its projection onto the Equator, and the angle between the local meridian and the Greenwich meridian, respectively. The scene center and scene corner coordinates in the Level 0R product metadata are expressed in the geodetic coordinate system.

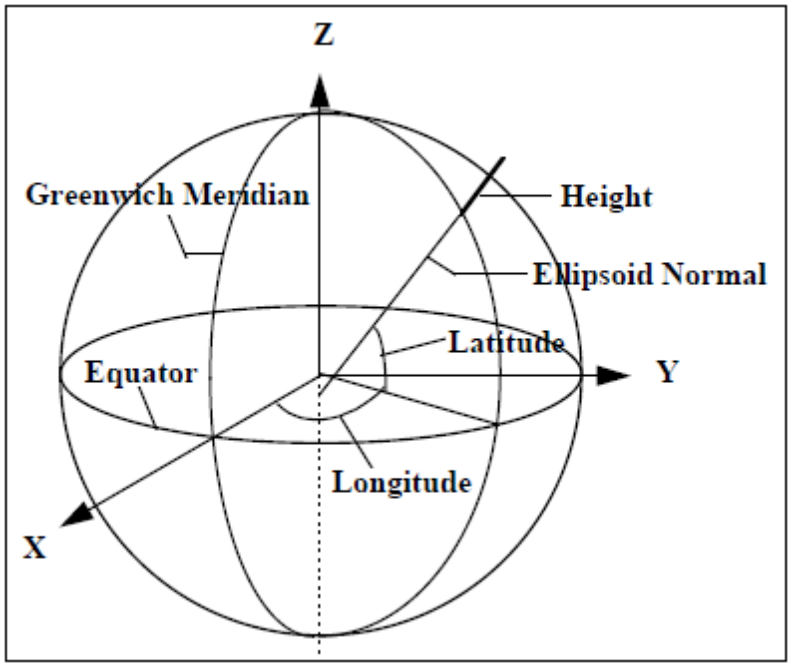

Figure B-6. Geodetic Coordinate System

B.11 Map Projection Coordinate System

Level 1 products are generated with respect to a map projection coordinate system, such as the UTM, which provides mapping from latitude and longitude to a plane coordinate system that approximates a Cartesian coordinate system for a portion of the Earth's surface. It is used for convenience as a method of providing digital image data in an Earth-referenced grid that is compatible with other ground-referenced datasets. Although the map projection coordinate system is only an approximation of a true local Cartesian coordinate system at the Earth's surface, the mathematical relationship between the map projection and geodetic coordinate systems is defined precisely and unambiguously.

Appendix C Metadata File (MTL.txt)

The MTL.txt file is included with all L8 Level 1 Data Products. Landsat MTL files contain beneficial information for the systematic searching and archiving practices of data. Information about data processing and values important for enhancing Landsat data (such as conversion to reflectance and radiance) are also included in this file.

Data Format Control Books (DFCBs) define and describe Landsat metadata. DFCBs for all sensors are located at https://www.usgs.gov/land-resources/nli/landsat/landsat-project-documents.

Sample L8 MTL.txt file:

```
GROUP = L1_METADATA_FILE
  GROUP = METADATA_FILE_INFO
    ORIGIN = "Image courtesy of the U.S. Geological Survey"
    REQUEST_ID = "0701809117441_00014"
    LANDSAT_SCENE_ID = "LC80330282018251LGN00"
    LANDSAT_PRODUCT_ID =
"LC08_L1TP_033028_20180908_20180912_01_T1"
    COLLECTION_NUMBER = 01
    FILE_DATE = 2018-09-12T22:00:27Z
    STATION_ID = "LGN"
    PROCESSING_SOFTWARE_VERSION = "LPGS_13.1.0"
  END_GROUP = METADATA_FILE_INFO
  GROUP = PRODUCT_METADATA
    DATA_TYPE = "L1TP"
    COLLECTION_CATEGORY = "T1"
    ELEVATION_SOURCE = "GLS2000"
    OUTPUT_FORMAT = "GEOTIFF"
    SPACECRAFT_ID = "LANDSAT_8"
    SENSOR_ID = "OLI_TIRS"
    WRS_PATH = 33
    WRS_ROW = 28
    NADIR_OFFNADIR = "NADIR"
    TARGET_WRS_PATH = 33
    TARGET_WRS_ROW = 28
    DATE_ACQUIRED = 2018-09-08
    SCENE_CENTER_TIME = "17:35:18.0691869Z"
    CORNER_UL_LAT_PRODUCT = 47.09933
    CORNER_UL_LON_PRODUCT = -103.71778
    CORNER_UR_LAT_PRODUCT = 47.02553
    CORNER_UR_LON_PRODUCT = -100.69517
    CORNER_LL_LAT_PRODUCT = 45.00187
    CORNER_LL_LON_PRODUCT = -103.76543
    CORNER_LR_LAT_PRODUCT = 44.93325
    CORNER_LR_LON_PRODUCT = -100.85461
```

```
    CORNER_UL_PROJECTION_X_PRODUCT = 597300.000
    CORNER_UL_PROJECTION_Y_PRODUCT = 5217000.000
    CORNER_UR_PROJECTION_X_PRODUCT = 827100.000
    CORNER_UR_PROJECTION_Y_PRODUCT = 5217000.000
    CORNER_LL_PROJECTION_X_PRODUCT = 597300.000
    CORNER_LL_PROJECTION_Y_PRODUCT = 4983900.000
    CORNER_LR_PROJECTION_X_PRODUCT = 827100.000
    CORNER_LR_PROJECTION_Y_PRODUCT = 4983900.000
    PANCHROMATIC_LINES = 15541
    PANCHROMATIC_SAMPLES = 15321
    REFLECTIVE_LINES = 7771
    REFLECTIVE_SAMPLES = 7661
    THERMAL_LINES = 7771
    THERMAL_SAMPLES = 7661
    FILE_NAME_BAND_1 =
"LC08_L1TP_033028_20180908_20180912_01_T1_B1.TIF"
    FILE_NAME_BAND_2 =
"LC08_L1TP_033028_20180908_20180912_01_T1_B2.TIF"
    FILE_NAME_BAND_3 =
"LC08_L1TP_033028_20180908_20180912_01_T1_B3.TIF"
    FILE_NAME_BAND_4 =
"LC08_L1TP_033028_20180908_20180912_01_T1_B4.TIF"
    FILE_NAME_BAND_5 =
"LC08_L1TP_033028_20180908_20180912_01_T1_B5.TIF"
    FILE_NAME_BAND_6 =
"LC08_L1TP_033028_20180908_20180912_01_T1_B6.TIF"
    FILE_NAME_BAND_7 =
"LC08_L1TP_033028_20180908_20180912_01_T1_B7.TIF"
    FILE_NAME_BAND_8 =
"LC08_L1TP_033028_20180908_20180912_01_T1_B8.TIF"
    FILE_NAME_BAND_9 =
"LC08_L1TP_033028_20180908_20180912_01_T1_B9.TIF"
    FILE_NAME_BAND_10 =
"LC08_L1TP_033028_20180908_20180912_01_T1_B10.TIF"
    FILE_NAME_BAND_11 =
"LC08_L1TP_033028_20180908_20180912_01_T1_B11.TIF"
    FILE_NAME_BAND_QUALITY =
"LC08_L1TP_033028_20180908_20180912_01_T1_BQA.TIF"
    ANGLE_COEFFICIENT_FILE_NAME =
"LC08_L1TP_033028_20180908_20180912_01_T1_ANG.txt"
    METADATA_FILE_NAME =
"LC08_L1TP_033028_20180908_20180912_01_T1_MTL.txt"
    CPF_NAME = "LC08CPF_20180701_20180930_01.02"
    BPF_NAME_OLI = "LO8BPF20180908172108_20180908180920.01"
    BPF_NAME_TIRS = "LT8BPF20180827051943_20180910114155.01"
    RLUT_FILE_NAME = "LC08RLUT_20150303_20431231_01_12.h5"
  END_GROUP = PRODUCT_METADATA
```

```
GROUP = IMAGE_ATTRIBUTES
  CLOUD_COVER = 28.71
  CLOUD_COVER_LAND = 28.71
  IMAGE_QUALITY_OLI = 9
  IMAGE_QUALITY_TIRS = 9
  TIRS_SSM_MODEL = "FINAL"
  TIRS_SSM_POSITION_STATUS = "ESTIMATED"
  TIRS_STRAY_LIGHT_CORRECTION_SOURCE = "TIRS"
  ROLL_ANGLE = -0.001
  SUN_AZIMUTH = 153.64775365
  SUN_ELEVATION = 46.63860470
  EARTH_SUN_DISTANCE = 1.0074499
  SATURATION_BAND_1 = "N"
  SATURATION_BAND_2 = "N"
  SATURATION_BAND_3 = "N"
  SATURATION_BAND_4 = "N"
  SATURATION_BAND_5 = "N"
  SATURATION_BAND_6 = "N"
  SATURATION_BAND_7 = "N"
  SATURATION_BAND_8 = "N"
  SATURATION_BAND_9 = "N"
  GROUND_CONTROL_POINTS_VERSION = 4
  GROUND_CONTROL_POINTS_MODEL = 369
  GEOMETRIC_RMSE_MODEL = 7.067
  GEOMETRIC_RMSE_MODEL_Y = 4.980
  GEOMETRIC_RMSE_MODEL_X = 5.015
  GROUND_CONTROL_POINTS_VERIFY = 160
  GEOMETRIC_RMSE_VERIFY = 4.368
  TRUNCATION_OLI = "UPPER"
END_GROUP = IMAGE_ATTRIBUTES
GROUP = MIN_MAX_RADIANCE
  RADIANCE_MAXIMUM_BAND_1 = 748.86316
  RADIANCE_MINIMUM_BAND_1 = -61.84137
  RADIANCE_MAXIMUM_BAND_2 = 766.84503
  RADIANCE_MINIMUM_BAND_2 = -63.32631
  RADIANCE_MAXIMUM_BAND_3 = 706.64111
  RADIANCE_MINIMUM_BAND_3 = -58.35465
  RADIANCE_MAXIMUM_BAND_4 = 595.87958
  RADIANCE_MINIMUM_BAND_4 = -49.20793
  RADIANCE_MAXIMUM_BAND_5 = 364.64859
  RADIANCE_MINIMUM_BAND_5 = -30.11280
  RADIANCE_MAXIMUM_BAND_6 = 90.68479
  RADIANCE_MINIMUM_BAND_6 = -7.48878
  RADIANCE_MAXIMUM_BAND_7 = 30.56563
  RADIANCE_MINIMUM_BAND_7 = -2.52412
  RADIANCE_MAXIMUM_BAND_8 = 674.37170
  RADIANCE_MINIMUM_BAND_8 = -55.68983
```

```
    RADIANCE_MAXIMUM_BAND_9 = 142.51294
    RADIANCE_MINIMUM_BAND_9 = -11.76877
    RADIANCE_MAXIMUM_BAND_10 = 22.00180
    RADIANCE_MINIMUM_BAND_10 = 0.10033
    RADIANCE_MAXIMUM_BAND_11 = 22.00180
    RADIANCE_MINIMUM_BAND_11 = 0.10033
  END_GROUP = MIN_MAX_RADIANCE
  GROUP = MIN_MAX_REFLECTANCE
    REFLECTANCE_MAXIMUM_BAND_1 = 1.210700
    REFLECTANCE_MINIMUM_BAND_1 = -0.099980
    REFLECTANCE_MAXIMUM_BAND_2 = 1.210700
    REFLECTANCE_MINIMUM_BAND_2 = -0.099980
    REFLECTANCE_MAXIMUM_BAND_3 = 1.210700
    REFLECTANCE_MINIMUM_BAND_3 = -0.099980
    REFLECTANCE_MAXIMUM_BAND_4 = 1.210700
    REFLECTANCE_MINIMUM_BAND_4 = -0.099980
    REFLECTANCE_MAXIMUM_BAND_5 = 1.210700
    REFLECTANCE_MINIMUM_BAND_5 = -0.099980
    REFLECTANCE_MAXIMUM_BAND_6 = 1.210700
    REFLECTANCE_MINIMUM_BAND_6 = -0.099980
    REFLECTANCE_MAXIMUM_BAND_7 = 1.210700
    REFLECTANCE_MINIMUM_BAND_7 = -0.099980
    REFLECTANCE_MAXIMUM_BAND_8 = 1.210700
    REFLECTANCE_MINIMUM_BAND_8 = -0.099980
    REFLECTANCE_MAXIMUM_BAND_9 = 1.210700
    REFLECTANCE_MINIMUM_BAND_9 = -0.099980
  END_GROUP = MIN_MAX_REFLECTANCE
  GROUP = MIN_MAX_PIXEL_VALUE
    QUANTIZE_CAL_MAX_BAND_1 = 65535
    QUANTIZE_CAL_MIN_BAND_1 = 1
    QUANTIZE_CAL_MAX_BAND_2 = 65535
    QUANTIZE_CAL_MIN_BAND_2 = 1
    QUANTIZE_CAL_MAX_BAND_3 = 65535
    QUANTIZE_CAL_MIN_BAND_3 = 1
    QUANTIZE_CAL_MAX_BAND_4 = 65535
    QUANTIZE_CAL_MIN_BAND_4 = 1
    QUANTIZE_CAL_MAX_BAND_5 = 65535
    QUANTIZE_CAL_MIN_BAND_5 = 1
    QUANTIZE_CAL_MAX_BAND_6 = 65535
    QUANTIZE_CAL_MIN_BAND_6 = 1
    QUANTIZE_CAL_MAX_BAND_7 = 65535
    QUANTIZE_CAL_MIN_BAND_7 = 1
    QUANTIZE_CAL_MAX_BAND_8 = 65535
    QUANTIZE_CAL_MIN_BAND_8 = 1
    QUANTIZE_CAL_MAX_BAND_9 = 65535
    QUANTIZE_CAL_MIN_BAND_9 = 1
    QUANTIZE_CAL_MAX_BAND_10 = 65535
```

```
    QUANTIZE_CAL_MIN_BAND_10 = 1
    QUANTIZE_CAL_MAX_BAND_11 = 65535
    QUANTIZE_CAL_MIN_BAND_11 = 1
  END_GROUP = MIN_MAX_PIXEL_VALUE
  GROUP = RADIOMETRIC_RESCALING
    RADIANCE_MULT_BAND_1 = 1.2371E-02
    RADIANCE_MULT_BAND_2 = 1.2668E-02
    RADIANCE_MULT_BAND_3 = 1.1673E-02
    RADIANCE_MULT_BAND_4 = 9.8436E-03
    RADIANCE_MULT_BAND_5 = 6.0238E-03
    RADIANCE_MULT_BAND_6 = 1.4981E-03
    RADIANCE_MULT_BAND_7 = 5.0492E-04
    RADIANCE_MULT_BAND_8 = 1.1140E-02
    RADIANCE_MULT_BAND_9 = 2.3542E-03
    RADIANCE_MULT_BAND_10 = 3.3420E-04
    RADIANCE_MULT_BAND_11 = 3.3420E-04
    RADIANCE_ADD_BAND_1 = -61.85373
    RADIANCE_ADD_BAND_2 = -63.33898
    RADIANCE_ADD_BAND_3 = -58.36633
    RADIANCE_ADD_BAND_4 = -49.21778
    RADIANCE_ADD_BAND_5 = -30.11882
    RADIANCE_ADD_BAND_6 = -7.49028
    RADIANCE_ADD_BAND_7 = -2.52462
    RADIANCE_ADD_BAND_8 = -55.70098
    RADIANCE_ADD_BAND_9 = -11.77112
    RADIANCE_ADD_BAND_10 = 0.10000
    RADIANCE_ADD_BAND_11 = 0.10000
    REFLECTANCE_MULT_BAND_1 = 2.0000E-05
    REFLECTANCE_MULT_BAND_2 = 2.0000E-05
    REFLECTANCE_MULT_BAND_3 = 2.0000E-05
    REFLECTANCE_MULT_BAND_4 = 2.0000E-05
    REFLECTANCE_MULT_BAND_5 = 2.0000E-05
    REFLECTANCE_MULT_BAND_6 = 2.0000E-05
    REFLECTANCE_MULT_BAND_7 = 2.0000E-05
    REFLECTANCE_MULT_BAND_8 = 2.0000E-05
    REFLECTANCE_MULT_BAND_9 = 2.0000E-05
    REFLECTANCE_ADD_BAND_1 = -0.100000
    REFLECTANCE_ADD_BAND_2 = -0.100000
    REFLECTANCE_ADD_BAND_3 = -0.100000
    REFLECTANCE_ADD_BAND_4 = -0.100000
    REFLECTANCE_ADD_BAND_5 = -0.100000
    REFLECTANCE_ADD_BAND_6 = -0.100000
    REFLECTANCE_ADD_BAND_7 = -0.100000
    REFLECTANCE_ADD_BAND_8 = -0.100000
    REFLECTANCE_ADD_BAND_9 = -0.100000
  END_GROUP = RADIOMETRIC_RESCALING
  GROUP = TIRS_THERMAL_CONSTANTS
```

```
    K1_CONSTANT_BAND_10 = 774.8853
    K2_CONSTANT_BAND_10 = 1321.0789
    K1_CONSTANT_BAND_11 = 480.8883
    K2_CONSTANT_BAND_11 = 1201.1442
  END_GROUP = TIRS_THERMAL_CONSTANTS
  GROUP = PROJECTION_PARAMETERS
    MAP_PROJECTION = "UTM"
    DATUM = "WGS84"
    ELLIPSOID = "WGS84"
    UTM_ZONE = 13
    GRID_CELL_SIZE_PANCHROMATIC = 15.00
    GRID_CELL_SIZE_REFLECTIVE = 30.00
    GRID_CELL_SIZE_THERMAL = 30.00
    ORIENTATION = "NORTH_UP"
    RESAMPLING_OPTION = "CUBIC_CONVOLUTION"
  END_GROUP = PROJECTION_PARAMETERS
END_GROUP = L1_METADATA_FILE
END
```

Appendix D References

Please see https://www.usgs.gov/land-resources/nli/landsat/landsat-acronyms for a list of acronyms.

Arvidson, Terry, Samuel Goward, John Gasch, and Darrel Williams. "Landsat-7 Long-Term Acquisition Plan." *Photogrammetric Engineering & Remote Sensing* 72, no. 10 (2006): 1137-1146.

Barsi, Julia A., John R. Schott, Simon J. Hook, Nina G. Raqueno, Brian L. Markham, and Robert G. Radocinski. "Landsat-8 Thermal Infrared Sensor (TIRS) Vicarious Radiometric Calibration." *Remote Sensing* 6, no. 11 (2014): 11607-11626.

Barsi, Julia A., Kenton Lee, Geir Kvaran, Brian L. Markham, and Jeffrey A. Pedelty. "The spectral response of the Landsat-8 operational land imager." *Remote Sensing 6*, no. 10 (2014): 10232-10251.

Cook, Monica, John R. Schott, John Mandel, and Nina Raqueno. "Development of an Operational Calibration Methodology for the Landsat Thermal Data Archive and Initial Testing of the Atmospheric Compensation Component of a Land Surface Temperature (LST) Product from the Archive." *Remote Sensing* 6, no. 11 (2014): 11244-11266.

Foga, S., Scaramuzza, P.L., Guo, S., Zhu, Z., Dilley, R.D., Beckmann, T., Schmidt, G.L., Dwyer, J.L., Hughes, M.J., Laue, B. (2017). Cloud detection algorithm comparison and validation for operational Landsat data products. Remote Sensing of Environment, 194, 379-390. http://doi.org/10.1016/j.rse.2017.03.026.

Gerace, Aaron, John Schott, Michael Gartley, and Matthew Montanaro. "An Analysis of the Side Slither On-Orbit Calibration Technique Using the DIRSIG Model." *Remote Sensing 6*, no. 11 (2014): 10523-10545.

Gerace, A., Montanaro, M., Derivation and validation of the stray light correction algorithm for the thermal infrared sensor onboard Landsat 8, Remote Sensing of Environment, Volume 191, 15 March 2017, Pages 246-257, ISSN 0034-4257, http://dx.doi.org/10.1016/j.rse.2017.01.029. (http://www.sciencedirect.com/science/article/pii/S0034425717300421)

Irons, James R., John L. Dwyer, and Julia A. Barsi. "The next Landsat satellite: The Landsat data continuity mission." *Remote Sensing of Environment* 122 (2012): 11-21.

Irons, James R., and John L. Dwyer. "An overview of the Landsat Data Continuity Mission." In *SPIE Defense, Security, and Sensing*, pp. 769508-769508. International Society for Optics and Photonics, 2010.

Knight, Edward J., and Geir Kvaran. "Landsat-8 operational land imager design, characterization and performance." *Remote Sensing* 6, no. 11 (2014): 10286-10305.

Markham, Brian, Julia Barsi, Geir Kvaran, Lawrence Ong, Edward Kaita, Stuart Biggar, Jeffrey Czapla-Myers, Nischal Mishra, and Dennis Helder. "Landsat-8 Operational Land Imager radiometric calibration and stability." *Remote Sensing* 6, no. 12 (2014): 12275-12308.

Mishra, Nischal, Md Obaidul Haque, Larry Leigh, David Aaron, Dennis Helder, and Brian Markham. "Radiometric Cross Calibration of Landsat 8 Operational Land Imager (OLI) and L7 Enhanced Thematic Mapper Plus (ETM+)." *Remote Sensing 6*, no. 12 (2014): 12619-12638.

Montanaro, Matthew, Raviv Levy, and Brian Markham. "On-orbit radiometric performance of the Landsat 8 Thermal Infrared Sensor." *Remote Sensing* 6, no. 12 (2014): 11753-11769.

Montanaro, Matthew, Aaron Gerace, Allen Lunsford, and Dennis Reuter. "Stray light artifacts in imagery from the Landsat 8 Thermal Infrared Sensor." *Remote Sensing 6*, no. 11 (2014): 10435-10456.

Montanaro, Matthew, Allen Lunsford, Zelalem Tesfaye, Brian Wenny, and Dennis Reuter. "Radiometric calibration methodology of the Landsat 8 Thermal Infrared Sensor." *Remote Sensing 6*, no. 9 (2014): 8803-8821.

Morfitt, Ron, Julia Barsi, Raviv Levy, Brian Markham, Esad Micijevic, Lawrence Ong, Pat Scaramuzza, and Kelly Vanderwerff. "Landsat-8 Operational Land Imager (OLI) radiometric performance on-orbit." *Remote Sensing 7*, no. 2 (2015): 2208-2237.

Rice, Robert F., Pen-Shu Yeh, and Warner H. Miller. "Algorithms for high speed universal noiseless coding." In *Proceedings of the AIAA Computing in Aerospace 9 Conference*, pp. 19-21. 1993.

Storey, James, Michael Choate, and Kenton Lee. "Landsat 8 Operational Land Imager On-Orbit Geometric Calibration and Performance." *Remote Sensing 6*, no. 11 (2014): 11127-11152.

Storey, James, Michael Choate, and Donald Moe. "Landsat 8 thermal infrared sensor geometric characterization and calibration." *Remote Sensing 6*, no. 11 (2014): 11153-11181.

Wenny, Brian N., Dennis Helder, Jungseok Hong, Larry Leigh, Kurtis J. Thome, and Dennis Reuter. "Pre-and post-launch spatial quality of the Landsat 8 Thermal Infrared Sensor." *Remote Sensing 7*, no. 2 (2015): 1962-1980.

Landsat Missions Factsheet: https://pubs.usgs.gov/fs/2015/3081/fs20153081.pdf

Landsat Missions Website: https://usgs.gov/landsat

Landsat 8 OLI and TIRS Calibration Notices: https://www.usgs.gov/land-resources/nli/landsat/landsat-8-oli-and-tirs-calibration-notices

EarthExplorer: https://earthexplorer.usgs.gov

GloVis: https://glovis.usgs.gov

LandsatLook Viewer: https://landsatlook.usgs.gov

LSDS-649. Landsat 8 (L8) Calibration and Validation (Cal/Val) Algorithm Description Document (ADD): https://www.usgs.gov/media/files/landsat-8-9-calibration-validation-algorithm-description-document

LSDS-749. Landsat 8 (L8) Mission Data Data Format Control Book (DFCB): https://www.usgs.gov/media/files/landsat-8-mission-data-data-format-control-book

LSDS-750. Landsat 8 (L8) Level 0 Reformatted (L0R) Data Format Control Book (DFCB): https://www.usgs.gov/media/files/landsat-8-level-0-reformatted-data-format-control-book

LSDS-809. Landsat 8 Collection 1 Level 1 (L1) Data Format Control Book (DFCB): https://www.usgs.gov/media/files/landsat-8-level-1-data-format-control-book

LSDS-810. Landsat 8 (L8) Calibration Parameter File (CPF) Data Format Control Book (DFCB): https://www.usgs.gov/media/files/landsat-8-calibration-parameter-file-data-format-control-book

Documents pertaining to the Landsat 8 mission and data products can be found on https://www.usgs.gov/land-resources/nli/landsat/landsat-project-documents.

Contact USGS Landsat User Services with any questions regarding these interfaces or Landsat data products, M-F 8:00 am to 4:00 p.m. CT:

www.usgs.gov/landsat
custserv@usgs.gov
1-605-594-6151
1-800-252-4547

Appendix E Acronyms

AAS	Anomaly Analysis Subsystem
ACS	Attitude Control System
ADD	Algorithm Description Document
ALI	Advanced Land Imager
ARB	Anomaly Review Board
ASCII	American Standard Code for Information Interchange
BATC	Ball Aerospace & Technologies Corp.
BIH	Bureau International De l'Heure
BPF	Bias Parameter File
BRDF	Bi-directional Reflectance Distribution Function
Cal/Val	Calibration/Validation
CCA	Cloud Cover Assessment
CCB	Configuration Control Board
CDED	Canadian Digital Elevation Dataset
CE	Circular Error
CE90	Circular Error 90
CFMask	C Function of Mask
CPF	Calibration Parameter File
CR	Change Request
CVT	Calibration and Validation Team
CVTK	Calibration Validation Toolkit
DEM	Digital Elevation Model
DFCB	Data Format Control Book
DMS	Data Management Subsystem
DN	Digital Numbers
DOQ	Digital Orthophoto Quadrangle
DPAS	Data Processing and Archiving System
DTED	Digital Terrain Elevation Data
ECEF	Earth-Centered, Earth-Fixed
ECI	Earth-Centered Inertial
EE	EarthExplorer
EO-1	Earth Observing 1
EROS	Earth Resources Observation and Science
ETM+	Enhanced Thematic Mapper Plus
FASCAL	Facility for Spectroradiometric Calibrations
FMask	Function of Mask
FOT	Flight Operations Team
FOV	Field of View
FPA	Focal Plane Array
FPM	Focal Plane Module
GCP	Ground Control Points
GDAIS	General Dynamics Advanced Information Systems

GeoTIFF	Georeferenced Tagged Image File Format
GloVis	Global Visualization Viewer
GLS	Global Land Survey
GLS2000	Global Land Survey 2000
GN	Ground Network
GNE	Ground Network Element
GPS	Geometric Processing Subsystem
GSD	Ground Sampling Distance
GSFC	Goddard Space Flight Center
GUI	Graphical User Interface
HCA	Horizontal Collimator Assembly
HDF	Hierarchical Data Format
HTTPS	Hypertext Transfer Protocol Secure
IAS	Image Assessment System
IC	International Cooperator
IGS	International Ground Stations
JPL	Jet Propulsion Laboratory
km	Kilometer
K	Kelvin
KPR	Key Performance Requirements
L0R	Level 0 Reformatted
L1Gs	Level 1 Geometric Systematic
L1Gt	Level 1 Systemic Terrain (Corrected)
L1R	Level 1 Radiometric (Corrected)
L1T	Level 1 Terrain (Corrected)
L1TP	Level 1 Precision Terrain (Corrected)
L7	Landsat 7
L8	Landsat 8
LE90	Linear Error 90 Percent
LOS	Line of Sight
LPGS	Level 1 Product Generation System
LSDS	Land Satellites Data System
LST	Land Surface Temperature
LTAP	Long-Term Acquisition Plan
LTAP-8	Landsat 8 Long-Term Acquisition Plan
Ltypical	Typical Spectral Radiance
LUT	Lookup Table
m	Meter
Mbps	Megabits per second
MLT	Mean Local Time
MMS	Multimission Modular Spacecraft
MOC	Mission Operation Center
MOE	Mission Operations Element
MSS	Multispectral Scanner
MTF	Modulation Transfer Function

MTL	Level 1 Metadata
NASA	National Aeronautics and Space Administration
NDVI	Normalized Difference Vegetation Index
NEΔT	Noise-equivalent change in temperature
NED	Natural Elevation Data
NEdL	Noise Equivalent Detector Radiance
NEOG	National Earth Observation Group
NGA	National Geospatial Intelligence Agency
NIST	National Institute for Standards and Technology
NMAS	National Map Accuracy Standards
NOAA	National Oceanic and Atmospheric Administration
NPOESS	National Polar-orbiting Operational Environmental Satellite System
OBC	On-Board Calibrator
ODL	Object Definition Language
OIV	On-orbit Initialization and Verification
OLI	Operational Land Imager
OSC	Orbital Sciences Corporation
Pan	Panchromatic
PCS	Process Control Subsystem
PDF	Portable Document Format
PICS	Pseudo-Invariant Calibration Site
PIE	Payload Interface Electronics
QA	Quality Assessment
QAS	Quality Assessment Subsystem
QWIP	Quantum Well Infrared Photodetector
RBV	Return Beam Vidicon
RF	Radio Frequency
RLUT	Response Linearity Look-Up Table
RMSE	Root Mean Square Error
ROIC	Read-Out Integrated Circuit
RPS	Radiometric Processing Subsystem
SCA	Sensor Chip Assemblies
SEU	Single Event Upset
SiPIN	Silicon PIN
SIRU	Scalable Inertial Reference Unit
SLC	Scan Line Corrector
SMD	Science Mission Directorate
SNR	Signal-to-Noise Ratio
SPOT	Satellite Pour l'Observation de la Terre
SRTM	Shuttle Radar Topography Mission
SSM	Scene Select Mechanism/Mirror
SSR	Solid State Recorder
STF	System Transfer Function
SWIR	Short Wavelength Infrared
TIR	Thermal Infrared

TIRS	Thermal Infrared Sensor
TM	Thematic Mapper
TOA	Top of Atmosphere
UI	User Interface
UP	User Portal
USGCRP	U.S. Global Change Research Program
USGS	U.S. Geological Survey
UT1	Universal Time Code Corrected
UTC	Universal Time Code
UTM	Universal Transverse Mercator
VNIR	Visible and Near Infrared
WGS84	World Geodetic System 1984
WRS	Worldwide Reference System
WRS-2	Worldwide Reference System 2